UCL Université catholique de Louvain

École polytechnique de Louvain (EPL)

epl

Understanding the flow behavior of end functionalized model polymers governed by both transient bond dynamics and interchain entanglements.

Dissertation presented by
Matin ROSTAMITABAR

for obtaining the master's degree in
Chemical and Materials Engineering

Supervisor(s)
Charles-André FUSTIN, Evelyne VAN RUYMBEKE

Readers(s)
Christian CLASEN, Jean-François GOHY

Academic year 2017-2018

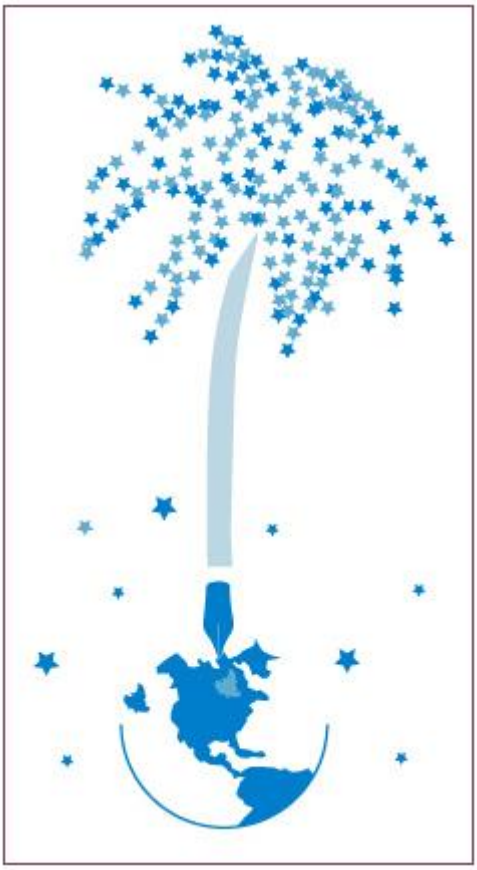

"If the three of human being gets the fruit of knowledge, you can bring the whole universe down".

(Naser Khosrow, (1004 – 1088 AD,)/ HNKB Cultural Center Logo)

Abstract

Massive production of polymer material proves the privileged position of them as the class of important materials. Scientists have constantly looked for new routes and methodologies to improve and modify synthetic polymers. One of the greatest treatment, inspired from the nature, is to incorporate non-covalent transient interaction into polymer to build supramolecular polymers. Supramolecular systems based on associating polymers are promising smart materials since they exhibit tunable properties achieved by the incorporation of stimuli responsive supramolecular moieties to polymer backbones. The great benefit of the self-assembling supramolecular network is their microstructure and dynamic which depends on many tunable parameters such as the strength of the transient bonds, temperature, chemistry and architecture of the polymer precursor.

One of the useful way to study behavior of supramolecular polymer is rheological characterization. Rheology is a complex study of the flow of matter and as a tool to investigate different properties. This dissertation joins a link between chemistry of polymers and their rheological properties. In other words, rheological properties and molecular structure of different metallo-supramolecular polymer based on linear chains will be investigated.

Functionalizing of hydrogenated, hydroxyl terminated polybutadiene by 2,2′;6′,2″-terpyridine in order to build metallo-supramolecular polymers is the main task which has been done in the synthesis part (chapter 3). This combination of polar end functional groups and nonpolar backbones would lead to microphase-separated morphologies in which the metal–ligand complexes form a ‘hard phase’ that physically crosslinks the polybutadiene ‘soft’ domains. The polymers self-assemble into different metallo-supramolecular bulk structures once metal ions are added. Therefore, the properties of the obtained materials can be finely tuned depending on the polymer chains and the type of metal.

In the rheological characterization (chapter 4) different aspect of polybutadiene polymers and their effect such as nature of metallic ions and their amounts, phase separation, etc. has been investigated. Therefore, these results can provide a clear vision about the effect of association by metal-ligand coordination and micro-phase separation on the dynamic and relaxation of the polymer chains. In addition, by studying all the supramolecular samples two plateaus were observed. We conclude that the first relaxation happens due to fast motion of the free linear assemblies, followed by the slower (Rouse) motion of the molecular segments trapped between two aggregates made of several metal-ligand complexes. These molecular segments, explore their surrounding at the rhythm of the entanglement/disentanglement of the free chains and dangling ends. The second (terminal) relaxation is not clear since it could be due to several mechanisms. Most probably, this relaxation is due to breaking of the complexes along the self-assemblies. However, it could also be due to the detachment of a complex from the phase separated domains. Finally, the experimental data was compared to the theoretical models predictions. These models are based on different assumptions concerning the relaxation processes and lifetime of the stickers.

ACKNOWLEDGEMENT

I would like to extend my thanks to Professor Evelyne van Ruymbeke and Professor Charles-André Fustin for their guidance and supervision throughout this project. Their comments and discussions provided much valuable information which is greatly appreciated. The suggestions and supervision of Dr. Jagadeesh Malineni and Fabio Lucaccioni in the synthesis part and Sina Ghiassinejad in rheological characterization are also greatly appreciated, as they helped to obtain much of the work presented. A great deal of assistance was supplied by various members of Bio and Soft matter (BSMA) and Institute of Condensed Matter and Nanosciences (IMCN) of Université catholique de Louvain, whose results for the analyses are presented throughout. Finally, I would like to express my profound gratitude to all members of FAME master by providing me the opportunity to study in this European program.

Contents

Abbreviations

ATRP atom transfer radical polymerization

CLF Contour Length Fluctuations

CR Constraint Release Rouse

DCM dichloromethane

DSC differential scanning calorimetry

GPC Gel Permeation Chromatography

LAOS Large Amplitude Oscillatory Shear

LVE Linear Viscoelastic

M*n* Number average Molar Mass

M*w* Weight Average Molar Mass

NMR Nuclear Magnetic Resonance

OH hydroxyl group

PBD Polybutadiene

SAOS Small Amplitude Oscillatory Shear

SAXS small angle X-ray scattering

SEC Size Exclusion Chromatography

TMA Time Marching Algorithm

TEM transmission electronic microscopy

THF tetrahydrofuran

TPY terpyridine

tTS Time Temperature Superposition

UPy Ureidopyrimidinone

List of Figures

List of Tables

Thesis objectives:

The aim of this master thesis is to prepare and study the rheological behavior of linear metallo-supramolecular polymers based on hydrogenated terpyridine-terminated polybutadiene polymer chains with different metal salts. In most of studies which has been done so far in field of metallo-supramolecular polymers the effect of aggregation by the metal-ligand associations have been neglected. In selected system composed of a non-polar polymer and a polar end-groups of terpyridine are able to phase separate and aggregation between end-groups can be predicted. Therefore, it is important to find out how this micro-phase separation can affect the relaxation mechanism of the metal-supramolecular polymer. Overall, this thesis has been divided into four main chapters:

In the first part of chapter one, an introduction and overview about type of supramolecular polymers, supramolecular interactions, examples of different supramolecular polymers, their applications, etc. are provided. In the second part of chapter one the theoretical fundamentals of rheology as a tool to investigate polymers and supramolecular polymer chain dynamics will be discussed.

In chapter two experimental techniques and protocol of ^{1}H NMR and rotational rheometry which has been used for characterization of samples during this master thesis is discussed.

In the third chapter, the strategy of functionalization of hydrogenated hydroxyl-terminated polybutadiene (as the initial sample) with terpyridine and preparation of metallo-supramolecular polymers with two metal salts are investigated.

In the last chapter the viscoelastic properties of the linear metallo-supramolecular samples by rheological characterization is obtained meanwhile different parameters effect (i.e. nature of metal ions and their amount, aggregation, etc.) on viscoelastic properties and relaxation of the supramolecular has been studied. Finally, this experimental data has been compared to available tube model.

Chapter1: Introduction and overview

Outline:

In this chapter the main focus is on the theoretical background of the supramolecular polymers and introduction into rheological characterization as an excellent tool for investigation of the mechanical and flow behavior of supramolecular polymers. It provides a clear vision of the type of supramolecular polymers and nature of interaction between chain of polymers that has been used in this master thesis. Furthermore, rheological measurements can reveal that the characteristic behavior of these gels critically depend on few important parameters. Therefore, this approach can offer an unprecedented control over gel properties and interesting stimuli-responsive properties that pave the way towards self-healing materials.

1.1.- INTRODUCTION & OVERVIEW OF SUPRAMOLECULAR POLYMERS

Polymer networks are commonly classified as ‘‘physical’’ or ‘‘chemical’’ networks. While chemical networks consist of chains that are interconnected by permanent covalent bonds, physical networks are obtained by non-covalent interactions between the chains. Typical examples for these non-covalent interactions are helical, glassy, or nanocrystalline chain associations; these crosslinks are strong, and the physical gels obtained from them usually

resemble the behavior of covalently jointed networks. By contrast, weak physical networks are obtained by transient interchain interactions such as hydrophobic or electrostatic associations; these interactions have finite lifetimes and are able to break and reform continuously on experimental timescales. Both physical and chemical networks have their specific pros and cons. A major advantage of chemical crosslinking is that it can be customized and designed to satisfy specific needs. Chemical networks are also strong and can be considered permanent on experimental timescales. This feature is favorable for applications that require tough polymer materials, but it is detrimental if these materials have to be processed or recycled; it also limits the utility of these networks for encapsulation and controlled release applications. By contrast, the reversibility of crosslinking in physical networks greatly facilitates their processing and recycling. However, physical crosslinking is hard to customize and often encountered in specific biopolymers, block copolymers, or polyelectrolyte systems only. To combine the versatility of custom-made, synthetic networks with the reversibility and flexibility of physical crosslinking, a recent development in polymer sciences has introduced a promising new class of materials: supramolecular polymer networks. These networks are formed by customized, highly directed supramolecular bonds such as hydrogen bonds, pi–pi interactions, or metal complexes, which either serve to construct the network chains by associating monomers, or which serve to non-covalently tie, covalently jointed, polymer chains together, as illustrated in Fig.1.1. Highly important directed supramolecular bonds such as hydrogen bonds, ionic interactions and metal complexes which is the topic of this thesis will be investigated more deeply in the next section.[1, 2]

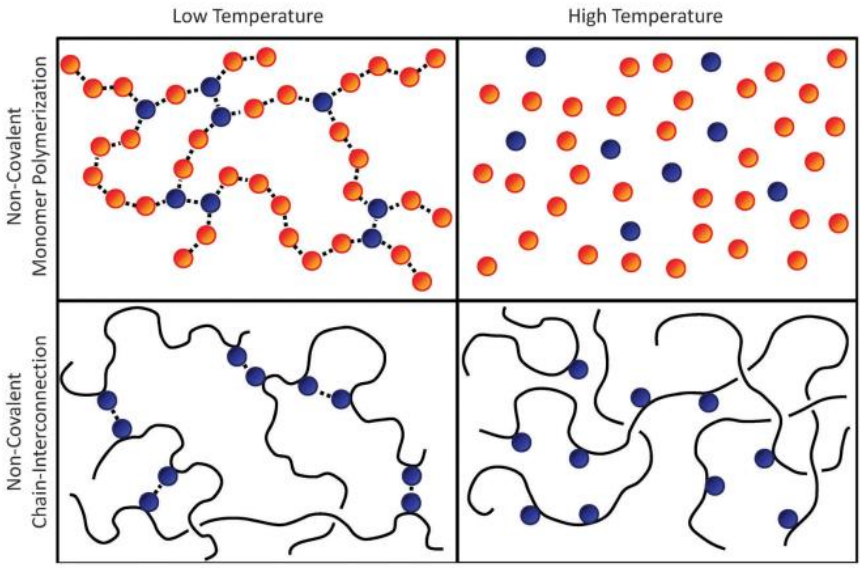

Figure 1.1-Schematic of two different types of supramolecular polymer networks. Upper row: supramolecular polymer chains which consist of noncovalently associating monomers. If some of these monomers have a functionality greater than two, a three-dimensional network forms. Lower row: a network of covalently jointed precursor polymer chains linked by non-covalent association of suitable side groups. Both systems are in a gel state at low temperatures, where supramolecular association is strong, whereas high temperatures break the supramolecular association, thereby favoring a sol state. [1]

The combination of the versatility of synthetic polymer networks with the flexibility of physical crosslinking is the basis for two major advantages of supramolecular polymer networks.

- First, their reversibility of crosslinking facilitates their processing and recycling; it also offers promising means to use supramolecular polymer networks as stimuli-sensitive matrices in sensing, actuation, and controlled release applications.

- Second, supramolecular polymer networks can have self-healing properties. As a result, the advent of supramolecular chemistry in the past decades has provided powerful tools to form "smart" materials based on the ability of molecules to self-assemble. It relies on (macro)-molecules able to adapt their properties and structures in response to external stimuli.[3, 4]

1.1.1-Supramolecular Interactions

Supramolecular polymers can be separated based on different aspects like synthetic strategies, polymer architectures, linear polymers or based on different polymers topologies (branched, star, etc.) which can form a network. In this section, they have been divided based on type of interactions. Although most of the examples which have been presented are based on linear polymer chains which is the goal of this master thesis too.

1.1.1.1- Hydrogen Bonding

The hydrogen bonding is the electrostatic association of two polar atomic groups. One of them is the hydrogen atom (H) being poor in electrons while the second group involves an atom presenting a high electronegativity such as the oxygen (O), nitrogen (N) or fluorine (F) atoms. The high difference of electronegativity between both sites allows the delocalization of the charges. The hydrogen atom is strongly polarized while the high electronegative atom is negatively polarized, which allows the association between the H atoms (positive poles) and the other atoms (O, N or F atoms carrying the negative charge). The weakness of those intermolecular bonds allows the formation of a reversible network and obtain tunable properties. The strength of the bonds, and thus of the network can be tuned in function of the number of the hydrogen links involved in the system. A point that should be noticed is that hydrogen bonds are weaker than covalent and ionic bonds, with an energy typically between 5 and 30 kJ/mol. A single hydrogen bond is not strong enough to fabricate supramolecular polymers. However, both the strength and the directionality can be increased when multiple hydrogen bonds are arrayed to create hydrogen bonding arrays. Multiple-hydrogen-bonding arrays also facilitate the fabrication of block or grafted copolymers. For example, UPy groups can be placed at the end of covalent polymer chains, such as polysiloxanes, poly(ethylene/butylene)s, polyethers, polyesters, and polycarbonates, which could then connect the polymer chains to form associations. Introduction of UPy end groups results in significant changes of the properties of polymers, and the obtained materials combine the mechanical properties of conventional polymers with the low melt viscosity of organic compounds (Figure 1.2). [2, 5]

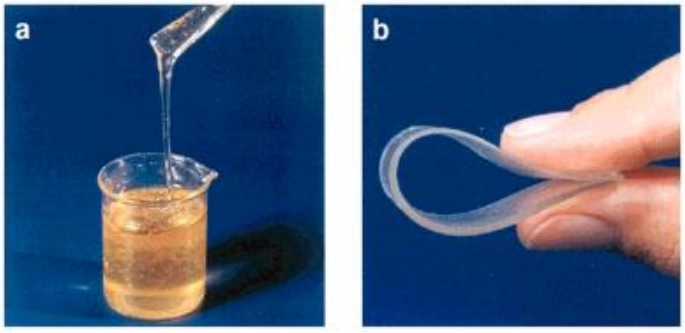

Figure 1.2-Poly(ethylene/butylene) with OH end groups (a) and poly(ethylene/butylene) functionalized with multiple-hydrogenbonded units (b). [5]

Another example of this kind of supramolecular interaction can be created by mixing multitopic molecules which interact by the hydrogen bonding. A multitopic molecule is a molecule which has several functional groups. In the Figure 1.3, there is a supramolecule composed of ditopic and tritopic molecules where the different molecules are linked through hydrogen bonding.

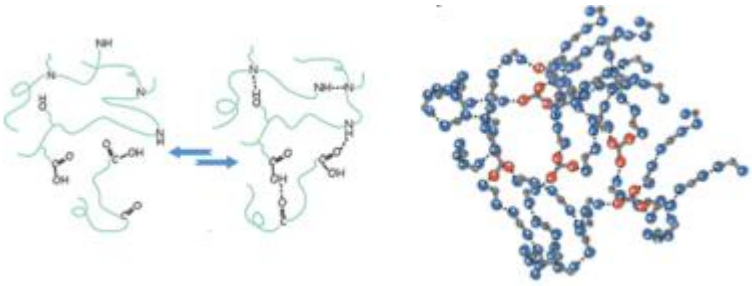

Figure 1.3- Supramolecule composed of ditopic and tritopic molecules.[6]

1.1.1.2- Ionic interaction

Ionic interactions exist widely in the inorganic world, present in minerals and silicate glasses, and in bio macromolecules, where they can serve as salt bridges to stabilize a specific three-dimensional structure. The early history of ionic interactions in polymers dates back to the concepts and uses of polyelectrolytes and ionomers, established in the early 20th century. Ionomers are copolymers where an ionic group (e.g., carboxylic acid) is doped into a polymer at a small amount (usually less than 15%) in order to modify the polymer properties. These materials were commercially available in the 1950s. One of the first examples of an ionomer was a copolymer of butadiene, acrylonitrile, and acrylic acid, where the acrylic acid was cross-linked with zinc salt to afford an elastomer. The resulting Zn-blended copolymers displayed increased tensile properties and adhesion compared to the non-Zn-doped materials. The ionic groups in ionomers tend to form aggregates with Zn due to the attraction between the ion pairs. As such, significant changes in thermal, morphological, and physical properties (e.g., phases, glass transitions, miscibility, rheology, and mechanical properties) can be realized using this approach, where different percentages of the ionic groups are added to the polymer. Polyelectrolytes, which were investigated even earlier, are similar except that they possess a high content of ionic groups and many of them are soluble in aqueous solution. The presence of concentrated ions on the polymer backbone chain leads to a repulsion between charges, which fundamentally alters the chains conformation. Such expanded, rigid, rod-like polymer chains, as opposed to random coil chains in conventional polymers, usually result in a change

in bulk properties, such as higher viscosity. The charged nature of polyelectrolytes also affords properties such as high hydrophilicity and electrical conductivity, enabling a variety of potential applications such as coatings on films and fibers, controlled drug delivery devices, solid-state conducting polymers in Li-ion battery and fuel cells, and so on.[7-9]

Ionomers and polyelectrolytes, with their ionic recognition groups, are widely used to create supramolecular polymeric assemblies. In case of supramolecular polymers, an example can be the supramoleculars containing involving ionic interactions which is based on the ability of the zwitterrion elements to delocalize their charges and exhibit, on a same molecule, a positive and a negative charge (Fig.1.4).

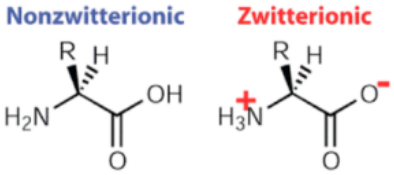

Figure 1.4- Ability of the zwitterion to delocalize its charges.[6]

For example, the amino-acid can easily transfer a hydrogen atom in order to obtain a charged molecule. The apparition of those charges allows the self-assembly of the molecules where the charges of a chain are able to interact with the other charges on another chain. The molecule association by ionic interaction leads to a reversible ionic clustering that manifests itself as a physical reversible cross-linking. This type of network is called ionomers.[8]

Fig1.5- Self-assembly mechanism by ionic interactions allowing the reversible network.[6]

Another example to investigate assemblies that were held together principally by electrostatic interactions is the work of Grinstaff and coworkers who explored alkyl phosphonium chloride compounds as building blocks which the formation of the ionic network is shown in Fig.1.6.[10]

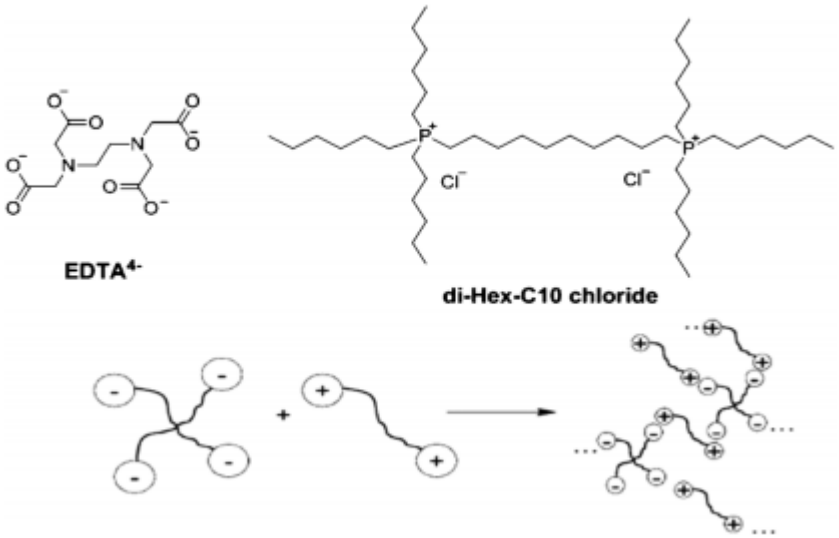

Figure 1.6-The formation of a supramolecular ionic network. Upper panel: chemical structures involved; lower panel: schematic of network formation reported by Grinstaff.[10]

1.1.1.3- Metal-ligand interactions

Metal-containing polymers have attracted great interest due to the combination of the properties of organic polymers and the magnetic, electronic, optical, and catalytic potential of metals. The interaction between a metallic ion and a ligand having a higher electronic density site, is the basis of the transition metal complexes. These are the supramolecular bonds which are studied in this present thesis.[11]

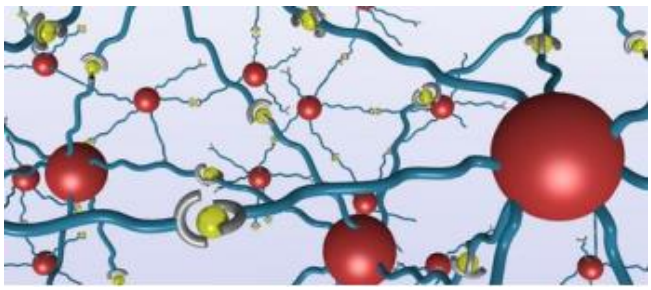

Fig 1.7-Supramolecular polymers whose associations are made by the metallo-ligand associations[12]

The ligands are generally used in order to functionalize polymer chains and thus give them the tunable properties thanks to the formation of a reversible network. These ligands can be added to the chains by both the pre-modification way and the post-modification way. The first way consists of functionalizing the chains during their synthesis while in the second way, the functionalization is a further step to the chain synthesis.

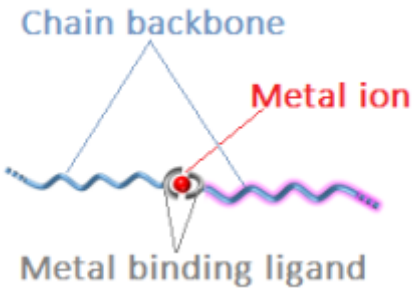

Fig 1.8-Metallo-supramolecular polymers.[12]

When those functionalized molecules are put together with the transition metal ions, they give place to a coordination complexation. The supramolecular polymers are thus composed of three elements; the chain backbone, the ligand and the transition metal ion. The characteristics of the chain backbone are very important and govern the properties of the final supramolecular bulk system. Indeed, the choice of the architecture, molecular weight, number of the involved chains of the different backbone which forms metal-ligand coordination (as some of them may not participate and form dangling chains) can tunes the properties of the system. The choice of the ligand and the metal ion will have an influence on the reversible character of the system. The equivalency of ligand/ions is important because it can determine the possible number of links between the ligands and ions therefore it an important role in the reversibility of the coordination complexes. The properties complexes can be influenced by external factors such as redox or thermo-mechanical stimuli or even the pH variation. [2]

To sum it up, the large range of interaction strength, directionality, and reversibility offered by supramolecular interactions (cf. Table 1.2) allows unprecedented control over the structure and properties of materials, enabling the synthesis of large and complex structures with diverse functions interesting for many different fields.

Interaction	Energy (kJ/mol)	Distance dependence	Stability	Illustration
Ion-ion	40-360	r^{-1}	High	
Ion-dipole	40-200	r^{-2}, r^{-4}	High	
Dipole-dipole	4-150	r^{-3}, r^{-6}	Medium	
Cation-π	4-80	r^{-2}, r^{-4}	Medium	
π-π stacking	4-20	r^{-3}, r^{-6}	Low	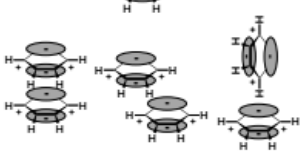
Dispersion	4-20	r^{-6}	Low	
Solvent effects	4-40		High	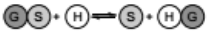

Table1.1- Supramolecular recognition interactions. [16]

1.1.2-Classification of metallo-supramolecular based on polymer structure

Metallo-supramolecular polymers can be classified according to their structure, i.e. poly addition-type supramolecular polymers vs. supramolecular block copolymers. In poly addition-type polymers, each monomer or macro monomer is linked to its neighbor by metal-ligand complexes. This approach requires the use of monomers or macro monomers bearing at least two binding sites that could be further condensed through supramolecular interaction. Some typical examples of building motifs for metallo supramolecular polymers is shown in Table-1.1. [13] In supramolecular block copolymers, metal-ligand linkers are introduced at specific locations in block copolymer architectures. This should lead to systems combining the characteristic features of block copolymers (*e.g.* microphase separation between immiscible constituent blocks) to the ones of supramolecular polymers (*e.g.* reversibility and tunability of the strength of the supramolecular bonds). The supramolecular linkers can be used to either bridge together different homopolymer blocks, or to link together different block copolymers. The first approach leads to diblock copolymers containing a supramolecular linker between the constituent blocks .The second strategy is based on the use of block copolymers containing a linking group specifically introduced at a defined locus of the copolymer chain (generally at the chain end or the block junction). These linking groups can further promote the formation of a supramolecular structure, e.g., star-like structures, by bridging two or more copolymer chains together. In this thesis, the focus of study would be on the use of metallo-supramolecular interactions.[14, 15, 17]

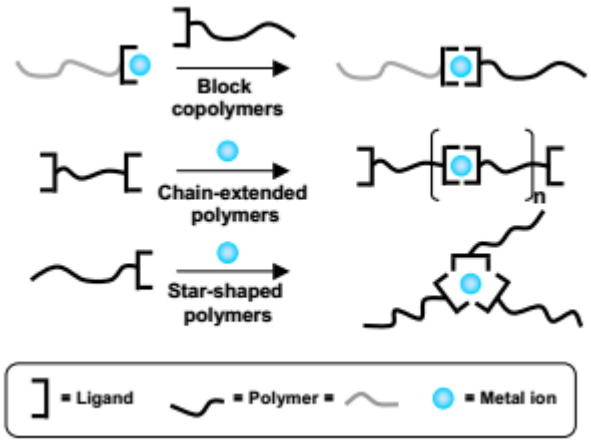

Figure 1.9-Metal ion induced self-assembly of polymers with metal coordinating end-groups resulting in block copolymers, chain-extended polymers or star-shaped polymers.[16]

Ligand Type	Metal	K_a	Solvent/Counterion
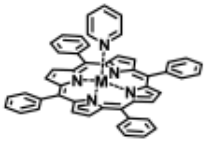	Zn^{2+} Co^{2+}	$4.1 \times 10^3\ M^{-1}$ $1.0 \times 10^6\ M^{-1}$	$CHCl_3$/— Pyridine/OAc^-
	Zn^{2+}	$\sim 10^{13}\ M^{-3}$	Aqueous KNO_3
	Zn^{2+}	$1 \times 10^{17}\ M^{-3}$	Aqueous KNO_3
	Zn^{2+} Fe^{2+}	$2 \times 10^{14}\ M^{-2}$ $\sim 10^{21}\ M^{-2}$	CH_3CN/ClO_4^-/TBAPF Water

Table1.2-Typical examples of building motifs for metallo-supramolecular polymers.[2]

1.1.3-Telechelic and side-chain polymers

As it mentioned in previous section the supramolecular materials are generally composed of polymer chains or oligomers functionalized by strongly interacting moieties. These moieties, sometimes called “stickers”. Therefore, it is also possible to classify those supramolecular materials into two categories according to the location of the stickers on the chains. Some systems present stickers placed laterally to the chain backbones. Other systems are based on the functionalization of their ends and are called the telechelic polymers. Some of the polymers that have been investigated based on different location of stickers are presented in Figure 1.10 It is this second system that interests us and will be investigated in this work.[2]

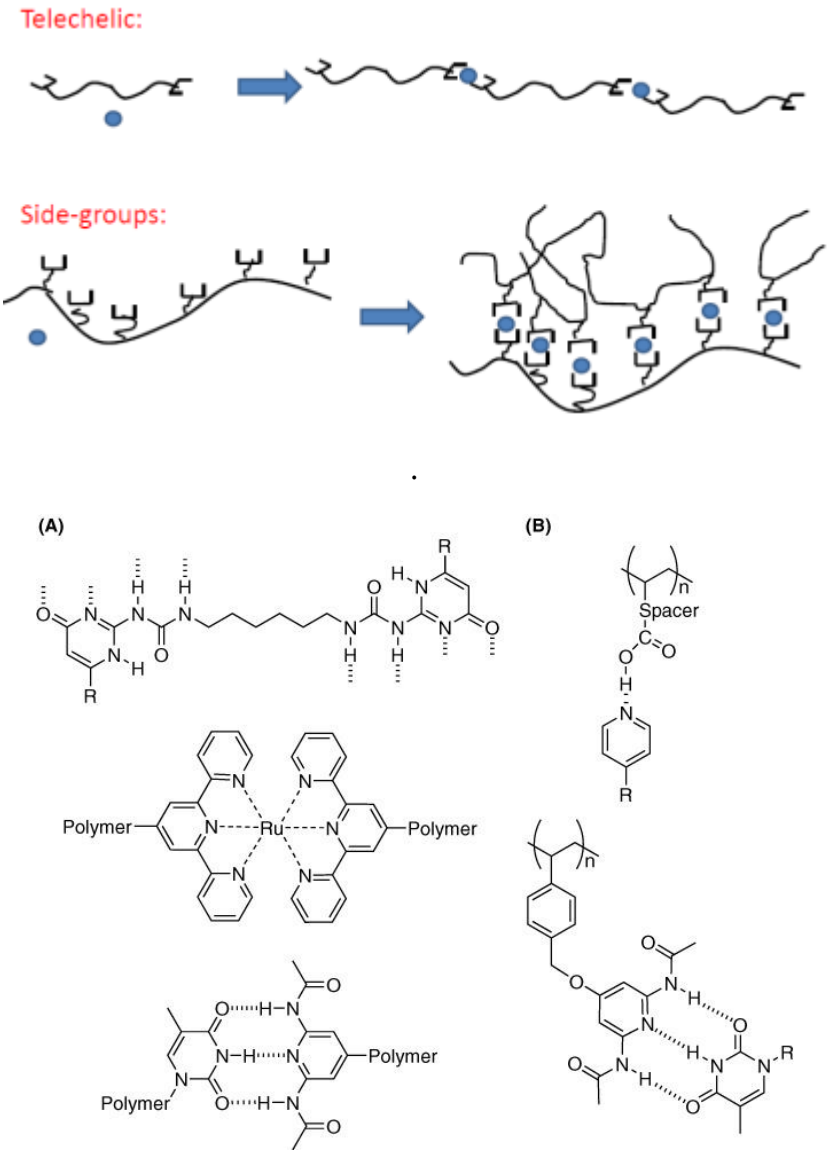

Figure 1.10- Different types of metallo- supramolecular polymers (above)- Examples of supramolecular polymers from the literature(bottom): (A) main-chain supramolecular polymers and (B) side-chain supramolecular polymers. [2]

1.2- RHEOLOGY: MAIN CHARACTERISTICS OF VISCOELASTIC MATERIALS

1.2.1- Introduction

Rheological properties of the melt are very sensitive to the molecular structure of a polymer. Rheological properties describe how stress develops in a sample undergoing a prescribed

deformation. They also describe the deformation that is caused by a prescribed stress. The most fundamental rheological experiment for a viscoelastic material is a step-strain test, and for melts this nearly always means a step shear strain.[18]

Rheology is a perfect tool to characterize visco-elastic which can take both an elastic behavior in a short lapse of time and a viscous behavior in longer periods of time. To better visualize this phenomenon, one can take as example the "silly putty", a commercially available toy based on a silicone polymer. When the silicone polymer is thrown onto a wall, i.e. the polymer is undergoing a fast deformation, it bounces and goes back quickly to its initial shape thanks to its elasticity. On the contrary, if it is left at rest on a table, then it is going to flow. Once again, time plays a crucial part in the explanation of that behavior. Rheology is a really interesting tool in polymer science and engineering. It makes it possible to establish a relationship between the behavior and the structure of materials. Indeed, the rheological properties are sensitive to some structures present in the material. The information given by this study are valuable for the processes of polymers in the molten state, given that those rheological properties govern the flow behavior. It also allows the scientist to anticipate undesirable behaviors during the manufacture of some products such as shark skin or other flow instabilities. Therefore, it is necessary to acquire a strong and solid knowledge on the behavior of these materials before using them in large scale.[19, 20]

1.2.2- The Maxwell model

Some models allow us to describe the different behaviors adopted by viscoelastic fluids. The most known model is the Maxwell model, in which the fluids are represented by an assembly of dashpots and springs, which characterize the different aspects of viscoelastic behavior. The dashpot presents the ability to dissipate the energy and is used to describe the viscous behavior of the liquids. Its force is proportional to the rate of displacement, while the spring force is proportional to the displacement (Fig.1.11). The spring is used to characterize the elastic behavior of solids. The strain undergone by these elements are;

$\tau_{spring} = G\gamma_{spring}$ (1.1)

$\tau_{dashpot} = \eta\, \dot{\gamma}_{dashpot}$ (1.2)

Where,

- τ_{spring} and $\tau_{dashpot}$ are respectively the spring and dashpot shear stress, in (Pa)
- G is the constant shear modulus expressing the resistance of the solid to deformation, in (Pa)
- γ_{spring} is the spring shear strain
- η is the viscosity, in (Pa.s)
- $\dot{\gamma}$ dashpot is the shear rate, in (s^{-1})

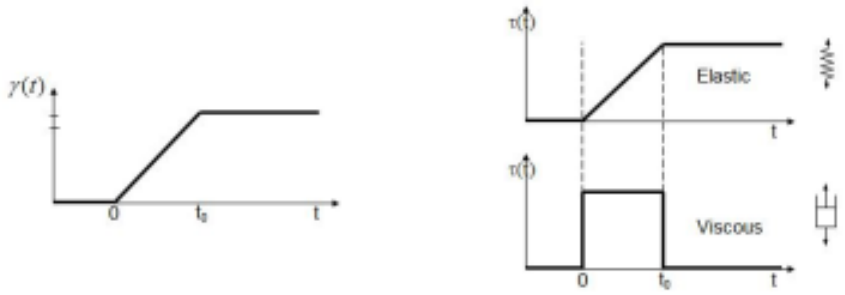

Figure 1-11-Response of the basic element submitted to a defined deformation.[20]

However, most fluids have a more complex behavior and cannot be described by these two simplistic models, which is also not sufficient to characterize simpler materials such as water in every context. Though liquid water is a Newtonian fluid, it can partly behave like a solid in certain situations. For example, a diver who dives at 50 meters deep. If the diver fails to stay in a vertical position and is rather in a horizontal position, in contact with water the constraint is so strong it could cause some aftereffects. Indeed, water does not dissipate all the energy immediately because it partially reacts as a solid which determines rate of deformation plays an important role in dissipation. To explain those viscoelastic behaviors, more complex models are developed with an association of dashpots and springs in parallel and/or serial. The two best known rheological models are the generalized Maxwell model and the Kelvin-Voigt models. The Maxwell element models the viscoelastic behavior of the material thanks to the assembly of a spring and a dashpot connected in series, as shown in Fig. 1-12.[20]

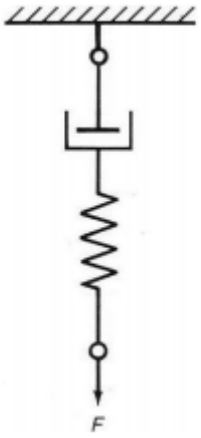

Figure 1.12- Maxwell element. Viscoelasticity of the material is represented by a spring and a dashpot in series. The spring is characterized by its modulus G_i and the dashpot by its viscosity η_i. The stress of each element is the same, while the deformation is different.[20]

This basic empirical model is particularly useful to characterize the behavior of materials called viscoelastic liquids. Those materials instantaneously react like a solid and so the model needs the presence of a spring. However, the material loses its memory afterwards and flows like a liquid. This second aspect of their behavior is characterized by a dashpot. The dashpot cannot instantaneously get out of shape because it needs time to adapt to the deformation. The spring which gives solid behavior to the material is being characterized by its modulus G_i,(which here only one spring exist and therefore i=1). It is characterized by its modulus G_i, while the viscous response is described by the dashpot and its viscosity η_i. In this model, each component of Maxwell element deforms independently of the others and therefore each component has its own constitutive equation, such as given above. The total strain corresponds to the sum of the strains of each component. The stress of each

component is the same and is equal to the total stress. When a deformation is applied, it is first applied to the spring and is slowly transferred to, the dashpot through time. The Maxwell element can be described by its constitutive equation;

$$\tau + \frac{\eta}{G}\dot{\tau} = \eta\,\dot{\gamma} \quad (1.1)$$

With $\eta/G = \lambda$, the relaxation time.

On the other hand, the Kelvin-Voigt model is used to characterize viscoelastic materials with a solid-like response by the connection of a spring and a dashpot in parallel. Those materials do not lose their memory and once the constraint is removed, the materials come back to their initial position thanks to their elastic behavior. That kind of material does not instantaneously react because, as mentioned before, the dashpot needs an adaptation time to deform itself. Therefore, the presence of dashpot in a parallel connection drags a delay effect on the deformation which is the same for each component put into parallel. In contrast to the Maxwell model, the paralleling of the components implies that the strain is the same for each component and the total stress is the addition of the stress of each component.

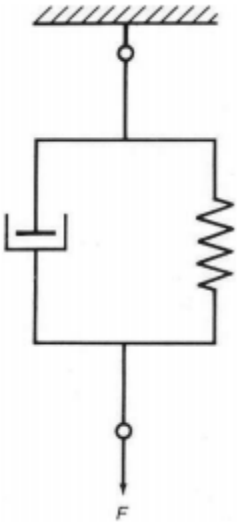

Figure 1.13-Element of Kelvin-Voigt model. The viscoelasticity of the material is described by a spring and a dashpot in parallel. The spring is characterized by its modulus Gi and the dashpot by its viscosity ηi. The deformation of each element is the same while the stress is different.[20]

At long time the deformation is fully dominated by the spring and the dashpot does not play any part. Its constitutive equation is given by;

$$\tau = G\gamma + \eta\,\dot{\gamma} \quad (1.2)$$

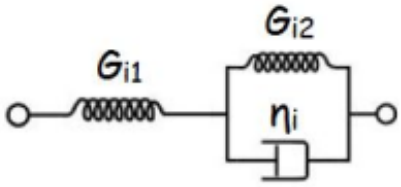

Figure1.14 - Model describing the viscoelastic solid. It is a combination of the Maxwell and Kelvin-Voigt models. [20]

Those basic empirical models can be modeled graphically showing the stresses undergone by viscoelastic solids and viscoelastic liquids for a given deformation as follows;

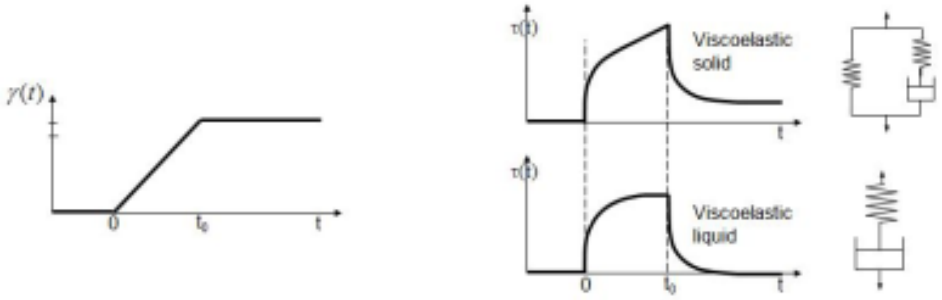

Figure1.15- Graphical representation of the stresses undergone by viscoelastic solids and viscoelastic liquids for a given deformation.[20]

Figure 1.16 shows a typical stress relaxation curve for a highly entangled, linear polymer sample in which all the molecules have the same molecular weight, i.e., a monodisperse sample. In this plot using linear scales, important phenomena that occur at very short times and at long times, where the stress is very small, cannot be seen. The same information is replotted in Fig. 1.17 using logarithmic scales for both axes. This has the effect of greatly expanding the behavior at very short times and very low stresses that were not visible using linear scales. The various features of this curve will be discussed in detail in sections 1.3.[20]

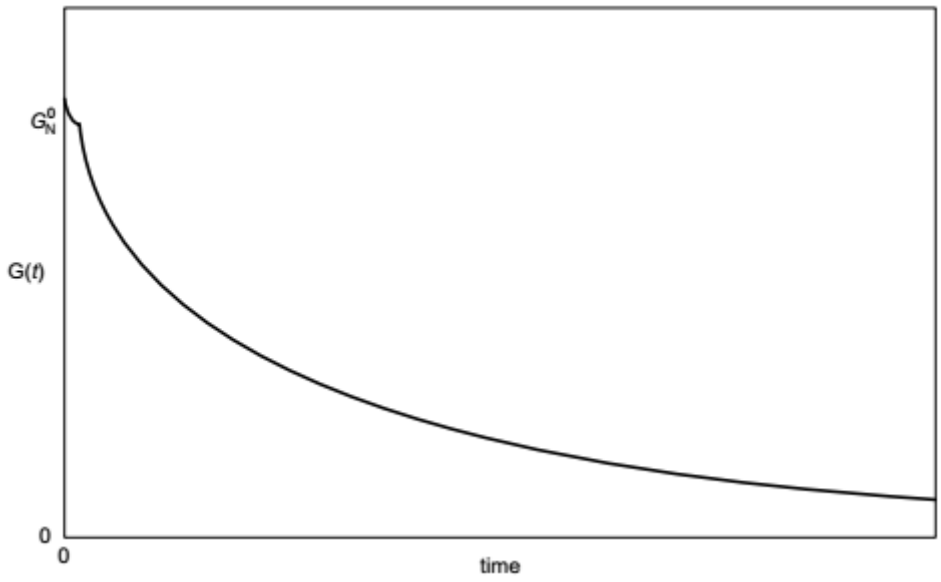

Figure 1.16- Typical stress relaxation curve for a molten polymer using linear scales for both axes. The pattern of the very fast relaxation at short times is not visible using a time scale that is suitable to show the final, long-term stage of the relaxation.[20]

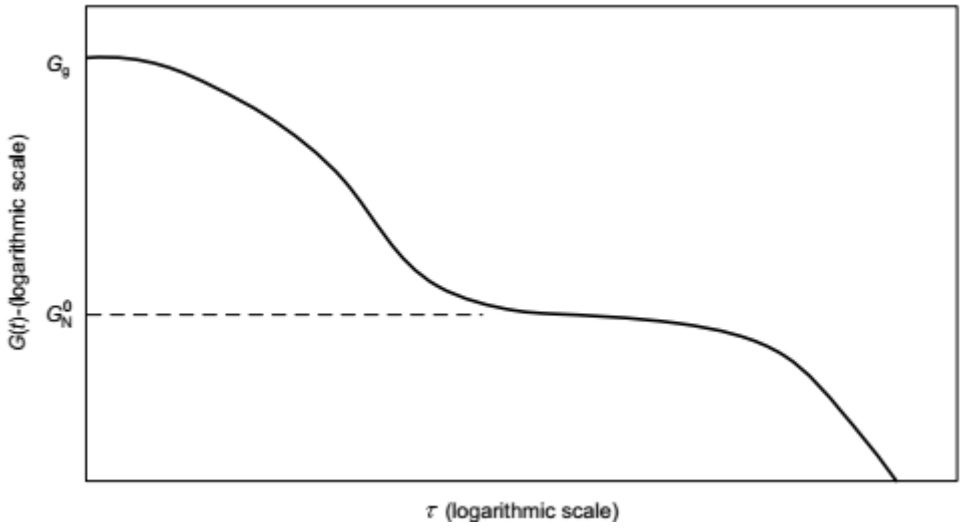

Figure 1.17- Stress relaxation curve for a linear, entangled, monodisperse polymer sample, where logarithmic scales are used for both axes. In this representation, distinct mechanisms of relaxation are apparent in the glassy, transition, plateau and terminal time zones. At least two Maxwell elements is needed in order to obtain this plot.[20]

1.2.3-Dumbell models and corresponding Rouse time

The theories of molecular motion are needed for a full understanding of polymer rheology. However, the size and complexity of the polymer molecules prohibit the use of truly realistic polymer models. Therefore, the molecular theories of polymers have been concentrated in simple models that only include the most basic characteristics of polymer molecules. Models developed to characterize the polymers are in a mesoscopic scale. It provides prediction of both static and dynamic properties. The mesoscopic scale states between the fundamental atomic and the macromolecule levels. In that scale, coarse-grained models would be used for

molecular modelling. It is a computational model that imitates the behavior of complex systems through a simplified representation. The model does not consider the chain in its entirety but only represents its simpler sub-components. Among the most frequently used models are representations consisting of a series of Hookean springs joined by beads like in Figure 1.18. In such a picture, the beads represent the friction of the polymer chain, while the spring takes into account that a polymer chain as an entropic object.

The real chain can also be approximated by a unique spring joined by two beads (one dumbbell only). This is described by vector $\vec{\boldsymbol{R}}$ that specifies the length and the orientation of the dumbbell representing the entire chain while r will be used in other cases (chain represented by several dumbbell).In both cases, each dumbbell has a Gaussian character. This model is called the Dumbbell model and is the simplest model (in case of single dumbbells model) to describe the polymer chains and their viscoelastic behavior but it is a reasonable model of the polymer chain dynamics. This model takes the internal structure of the material into account and considers a molecular approach allowing us to understand the physical origin of viscosity and develop molecular rheology.

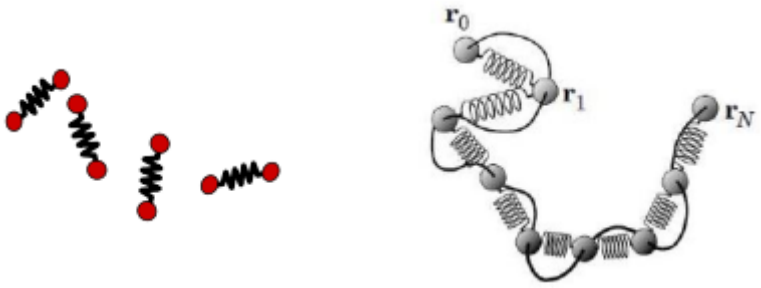

Figure 1.18- Dumbbell model where chains are represented by a single (left) and series of springs connected by beads (right).[12]

The springs characterize the elastic force due to the Brownian motion of the real chain and represent the internal degree of freedom of a polymer molecule. The entropic elastic force generated in a spring (here characterizing the entire chain) is;

$$F_{entropic} = k_{sp} = \frac{3kBT}{(Nb^2)R} \quad (1.19)$$

Where

• k_{sp} is the entropic elastic force generating in a spring

• k_B est the Boltzmann constant

• T is the temperature

• N is the number of Khun segments in the chain

• b is the length of a Khun segment

• R is the end to end distance

In case of series of springs connected by beads, however, to obtain a more accurate characterization, we consider that each Khun segment represents one chain dumbbell. The Khun segments have three characteristics;

• The length of each khun segment is identical and depends of the polymers

• The Khun segments are independent from one another.

• The Khun segments have a random orientation with follows the primitive path

The beads act as the centre of the anisotropic hydrodynamic and/or systematic forces represent the friction of chains with their environment (linear chains or solvent). Each bead has its own friction ζ_0 that corresponds to the friction coefficient of a Khun segment. The friction force is opposed to the motion of the chain.

$$F_{friction} = n\zeta_0 \left(\frac{dR}{dt}\right) \quad (1.20)$$

The chains being entropic objects, they take a configuration by Brownian motion in which the system tends to maximize its entropy. Therefore, their entropic nature tends to bring back each molecule to its stable coil shape and to minimize its end to end distance R.

At rest, the dumbbells are randomly oriented and follow the general path of the chain in a non-stretched state. Under flow, the dumbbells are stretched in the flow direction by viscous or convection (friction generated by the solvent) forces. When the shear rate is increasing, the dumbbells are more stretched and orient in the flow direction. The resulting tension in the spring makes them want to return to their non-stretched state

After the flow, the chains progressively take their equilibrium length again through Brownian forces. The chain is completely relaxed when one of its ends has diffused to the other one.

At initial time $R(0) \neq 0$, we assume an equilibrium situation where the following equation is verified.

$$F_{entropic} = F_{friction} \quad (1.21)$$

This equality allows to get the relaxation time needed to the chains to come back to their non-stretched state.

$$\tau_R = \frac{\zeta 0 n^2 b^2}{3kBT} \quad (1.22)$$

Where τ_R is the characteristic time required by the chain to come back to its equilibrium. This relaxation time varies proportionally with the square of the length of the sub-chain and is valid only no entanglements exist.

1.2.4-Complex fluids

The viscoelastic can be classified in different categories according to their behavior when submitted to a constraint. In other words, they are classified according to the relationship between their shear stress and their shear strain rate. Four different behaviors can be observed, as summarized in Figure 1.19.

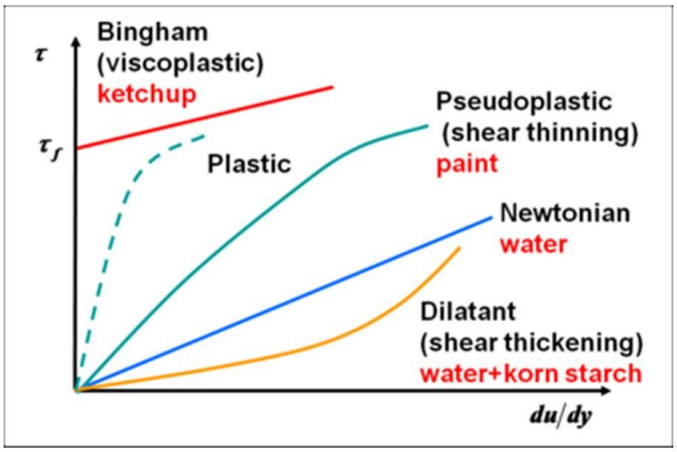

Figure 1.19- type of fluids.[12]

• The Bingham fluid is a fluid that does not flow at all until the shear stress exceeds a certain critical value called yield stress. In this fluid, once the system begins to flow, its behaviors is similar to the one of Newtonian. There is an internal structure within this type of fluid which breaks down before the fluid can start to flow. It adopts an elastic solid behavior under low constraints but acts as a viscous fluid at higher constraints. For example, toothpaste and ketchup have this particular behavior.

• The shear thickening fluid is a fluid in which the viscosity increases with the strain rate. The shear stress increases much more rapidly than the shear rate in that kind of fluid, which can also be called "dilatant fluid".

• The shear thinning or pseudo plastic fluid becomes less viscous as the shear stress increases. The behavior of this fluid is opposed to that of the shear thickening fluid. It represents most of the polymer melts behavior.[19]

1.2.5-Importance of time scale

As mentioned before, the time scale on which the experiment is observed has a crucial importance on the behavior of fluids. It governs the dynamic behavior of those fluids. Indeed, the same substance can behave like a solid or a liquid, according to the observation time or the deformation frequency. Hence the importance of a dimensionless number to characterize the materials. This dimensionless number is called the "Deborah number" and puts in relation the relaxation time with the observation time.

$De = \tau_{rel}/\tau_{exp}$ (1.4)

Where

• τ_{rel} is the characteristic relaxation time of the material. It is the time necessary for the material to relax and free itself from its constraints. It is in (s).
• τ_{exp} is the characteristic time of the experiment. It is the time during which the constraints are applied. It is also expressed in (s).

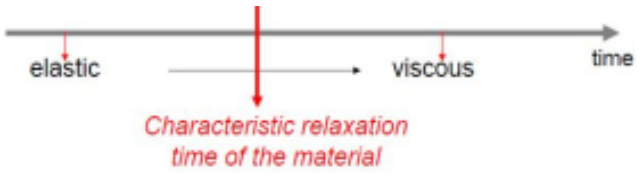

Figure 1.20 -Importance of observation time on the behavior of fluids. If the experimental time is quite short, the fluids will tend to react as an elastic solid. On the other hand if this experimental time is much longer, then fluids behave like viscous liquids.[6]

The Deborah number allows to characterize the behavior of materials according to the deformation/experimental time and defines the rate at which the elastic energy is stored or released.

• De « 1 : viscous behavior
• De = 1 : viscoelastic behavior
• De » 1 : elastic behavior

The Deborah number represents the fact that a solid substance can flow if it is observed on a long enough period of time. That is why that dimensionless number was called after the name of prophetess Deborah who said "The mountains flowed before the Lord" in a song. In the same way, a viscous liquid can adopt an elastic behavior if observed during a short lapse of time. A nice example has been explained in the picture. The fluid in the pool is a non-Newtonian fluid made of cornstarch and water. The cornstarch has the appearance of a powder and once diluted in water the mixture develops interesting properties. Quickly loaded, it reacts with the behavior of a solid and slowly loaded, it adopts the behavior of a liquid.

Figure 1.21- Non-Newtonian fluid illustrating the dynamic behavior concept and the Deborah relationship. This cornstarch pool has an interesting behavior, depending on the experimental time. Quickly loaded, it reacts as a solid and slowly loaded, it behaves as a liquid.[6]

Running in the swimming pool, the fluid behaves as an elastic material in accordance with the Deborah relationship. Indeed, the time during which the constraint is applied is shorter than the characteristic relaxation time of fluids. But if the person stops moving in the pool, the experimental time is longer, and the fluid behaves as a viscous fluid. The person will therefore immediately sink. A good knowledge of what the Deborah number is necessary to understand the time-temperature superposition principle.[20]

1.2.6 Time temperature superposition

Time-temperature superposition is of interest in two contexts. For the experimentalist it is the basis of a technique for substantially increasing the range of times or frequencies over which linear behavior can be determined. And for the polymer scientist, it may provide additional information about molecular structure. It was Ferry who first provided a scientific basis for this procedure. The essence of the concept is that if all the relaxation phenomena involved in G(t) have the same temperature dependency, then changing the temperature of a measurement will have the same effect on the data as increasing the time of the experiment i.e, shifting the data horizontally on the log(time) or log(frequency) axis.[20]

This principle is particularly useful for materials which relax on a long time scale under a certain temperature. The solicitation frequency (at which the constraints are applied) influence the viscoelasticity properties of the polymers and is inversely proportional to the temperature effects. The effects of frequency and temperature are therefore dependent. Actually, at a high temperature, the polymeric chains have a higher mobility and therefore the relaxation time decreases with the temperature. In other words this time-temperature superposition principle means that a polymer at a low temperature with a long experimental or relaxation time behaves like the same polymer at high temperature and short experimental or relaxation time if the Deborah number remains the same. The use of this principle allows us to draw the master curve showing the effects of frequency on a very wide range of materials, on the basis of experimental data.

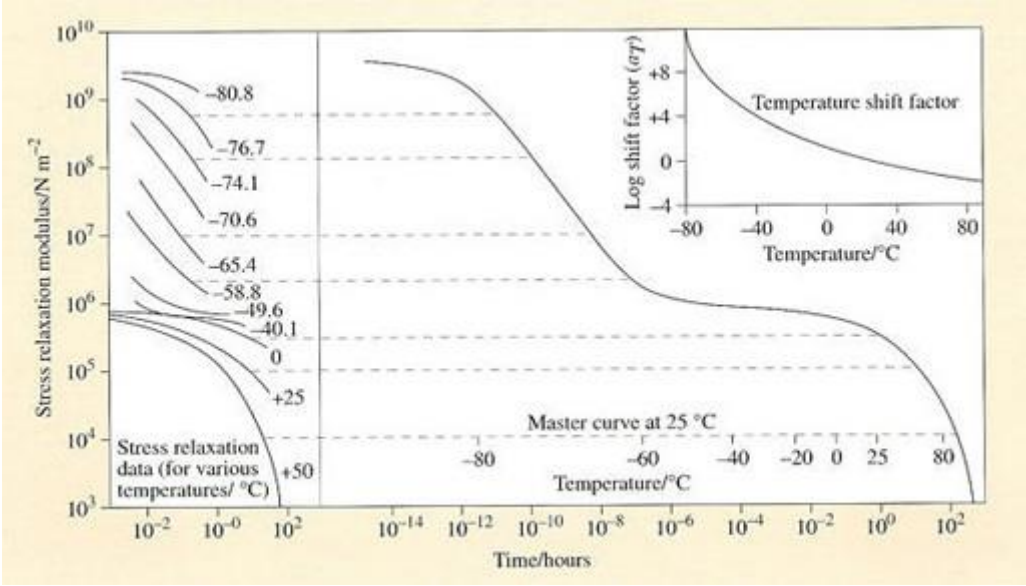

Figure1.22- Construction of the viscoelastic master curve for PIB at 25 °C reference temperature by shifting stress relaxation curves obtained at different temperatures horizontally along the time axis. The shift factor, aT varies with temperature as shown in the inset at upper right.[21]

In fact, after determining G(t) isothermal curves for different temperature, the TTS principle is used with a horizontal shift. The change in temperature from a temperature T to the reference temperature T_0 is translatedby the relationship below;

$$\tau_i(T) = a_T . \tau_i(T_0) \quad (1.5)$$

Where
•$\tau_i(T)$ is the relaxation time of the material at temperature T, (s)
•$\tau_i(T_0)$ is the relaxation time for the material at the reference temperature, (s)
•a_T is the horizontal shift factor for the rheological data at temperature T to draw the master curve at the reference temperature T_0,

The horizontal shift factors allow to shift the experimental data taken at different temperature *T*
along the time axis so that they will equal the data taken at the reference temperature *T*0. Some empiric expressions have been developed to describe the dependence of the shift factors on the temperature. The two most used laws are the Arrhenius and Williams-Landel-Ferry (WLF) laws.
They are respectively given by;

$$a(T) = \exp[\frac{Ea}{R\left(\frac{1}{T}-\frac{1}{T0}\right)}] \quad (1.6)$$

And

$$a(T) = [\frac{-C1(T-T0)}{C2+(T-T0)}] \quad (1.7)$$

Where

• Ea is the activation energy for flow, (J. mol^{-1})

• R is the constant of perfect gas, (8,314 J K^{-1} mol^{-1})
• T is a temperature T, (K)
• T_0 is the reference temperature, (K)
• C_1 and C_2 are empirical constants which depend on the nature of the polymer melt and not on the structure

The WLF equation can be derived from the empirical Doolittle equation that relates viscosity to fractional free volume together with assumption that the free volume is linearly related to the temperature.[20]

Equation 1.6 is generally used when the temperature is at least one hundred degrees above the glass transition temperature, while the WLF Eq.1.7 usually provides a better fit of data at temperatures closer to T_g. Both of the above equations are basically empirical, and one should not expect them to be strictly obeyed by any material.[19, 22]

1.3-RELAXATION FUNCTION AND MODULI

1.3.1-Relaxation modulus

The polymer viscoelastic response leads to relaxation modulus curves G(t). Those curves have an important source of information about molecular structure.

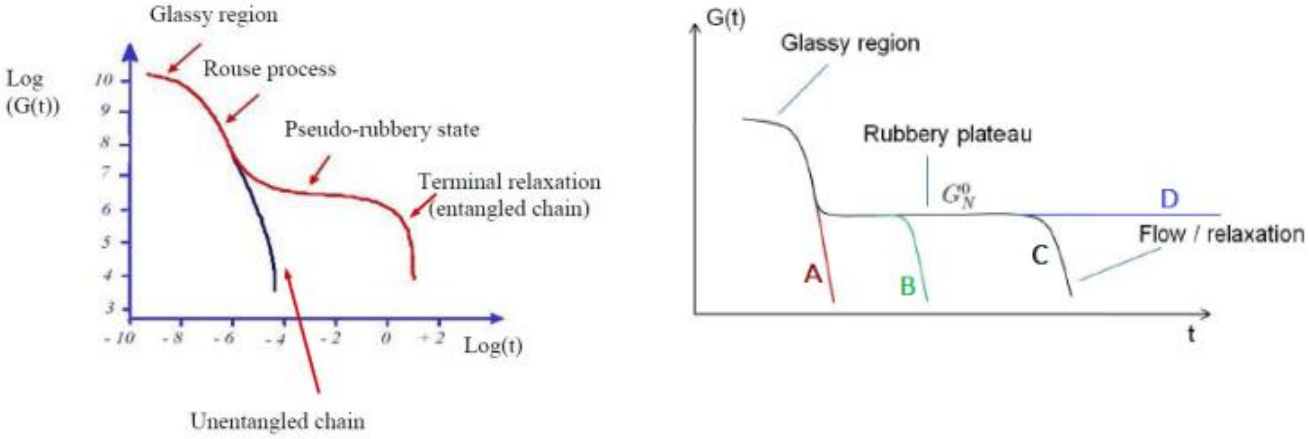

Figure 1.23-Curves of relaxation modulus. Those curves give information about the molecular structure. The graph on the left shows the different regions of polymer response. The second graph represents the behavior of polymers with different molecular structures.[12]

As shown in the graph on the left and more specifically on the red curve, there are three zones corresponding to the relaxation of different characteristics of the molecular structure.

• The Glassy region;

• The transition zone between Glassy and rubbery plateau;

• The Plateau modulus;

• The Terminal relaxation or flow region;

The glassy region describes the polymer in a frozen state with a reduced chain mobility. It represents the behavior of a polymer at very low temperature or during an extremely short experimental time. In this region, the chains cannot diffuse by Brownian motion. The only relaxation mechanism is the stretching and the bending of bonds. The "glassy" modulus is relatively similar to the polymer at glassy state, around 10^9 Pa. Indeed, the molar mass and structure of the polymers have no significant influence neither on the length and angle of chains nor on the disentanglements which do not have time to relax. Here, the polymer has an elastic behavior and the response is characterized by a high Deborah number. This rigid state gives a very high relaxation modulus compared to the rest of the curve. Then, the chains quit slowly their frozen state and diffuse to maximize the system entropy. The chain mobility increases and consequently, their relaxation modulus decreases until reaches the reach the plateau modulus, G^0_N. By entering in the transition zone between Glassy and rubbery plateau During this transition, the relaxation of the chain is well described by the the Rouse process which is explained in the next sections.[19]

At a long timer (or at an intermediate temperature) a plateau called "plateau modulus" appears. It comes from the entangled state of the chains. As short time, these entanglements between chains act as a "physical cross-links", and prevent the full mobility of the chains which hinders the polymer flow. This, explains the appearance of a rubbery plateau transition into a rubbery

plateau and why the polymer cannot flow immediately after the glass transition. The length of the plateau is strongly influenced by the molar mass and the architecture of the macromolecules. An increase in the molar mass delays the flow of polymers which is represented by a longer plateau Indeed, the longer the chains are, the more time is needed to disentangle them and allow them to flow.

The plateau modulus, represents the rigidity of the chains, and is directly related to the entanglements density in a polymer melt. Contrary to the relaxation time, it does not depend on the chain architecture or molar mass can be calculated by;

$$G^0{}_N = \frac{\rho RT}{Me} \quad (1.8)$$

Where

- ρ is the density of polymer, in (kg/m^3)
- R is the gas constant, in ($J.K^{-1}.mol^{-1}$)
- T is the temperature, in (K)
- M*e* is the average molecular weight between two entanglements, in (kg/mol)

M_e can be considered as the longest sub chain which can be relaxed by Rouse relaxation. Therefore, if the molecular weight of the chain is below the critical value for entanglement, M_e, there are no entanglements and thus no plateau modulus. For entangled chains, after a sufficiently long time allowing the disentanglement of the chains, the polymer begins to flow. The chains are stress-less and the polymer tends to behave like a viscous liquid. At high temperatures, the same effect is obtained (time-temperature superposition). This phenomenon is characterized by a low Deborah number and a relaxation modulus drop. However, this terminal relaxation does not exist for all polymers as for example, permanent chemical network. Indeed, in this in case, the cross-linked polymers cannot disentangle and thus cannot flow. In case of a supramolecular system with a reversible network, a longer period of time is needed because the reversible association must be broken before the two sub chains can be disentangled. Figure 1.21 on the right shows the response of different polymers. A first distinction can be made between two important types of polymeric systems.

- The thermoset polymers
- The thermoplastic polymers[20]

The thermoset polymers are made of polymers that are cross-linked to form an irreversible chemical link. It eliminates the risk of the product re-melting when some heat is applied. A well-known example of a thermoset polymer is the rubber which is vulcanized. Their permanent network prevents flowing at long times and is characterized by an infinite plateau modulus. This category of polymers is represented by curve D on the right graph in Figure 1.23. The thermoplastic polymers are characterized by a reversible physical network and they soften when heated. The reversible character of those systems allow them to break their bonds and disentangle, making it possible for the polymers to flow at long times. These responses are characterized by curves A, B and C in figure 1.23 on the right. Curve A describes the behavior of polymers with a molecular weight below *M*e which have no entanglement. Those polymers flow immediately after the glass transition. The difference between curves B and C is the molecular weight. If the chains are short, there will be few entanglements and this results in a short plateau modulus. *M*e being the average molecular weight between two entanglements, it

is easy to understand that if the molecular weight increases, the number of entanglements along the chains increases and therefore a longer time is needed before the chains are able to flow. The response of the polymers in the plateau modulus and during the terminal relaxation can be explained by the tube model and the relaxation by reptation, fluctuation and constraint release which will be discussed later.[20]

To Sum it up, two characteristics of plateau modulus are important to study; the height of the plateau modulus, G^0_N, and its length. The length of the plateau gives information on the molecular weight of the polymer, while the G^0_N depends on the architecture of the chains.;[23]

In the case of more complex systems, two (or more) distinctive plateaus can be observed. This is due to the relaxation of chains having different molecular weights or different architectures.

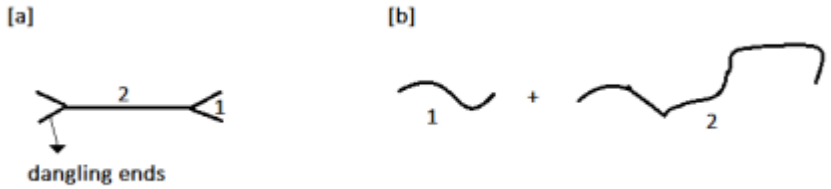

Figure 1.24 -Systems presenting a second plateau modulus.[20]

The molecular weight between two entanglements, M_e has a crucial importance in the rheological study. As indicated above, it is closely related to the plateau modulus. "Another parameter to be taken into consideration to determinate the plateau modulus is the concentration of the system. But here again, this parameter is related to M_e.[19, 22]

A relationship between G^0_N and c can be found;

$G^0_N \propto c^2$

The polymer concentration also influences the terminal relaxation time of the melts. This relaxation can be modeled by the enhanced contour length fluctuation process (CR-CLF) which is explained in next sections.[20]

1.3.2 Storage and loss moduli

In this section the viscoelastic properties through the storage and loss moduli curves, notified respectively by G' and G" would be investigated. Those data come from the dynamic measurement and more specially by Small Amplitude Oscillatory Shear (SAOS).

To define the G' and G" expression, we consider a small amplitude oscillation shear strain having the following form;

$$\gamma_{xy}(t) = \gamma_0 \sin(\omega t) \quad (1.9)$$

The system answers to this oscillatory strain by a stress whose expression is given by;

$$\tau_{xy}(t) = \tau_0 \sin(\omega t + \delta) = \gamma_o \left[\frac{\tau 0}{\gamma 0} \sin(\omega t)\cos(\delta(\omega)) + \frac{\tau 0}{\gamma 0} \sin(\delta(\omega))\cos(\omega t) \right] \quad (1.10)$$

Where

• γ_0 and τ_0 are respectively the deformation and response amplitudes

• δ is the phase shift compared to the deformation. It is defined as; $0 < \delta < \pi/2$.

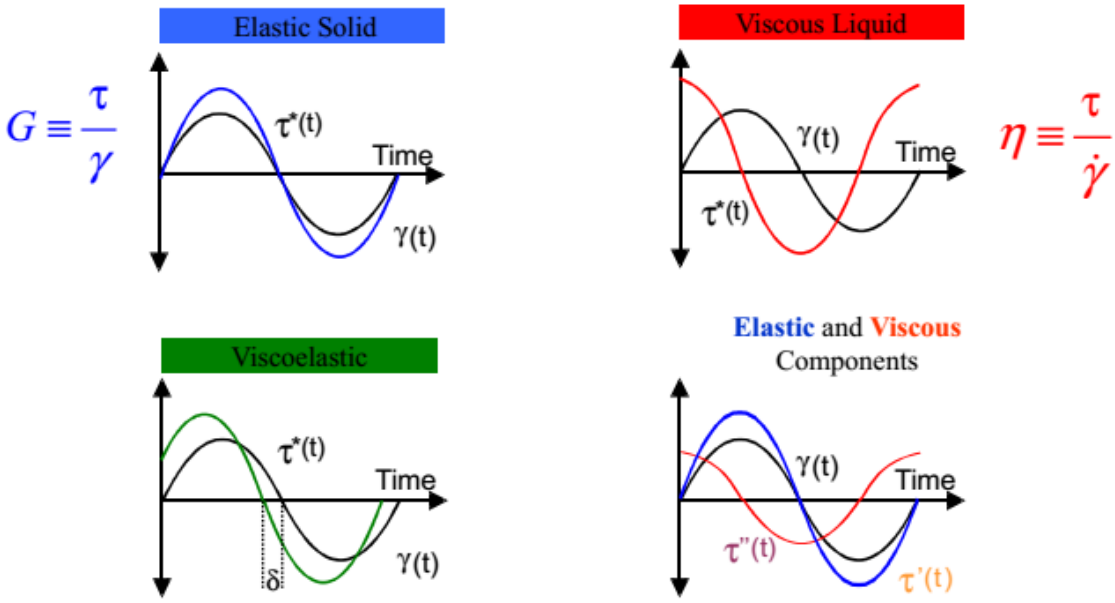

Figure 1.25 -Graphic illustration of the elastic, viscous and viscoelastic responses.[12]

According to expression above, the response of the elastic solids is proportional to the applied deformation. According to Equation 1.10, the viscous response is proportion to shear rate. This suggests that the Newtonian fluids react with a shift factor, δ of $\pi/2$, compared to its oscillatory deformation. On the other hand, as illustrated in Fig.1.25, the shift factor equals zero for the elastic response. This scaling is easily found from the equation here above:

$$\tau_{xy,elastic}=\gamma_0 G'(\omega)\sin(\omega t) \quad (1.11)$$

$$\tau_{xy,viscous} = \gamma_0 G''(\omega)\cos(\omega t) \quad (1.12)$$

Equations 1.11 and 1.12 define the storage modulus, G', which represents the elastic response of the material and the loss modulus, G", which characterize characterizes the viscous part of its response.

The viscoelastic material being defined as a material displaying an elastic part and a viscous part, its viscoelastic response is defined as the sum of its elastic part and viscous part responses.

$$\tau_{xy}(t) = \gamma_0 G_0(\omega)\sin(\omega t) + \gamma_0 G''(\omega)\cos(\omega t) \quad (1.13)$$

From Equations 1.11 and 1.12, we can find the equations of G' and G":

$$G'=\frac{\tau}{\gamma_0}\cos(\delta(\omega)) \quad (1.14)$$

$$G''=\frac{\tau}{\gamma_0}\sin(\delta(\omega)) \quad (1.15)$$

By their definition G' and G" are the Fourier transform of the relaxation modulus, G(t). Thus, we can note that both dynamic and relaxation moduli give us the same information.

The important result for single Maxwell model obtained are summarized below:

$$\frac{G'}{G0} = \frac{(\lambda\,\omega)^2}{1+(\lambda\,\omega)^2} \quad (1.16)$$

$$\frac{G^{"}}{G0} = \frac{(\lambda\,\omega)}{1+(\lambda\,\omega)^2} \quad (1.17)$$

From those equations relating the frequency to G' and G", we can analyses the extreme case of the very low frequency

• If $\lambda\omega << 1$:

$$G'(\omega) \propto \omega^2 \quad (1.16) \qquad G''(\omega) \propto \omega \quad (1.18)$$

This result means that the slope of the storage modulus at low frequency is -2 while the slope of the loss modulus is -1 as shown in Figure 1.26.

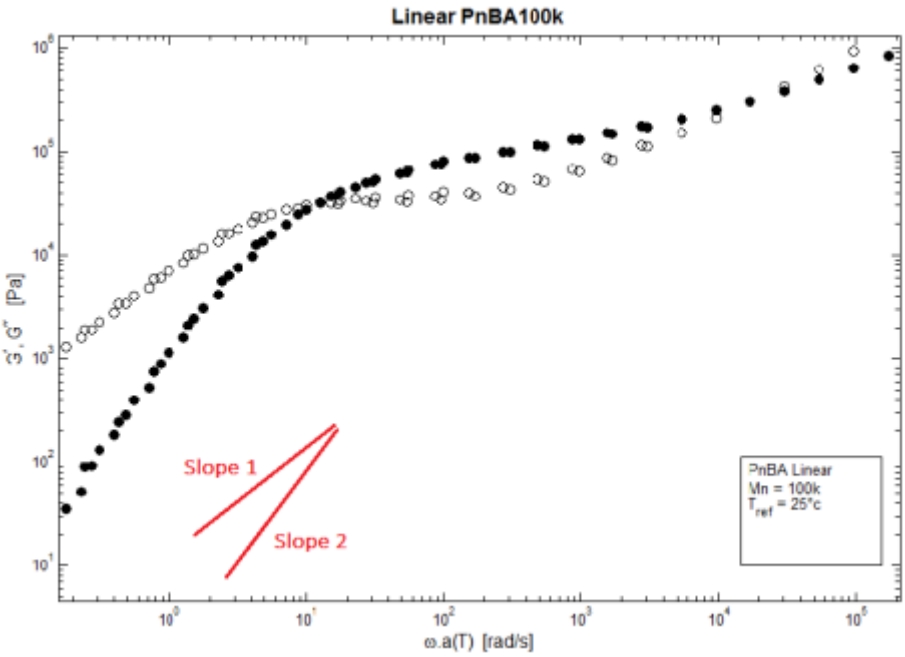

Figure 1.26 -Experimental storage and loss moduli versus angular frequency of linear PnBA with Mn=138kg/mol. Those master curves are drawn thanks to time-temperature superposition and the data are shifted for a reference temperature of 25 °c.[6]

A low frequency corresponding to a long time by the relationship $\omega = 1/t$, the $G(\omega)$ is similar to the reverse of G(t) curve. The different regions discussed in section 1.3.1 for G(t). Here again, the plateau modulus and terminal relaxation are really sensitive to the molecular structure.

1.4 FUNDAMENTALS OF TUBE MODELS

The tube model was introduced by de Gennes and by Doi and Edwards in order to explain how an entangled polymer (either melt or highly concentrated solution) relaxes the anisotropy and related stress induced by a step strain. This model reduces the complex dynamics of inter-chain topological interactions to a "single-body" process, in which the molecular environment of an observed chain (usually called the "test" chain) is represented by a mean field called the "tube". The test chain, which is unable to cross another molecule, is indeed behaving as if it were confined in a tube since only motions parallel to the curvilinear tube axis are unhindered, while lateral motions are limited to a characteristic distance, the tube diameter a. Since the tube is an average object, its diameter has a constant value along the chain and for all chains. While it depends on the nature of the polymer and concentration, it is independent of chain architecture.[24, 25]

Since it is assumed that a sub-chain between two entanglements is Gaussian, its end-to-end distance *l* is given as $l^2 = Neb^2$, where *b* is the length of a Kuhn segment and N_e is the number of Khun segments between two entanglements. It is useful to imagine that in the tube picture, the chain is coarse-grained at the scale of the segments between entanglements (Figure 1.27). They define the primitive path of the chain, having a length $L_{eq}(M)=Z.l=(M/M_e)l$. The primitive path can be considered as a (discretized) representation of the curvilinear axis of the tube.[26]

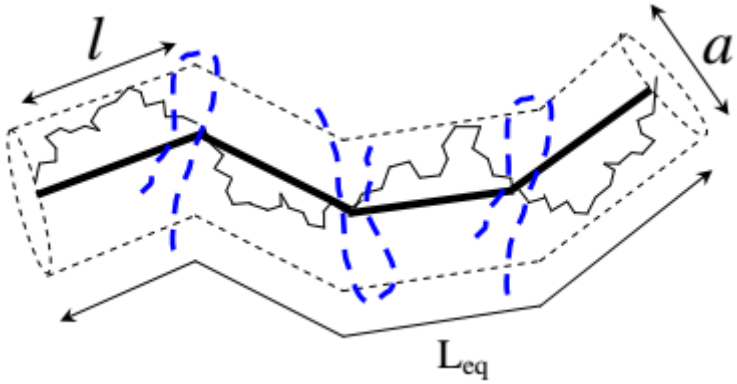

Figure 1.27- Schematic representation of a chain in the tube. Real chain: thin broken line; primitive path: thick line; entanglements : dotted line.[27]

Since we assume a Gaussian chain confined in a tube of diameter a, the most probable curvilinear path length L_{eq} is proportional to molecular weight through the relation:

$R^2=L_{eq}.a=Zl_a$, (1.23)

where R is the quadratic end-to-end distance of the relaxed chain. On the other hand:

$R^2=Nb^2=ZN_eb^2=Zl^2$, (1.24)

where $N=ZN_e$ is the total number of Kuhn segments. Hence: a=l.

The second transition in Figure-1.23 corresponds to the escape of the chain from the stressed entanglement network toward the relaxed equilibrium state, via tube. This includes different relaxation processes (reptation, contour length fluctuations, constraint release mechanisms) described in detail below. Neglecting the glassy region, the relaxation modulus of an entangled polymer, G(t), is thus described by two terms: the first takes into account the Rouse relaxation and the second describes the tube renewal process, which is proportional to the unrelaxed fraction, F(t), of the polymer:

$G(t) = G_{Rouse}(t) + G^0_N. F(t)$. (1.25)

Equation 6 is obviously not valid at very short times corresponding to the glassy region. Indeed, the Rouse modulus diverges at time zero. Different models based on the generic tube theory have been proposed in order to correctly describe the relaxation function F(t) of a linear polymer (see Section 4). While significant qualitative and quantitative differences are found between the various models, they use the same basic ingredients to describe the relaxation of a chain: reptation, contour length fluctuations and constraint release mechanisms. These are introduced in the following sections.[28]

1.4.1 Reptation

For times larger than the Rouse time of an entangled segment, τ_e, the tube is active. This means that topological constraints restrict the motion of the chain laterally. Therefore, the only possible motion of the center of mass is a diffusion along the curvilinear axis of the tube. This process is defined by a one dimensional diffusion equation. By back and forth motions along the primitive path (which are associated to a Brownian motion of the center of mass), the chain can move few by few outside the initial tube to create a new one. This is illustrated in Figure 1.28 According to Equation 1.26, the stress resulting from a small step strain will progressively relax by the disappearance of the oriented segments because new tube segments created around the advancing chain end are randomly oriented. Hence, the chain will relax from the outer to the inner segments. According to reptation theory, the time needed to relax the entire chain by reptation, τ_d, is proportional to the cube of the molecular weight of the test chain:[25, 26]

$$\tau_d = \frac{Leq^2}{\pi 2Dc} \propto \frac{M^2}{M^{-1}} = M^3 \quad (1.26)$$

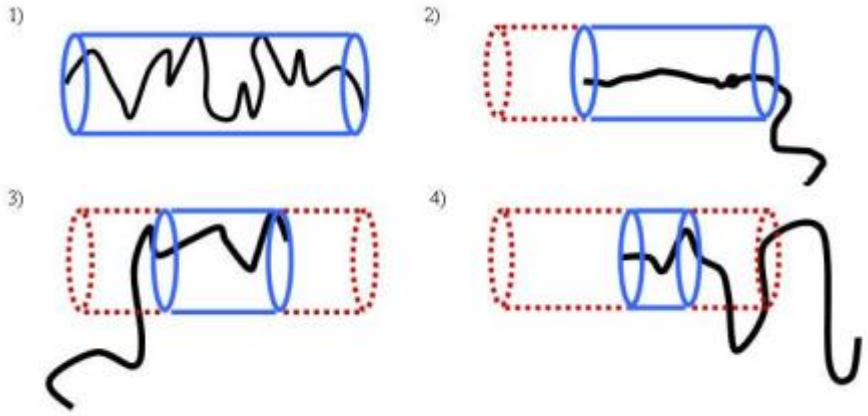

Figure1.28- Reptation process[27].

where *Dc*, the curvilinear diffusion coefficient, is equal to *kT/Nζ0*, results from the summed drag of all the monomers along the chain and is thus proportional to the number of monomers, *N*, and the monomeric friction coefficient *ζ0*. Expressing the primitive path length L_{eq} and the curvilinear diffusion coefficient in terms of tube model parameters gives the important relation :[26]

$$\tau_d(M) = \frac{\zeta 0\ Ne^2.b^2.\pi^2}{kT}\left(\frac{M}{Me}\right)^3 = 3\tau_e Z^3 \quad (1.27)$$

This M^3 dependence of the reptation time must be compared to the M^2 dependence of the Rouse time. The same M^3 scaling is predicted for the zero shear viscosity, η_0 , since:

$$\eta_0 \propto G_0^N.\tau_d \quad (1.28)$$

and the plateau modulus is (in this picture) molecular-weight independent.

1.4.2 Contour length fluctuations

Because the experimental dependence observed for zero shear viscosity of entangled polymer melts follows a $M^{3.4}$ scaling rather the anticipated M^3 predicted by pure reptation, it is clear that

additional relaxation mechanisms besides curvilinear diffusion of the center of mass are required to correctly describe the relaxation of linear chains[29]. Initially proposed by Doi and later expanded by Milner and Mc Leish, contour length fluctuations (CLF) are the second key ingredient of quantitative tube models. This process is a Rouse relaxation of the chain ends, which does not require the motion of the center of mass, already described by reptation. As shown in Figure 1.29, when the chain contracts within the tube and then stretches out again, the orientation of the ends of the initial tube is forgotten, and the stress associated with those portions is relaxed.

Contour length fluctuations arise because the equilibrium length of a chain is only the most probable length, representing the most stable configuration. However, other chain lengths are possible, by thermal fluctuations around this equilibrium and include Rouse modes associated to sub-chains possibly larger than M_e. The CLF process is a typical first passage problem: it is not related to the most probable location of a chain end, but rather to the deepest tube segment reached by the fluctuating chain end. Before the reptation process can be completed, the outer chain segments are already relaxed by CLF. Therefore, CLF will speed up the overall relaxation of the polymer. The experimental 3.4 scaling for viscosity and reptation time has been attributed to CLF by Doi, arguing that the fraction of tube relaxed by CLF should scale as $Z^{-1/2}$ .Therefore, the importance of CLF becomes less as Z increases. As a consequence of CLF, viscosity increases faster than the asymptotic Z^3 reptation prediction.[30]

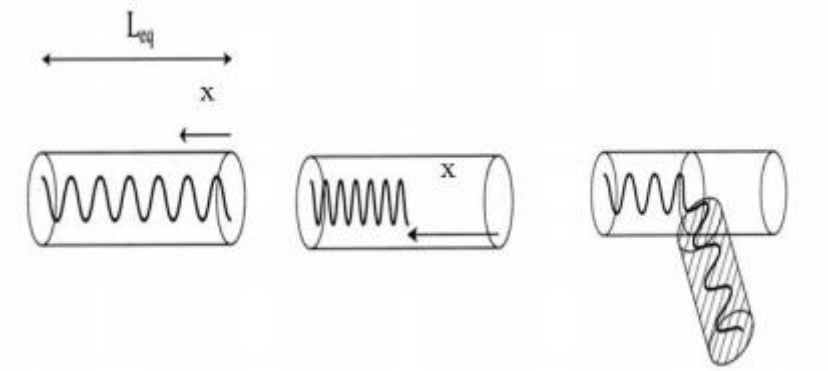

Figure 1.29- Contour Length Fluctuations process.[27]

Since chain reptation needs only to relax the remaining (central) parts of the primitive path, the reptation time has to be renormalized in order to include the effect of CLF.

1.4.3- Constraint release and tube dilation

Since the tube represents the topological constraint on a given chain from its molecular environment, the tube itself is able to move according to the motion of the surrounding chains. This tube motion, neglected in the Doi and Edwards model, is in particular important for polydisperse systems. Tube motions are extremely complicated to describe in their generality and therefore only simplifications of the real situation are tractable. Tube motions chiefly affect the test chain in two different but related ways. First, "slow" tube motions allow large-scale lateral motions of internal segments, i.e. they induce a constraint release mechanism (CR) (Figure 1.30).[31] Second, when motions of surrounding chains become fast at the observed time scale, the effect is equivalent to an increase of the "effective" tube diameter, which leads

to an acceleration of the other relaxation processes (reptation, CLF). This mechanism is called "Dynamic Tube Dilation" (DTD).[32]

Figure 1.30-constraint release process.[27]

1.4.4- Dynamic Tube Dilation (DTD)

This approach has first been proposed by Marrucci. It is based on the concept that the "effective" tube of constraints around a chain widens as the relaxation proceeds. Indeed, the tube diameter is directly linked to the average distance that a chain can laterally cover without hitting topological constraints by the surroundings molecules. Were these obstacles fixed (i.e. a permanent network), the tube diameter would be a well-defined, time-independent quantity. However, because of the mobility of the surrounding chains, obstacles continuously disappear and reform, some of them more rapidly (near the chain end), others more slowly (far from the chain ends). Therefore, the test chain will be able to move laterally and explore the surroundings more and more with time. In other words, the tube diameter must be taken as an increasing function of time during relaxation. [32]This increase is calculated by assuming that the relaxed part of the polymer behaves like a solvent. Therefore, the effective tube diameter depends on the unrelaxed fraction of the polymer, $\Phi(t)$ as:

$$M_e=\frac{Me(0)}{\Phi(t)^{\alpha}} \qquad (1.29)$$

$$L_{eq}=L_{eq}(0).\,\Phi(t)^{\alpha/2} \qquad (1.30)$$

$$\alpha_e=\frac{\alpha(0)}{\Phi(t)^{\alpha/2}} \qquad (1.31)$$

Note that the time dependent values are described as "effective" and are different from the true material parameters (except at time zero). Indeed, since the polymer density remains constant through time, the equilibrium values do not change.

From Equation 1.33 and Equation 1.35, it would be concluded:

$$G(t)=\frac{\rho RT}{Me(t)^{\alpha}}\,\Phi(t)=G^0_N\,\Phi(t)^{\alpha/2} \qquad (1.32)$$

The exponent α, called the dilution exponent takes a value between 1 and 1.3. Still today, there is no real consensus on its value even if the last trend seems to take 1 . Equation 1.36 is similar to the one obtained from the double reptation approach. However, a fundamental difference between both approaches is the fact that Dynamic Tube Dilation affects the reptation dynamics because the reptation time is proportional to $L_{eq}(t)^2$ and thus, to $\Phi(t)^{\alpha}$. On the other hand, it is considered constant in the double reptation model.[30] In the DTD model, the relaxed part of the polymer is immediately taken as solvent. However, Struglinsky and Graessley have shown that this assumption is not always valid.It works only if the different relaxation times are well separated on the time scale.[33, 34]

Refined tube dilation models have further been developed for monodisperse star molecules. In particular, Ball and McLeish have extended the Dynamic Tube Dilation concept to contour length fluctuations in order to explain the relaxation of star polymers. This model was improved by Milner and McLeish who solved the first passage problem to obtain more accurate expression of the activated fluctuations times and considered the early (non-activated) Rouse fluctuations. [35]

1.5-VISCOELASTICITY PROPERTIES OF SUPRAMOLECULAR POLYMERS

1.5.1 Metallo-supramolecular polymers of bifunctional macromolecules

In this section the effect of aggregation is neglected completely and therefore, the entanglements between polymer chains and associations-dissociation time of metal-ligand bond plays the important role in the relaxation mechanism of supramolecular polymers. In a work done by Zhuge et.al, at 25 °C the reference polymer, i.e., a PnBA bifunctional polymer without metal ions, relaxes easily as it contains only 6.7 entanglements. Its terminal relaxation zone is reached at time τ_{rel} = 45 ms, and its relaxation is well described by reptation combined with CLF and CR mechanisms. However, when metal ions are added, the polymer with active stickers behaves quite differently. Even with zinc ions, the bifunctionalized metallo-supramolecular bulk material has a longer terminal relaxation time, τ_{rel},Zn(II) = 134 ms.[36]

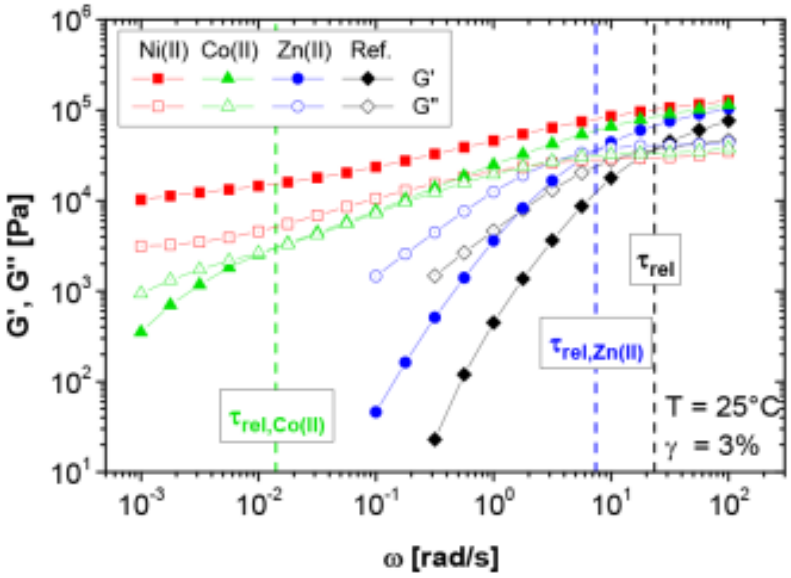

Figure 1.31-Linear rheology curves at 25 °C of linear bifunctional PnBAtpy2 (melts) with different transition metal ions. The reference corresponds to a polymer without metal ions. The storage modulus G′ is represented by filled symbols and the loss modulus G″ by empty symbols.[36]

This first example shows the large influence of the nature of the metal ion. In the present work, Zn and Co metal ions have been selected.

1.5.2- Effect of collective assemblies

Based on the viscoelastic investigations it can be stated that collective assemblies play a key role in controlling dynamics of supramolecular networks.

With respect to participation in collective assemblies, polymer segments can be divided into five categories, illustrated schematically in Figure. 1.32. (i) free linear chains that are not attached to any collective assembly, and have freely moving extremities (ii) star-like chains that are attached to only one long lifetime collective assembly, (iii) trapped segments that are

connected to more than two collective assemblies, and (iv) dangling ends of the trapped segments. Free linear chains, star-like molecules and dangling end of the trapped segments constitute the mobile polymer fraction of the system as they are able to relax by tube escape mechanisms. In contrast, sections of trapped chains between two collective assemblies are essentially immobile since renewal of their orientation is restrained until dissociation of this long lifetime stickers. This classification of segments in a supramolecular network enables us to describe complex shape of the relaxation modulus by considering hierarchy of relaxation times, shown in Figure 1.32. Note that dynamic moduli and angular frequencies are normalized by the plateau modulus (G^0_N) and the reptation time (τ_d) of linear chains, respectively.

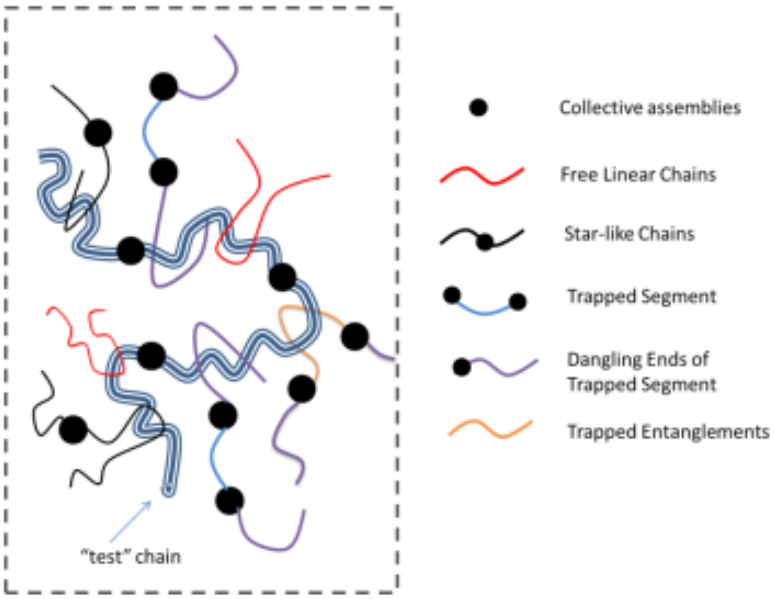

Figure 1.32-Schematic illustration of different categories of segments in enatgled supramolecular networks formed via collective assemblies of moieties. A probe chain is shown. It is surrounded by free linear chains not attached to collective assemblies, star-like chains that are only attached to one collective assembly, and trapped chains that are connected to at least two long life time collective assemblies.

Zone 1: When early timescales Rouse motions occur, which involve relaxation of subchains of increasing lengths. At short times, the relaxing segments do not feel the tube. Note that the segments which can relax by Rouse are shorter than the distance between physical constraints, *i.e.* entanglements, binary and collective assemblies. At longer times, Rouse modes are restricted, as longer segments feel the constraint imposed by the surroundings environment. The transition to the first plateau modulus (Zone 2 , Fig.1.33) marks the saturation of the Rouse modes, and the tube picture starts to be relevant. In other words, the length of the subchains reaches the average spacing between physical constraints. It is worth noting that binary assemblies only alter Rouse modes, when their corresponding association time exceed τ_e.

Zone 2: At the second relaxation step, the dangling branches of the trapped chains as well as the star-like chains will renew orientation by CLF. Moreover, the free linear chains will relax by reptation and CLF. As the level of the first plateau modulus is determined by the average distance between physical constraints, higher plateau modulus can be expected for the supramolecular network, compared to linear chains.

Zone 3: Once the mobile components have relaxed, the CR process becomes active. Trapped strands between successive sticky junctions partially renew configuration through local CR events. In other words, the segments of the trapped strands will undertake Rouse-like hops. These events occur at time scale by which entanglements between the trapped strands and the surrounding mobile material disappear/re-appear. They provide extra freedom to the trapped strands, which can now explore the surrounding space on a larger length scale than the one corresponding to the original tube diameter.

Zone 4: The terminal relaxation of the trapped chains is delayed until dissociation of the collective assemblies takes place. As mentioned earlier in most cases it is outside the experimental window. Nevertheless, the beginning of this regime can be observed with specific samples at high temperatures.[37, 38]

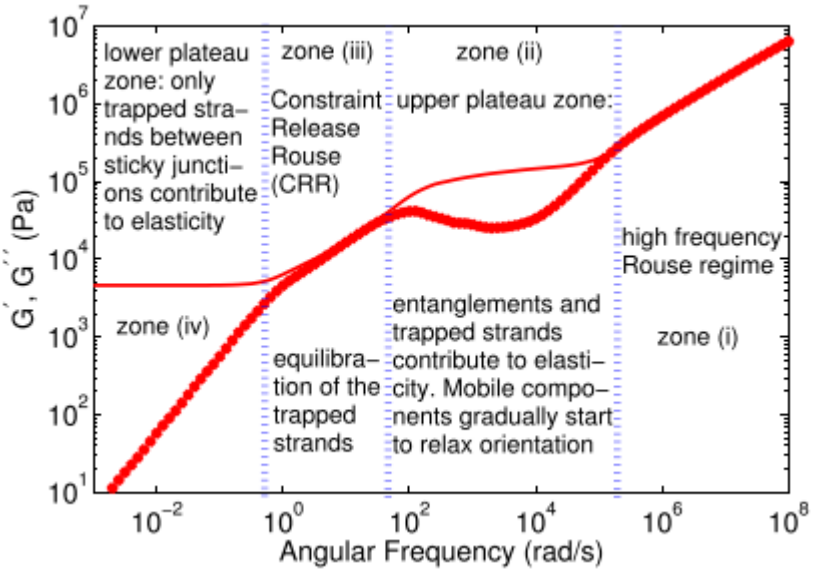

Figure 1.33-A graphical illustration of the four relaxation regimes (zones) considered in the model. The different zones are discussed in the text. The solid curve corresponds to G' while the dotted one to G".[38]

1.5.3-Some examples of the effect of aggregations on the rheological behavior of PB

It is essential to notice the Hydrogenated, hydroxylated polybutadiene also has different behavior from linear polybutadiene because low-molar-mass polybutadienes, as well as their hydrogenated analogues, form hydrophobic domains which contribute to existence of supramolecular clusters detectable by dynamic light scattering. These domains, and hence also the clusters, gradually and reversibly disintegrate with increasing temperature for original polybutadienes but persist in their hydrogenated derivatives.[39]

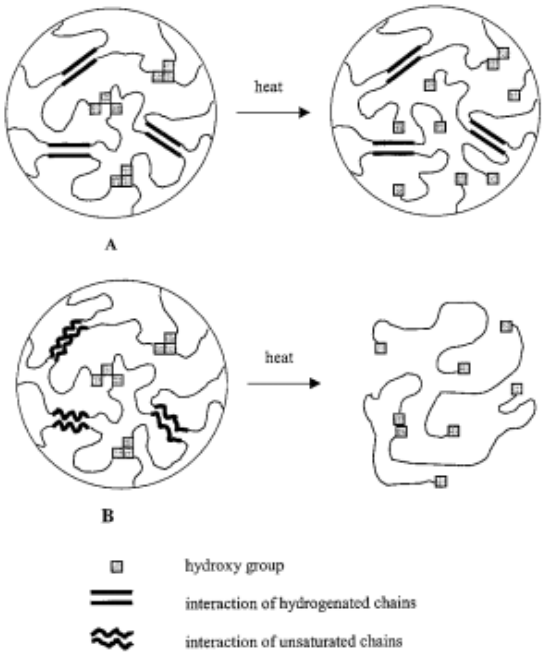

Fig 1.34-Hypothetical representation of OH/OH and aliphatic knots in bulk hydroxylated Polymers and their dissociation upon heating: hydrogenated Polymer (above), unsaturated polymer (bottom).[40]

In Addition, OH end groups contribute substantially to the formation and preservation of the clusters: hydrophilic micro domains based on hydrogen bonds between three and more OH groups exist in bulk OH-telechelic Polybutadiene (be it unsaturated or hydrogenated analogues) at room temperature. These OH microdomains represent knots connected by hydrophobic links forming a physical network which hinders the segmental motion. With increasing temperature, however, the microdomains reversibly dissociate. [40, 41]

In a research study by Jir Podesˇva et.al, it has been reported by IR spectroscopy method, with unsaturated, hydroxylated samples, an interaction between an OH end group and the corresponding C=C bond of the adjacent terminal monomer unit takes place both in bulk and in dilute heptane solution due to the existence of coiled conformation of the chain ends. This intramolecular OH/C=C interaction makes the OH/OH hydrogen bonding less probable. After hydrogenation, OH end groups lose their C=C counterparts and the coiled conformations of the chain ends are no longer probable. In case of dilute heptane solutions, only intramolecular end-to-end OH/OH hydrogen bonding is possible, which leads to macrocycles.[40]Finally, V. *R. Raju* et.al has studied that polybutadiene could be hydrogenated without apparent change in large-scale molecular structure. [40]

Definitely the polymer chain dynamics in supramolecular polymer melts is quite complex due to reduction of chain mobility, chain entanglements, phase-segregation of macromolecular parts, and aggregation or crystallization of associating groups (collective assembly). According to Lewis *et al.* most experimental studies of supramolecular polymer melts deviate significantly from the idealized picture of reversibly binding chains. Very few studies have been conducted on model systems that isolate how specific variables influence association/dissociation dynamics of the stickers within polymer melts.[42]

Another nice example is the work that has been done by Stadler et al. in which they investigated the dynamics of PB modified with 4-phenyl-1,2,4-triazoline-3,5-dione (urazole) groups at 1, 2, 3 and 4 mol% grafting density. The molecular mass of the PB precursor was 29 kg/mol thus it contained over 18 entanglements.[43]

Figure 1.35 shows reduced pseudomaster curves of dynamic moduli for PB-urazole at 2, 3 and 4 mol%. It is clear that tTS fails in these supramolecular polymers, as indicated by the poor matching of the shifted curves. The level of thermo-rheological complexity increases with increasing urazole content along the PB chains. Figure 1.35 demonstrates 3 main effects which are usually found in hydrogen bonding and coordination supramolecular networks. i) terminal relaxation is hindered or G'/G'' the cross-over is shifted to lower frequencies, ii) there is considerable broadening of relaxation time spectrum and iii) zero shear viscosity is increased dramatically. These observations are in common with basic observations in ionomers, as discussed in first chapter.[43, 44]

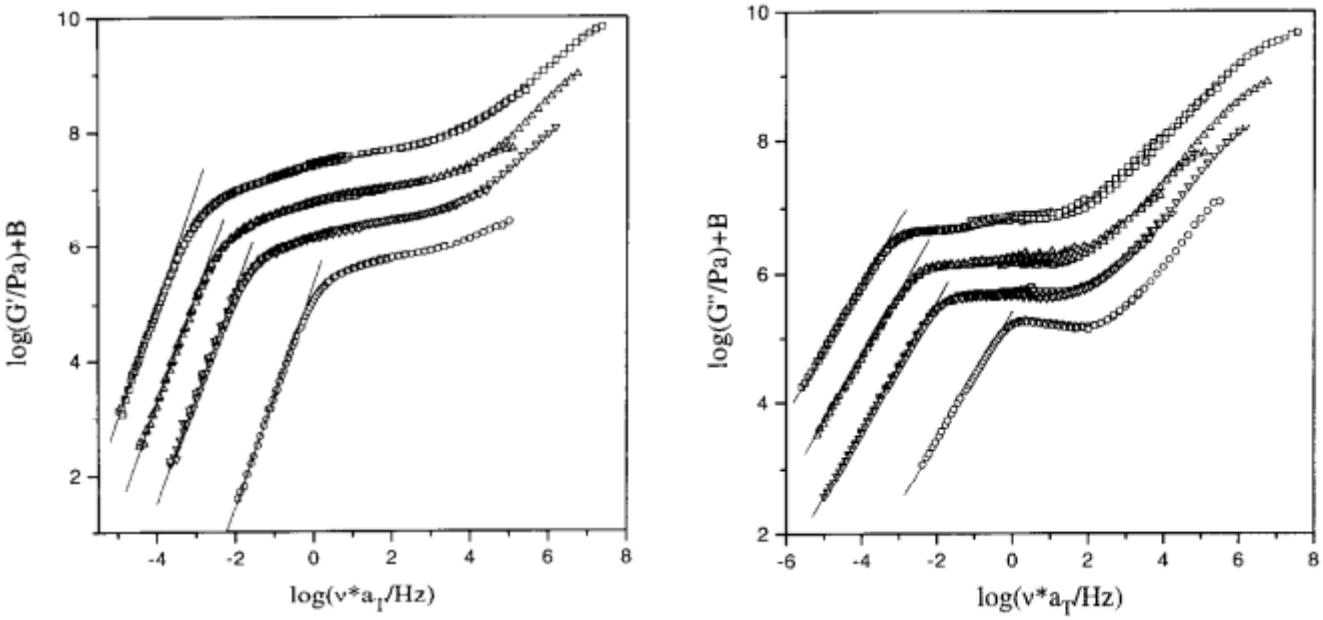

Figure 1.35- (left) Storage and (right) loss modulus psuedomaster curves for urazole functionalized polybutadienes at different degrees of substitution (Tr = −40 ◦C). The master curves are vertically offset against each other by half a decade for clarity. Adopted from Müller et al. Polymer 1995.[43]

Hilger et al. have investigated polybutadienes of narrow molecular-weightdistribution, carrying statistically distributed polar phenylurazole (1),4-ethoxycarbonylphenylurazole(2) and 4-carboxyphenylurazole(3) groups along the polymer chain. They were analyzed with respect to their dynamic mechanical properties in the linear viscoelastic region. In these systems thermoreversible networks are formed by hydrogen-bond complexes. In the case of (1) and (2), where only binary complexes are formed, the systems show thermo-rheologically simple behavior, i.e. the construction of viscoelastic master curves is possible and the temperature dependencies described by an average apparent activation energy of flow for all relaxation processes. For polybutadiene carrying between 0.5 and 4 groups of (3) per 100 repeat units, thermo-rheologically complex behavior is observed, which is related to the multiphase structure formed by phase separation between the covalent polybutadiene backbone and supramolecular ordered association polymers formed by the polar functional groups.[45]

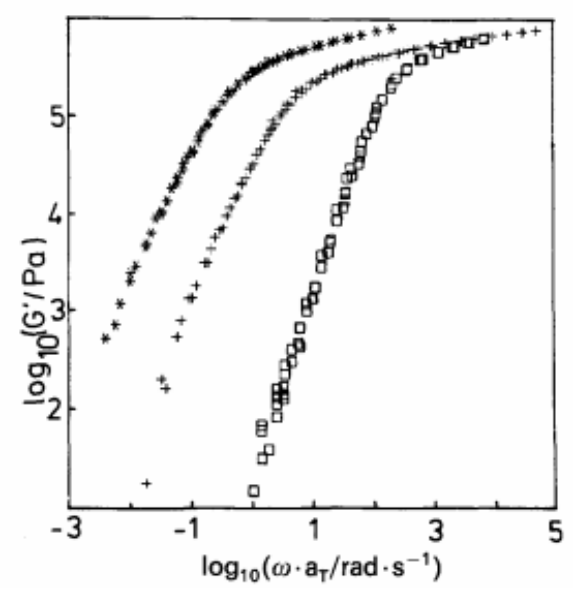

Figure 1.36- Storage modulus master curves for PB-30-0 (□), PB-30- UE-2 (+) and PB-30-UE-4 (*); reference temperature 273 K.[45]

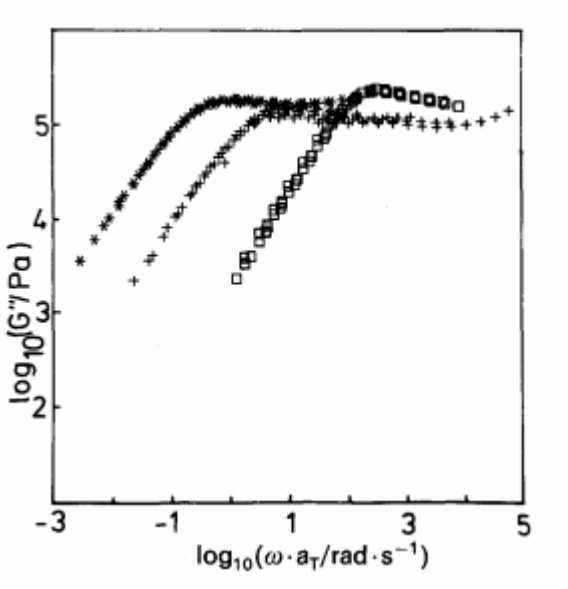

Figure 1.37- loss modulus master curves for PB-30-0 (□), PB-30- UE-2 (+) and PB-30-UE-4 (*); reference temperature 273 K.[45]

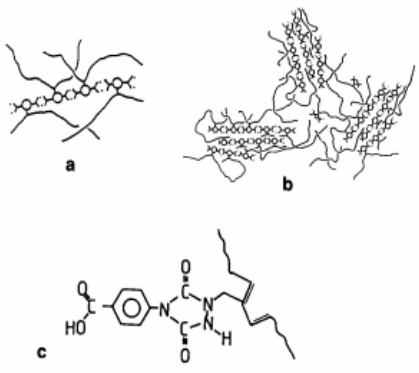

Figure 1.38- Schematic structural model for the build-up of a multiphase structure from statistical copolymers:(a) formation of the association polymer; (b) phase separation by cooperative aggregation; and (c) resulting structure from the addition of 4-(4'-carboxyphenyl)-l,2,4- triazoline-3,5-dioneto a polybutadiene chain. The -COOH and the-NHCO- units are able to form hydrogen-bond complexes.[45]

The physical origin of this failure is attributed to the different temperature dependence of the chain relaxation time (which follows the temperature dependence of τ_e) and the association lifetime, τ_{ass}, and consequently the average number of associated end groups. That is, the motions of the chains are dictated by two different processes: (i) Dynamics of stickers and (ii) reorientation of the entanglement segments (disentanglement), which have different temperature dependence and also doesn't exist in the intial samples. This failure of TTS principle is analyzed in details by Zhang et al., who demonstrate that in the case of unentangled associative chains, the shift factors used in the terminal regime for building a mastercurve are influenced by both the transient bond dynamics and the segmental dynamics. In consequence,

these shift factors cannot be directly used to determine the sticker activation energy. To do so, the authors show that one should rather consider the temperature influence on the ratio between the sticker lifetime and the segmental time.[46]

In case of entangled associative chains, the failure of TTS principle can be even more pronounced, without any possibility to build a mastercurve in the low frequency regime of deformation. The importance of this failure seems to depend on the lifetime of the stickers along the chains, compared to the disentanglement time of the unassociated chains.[47]

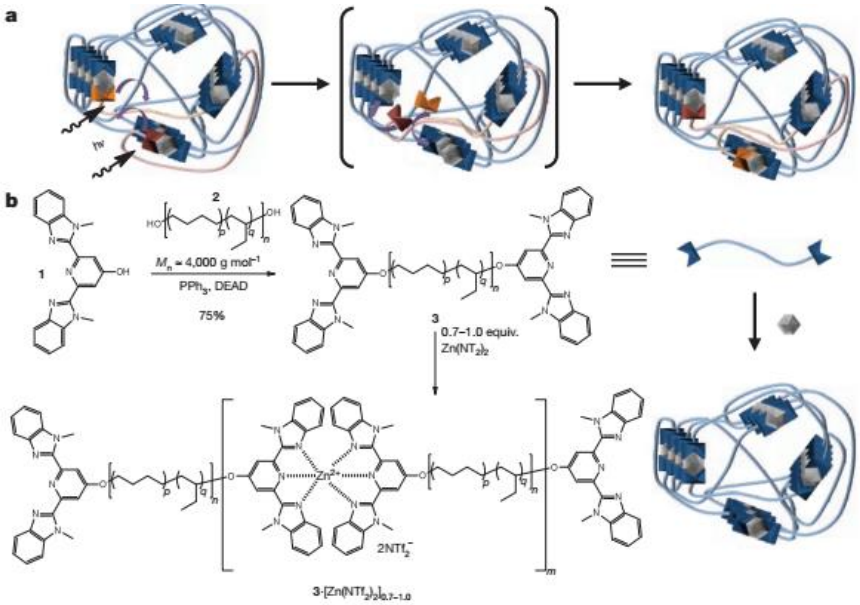

Figure1.39- Mechanism and synthesis of photo healable metallosupramolecular polymers. Proposed optical healing of a metallo-supramolecular, phase separated network. b, *Synthesis of macromonomer* 3 *and polymerization by addition of Zn(NTf2)2.[39]*

In a work done by Rowan et.al, which is similar to this master thesis they prepared a a macromonomer comprising a rubbery, amorphous poly(ethylene-co-butylene) core with 2,6-bis(19 methylbenzimidazolyl)pyridine (Mebip) chain ends. This design was based on the assumption that the hydrophobic core and the polar metal–ligand motif would phase separate. To probe how the metal ion affects the materials' properties, the polymer was self-assembled with $Zn(NTf_2)_2$ or ligands at the termini $Zn(NTf_2)_2$ revealed microphase-separated lamellar morphologies in which the metal–ligand complexes form a 'hard phase' that physically crosslinks the poly(ethylene-co-butylene) 'soft' domains (Fig 1.39).Therefore, the formation of lamellar morphologies in which a hard phase comprising the metal–ligand complexes physically crosslinks soft domains of the poly(ethylene-cobutylene) cores is the main determinant for the thermomechanical characteristics of the materials has been studied.[39]

References

1. Sebastian Seiffert, J.S., *Physical chemistry of supramolecular polymer networks.* Chem. Soc. Rev, 2012. **41**: p. 909–930.

2. Liulin Yang, X.T., Zhiqiang Wang, and Xi Zhang, *Supramolecular Polymers: Historical Development, Preparation, Characterization, and Functions.* Chemical reviews, 2015. **15**: p. 7196-7239.

3. Brassinne, J.Z., F.; Fustin, C.-A.; Gohy, J.-F. , *Precise Control over the Rheological Behavior of Associating Stimuli-Responsive Block Copolymer Gels.* Gels 2015. **1**: p. 235−255.

4. P. Cordier, F.T., C. Soulie-Ziakovic and L. Leibler, *Self-healing and thermoreversible rubber from supramolecular assembly.* Nature, 2008. **451(21)**: p. 977–980.

5. Folmer, B.J.B.S., R. P.; Versteegen, R. M.; van der Rijt, J. A. J.; Meijer, E. , *Supramolecular Polymer Materials: Chain Extension of Telechelic Polymers Using a Reactive Hydrogen-Bonding Synthon.* Adv.Mat., 2000. **12**: p. 874−878.

6. BLOND, J., *Rheology of metallo-supramolecular model polymer based on telechelic poly(n-butyl acrylate)s and metal-ligand interactions*. 2017, uclouvain.

7. De Smedt SC, D.J., Hennink WE., *Cationic polymer based gene delivery systems.* Pharm Res. , 2000. **17(2)**: p. 113-26.

8. Xinrong Lin, M.W.G., *Ionic Supramolecular Assemblies.* Israel Journal of chemistry, 2013. **53**: p. 1 – 13.

9. M. Leclercq, M.B., *Dynamics of polyelectrolyte complex formation and stability as a polyanion is progressively added to a polycation under modeled physicochemical blood conditions.* Bioactive and Compatible Polymers, 2011. **26**: p. 301-316.

10. Michel Wathier, M.W.G., *Synthesis and Properties of Supramolecular Ionic Networks.* J. Am. Chem. Soc., 2008. **30**: p. 9648–9649.

11. Sivakova, S.J.R.P.S.S., *Nucleobase-induced supramolecular polymerization in the solid state.* Polym. Chem, 2003. **41**: p. 3589-3596.

12. Ruymbeke.E, B.C.a.v., *Rheometry and Polymer Processing*, in *MAPR 2018*. 2018.

13. Meier, M.A.R.W., D.; Ott, C.; Guillet, P.; Fustin, C. A.; Gohy, J.-F.;, *Supramolecular Self-Assembled Ni(II), Fe(II), and Co(II) ABA Triblock Copolymers.* Macromolecules 2006. **39**: p. 1569–1576.

14. Hoogenboom, R.S., *The use of (metallo-)supramolecular initiators for living/controlled polymerization techniques.* U. S. Chem. Soc, 2006. **35**: p. 622–629.

15. Schubert, M.A.R.M.U.S., *Terpyridine-modified poly(vinyl chloride): Possibilities for supramolecular grafting and crosslinking.* Polym. Chem, 2003. **41**: p. 1413–1427.

16. Guillet, P., *Metallo-Supramolecular Block Copolymers: From Synthesis to Smart Nanomaterials*. 2008, Uclouvain.

17. Goshe, A.S., I.; Ceccarelli, C.; Rheingold, A.; Bosnich, B. , *Supramolecular recognition: On the kinetic lability of thermodynamically stable host–guest association complexes.* Proc. Natl. Acad, 2001. **99**: p. 4823–4829.

18. Tschoegl, N.W., *The phenomenological theory of linear viscoelastic behavior*. 1989, Berlin: Springer-Verlag.

19. Ferry, J.D., *Viscoelastic properties of polymers*, ed. 3rd. 1980, New York: John Wiley & Sons.

20. Larson, J.M.D.R.G., *Structure and Rheology of Molten Polymers*. 2005, Munich: Hanser.

21. ; Available from: http://www.open.edu/openlearn/science-maths-technology/science/chemistry/introduction-polymers/content-section-5.3.1.

22. Ferry, J.D., *Mechanical properties of substances of high molecular weight. .* Am. Chem. Soc. , 1953. **72**: p. 3746–3752.

23. Macosko, C.W., *Rheology: Principles, Measurements, and Applications*. (1994) VCH, New York: VCH.

24. P.G., d.G., *Reptation of a polymer chain in the presence of fixed obstacles.* J. Chem. Phys., 1971. **55** p. 572–579.

25. Doi M., E.S.F., *Dynamics of concentred polymer systems.* J. Chem. Soc., 1978. **74**: p. 1789–1832.

26. Larson, *The Structure and Rheology of Complex Fluids*. 1999: Oxford University, press.

27. E. van Ruymbeke, L.B., S. Coppola, S. Righi, D. Vlassopoulos, *Decoding the viscoelastic response of polydisperse star/linear polymer blends.* Journal of Rheology, 2010. **54**.

28. Rouse P.E., A., *Theory of the Linear Viscoelastic Properties of Dilute Solutions of Coiling Polymers.* J. Chem. Phys., 1953. **21**: p. 1272–1280.

29. Colby R.H., F.L.J., Graessley W.W., , *Melt Viscosity–Molecular Weight Relationship for Linear Polymers, .* Macromolecules,, 1987. **20** p. 2226–2237.

30. Doi M., G.W.W., Helfand E., Pearson D.S.,, *Dynamics of polymers in polydisperse melts.* Macromolecules, 1987. **20**: p. 1900–1906.

31. McLeish T.C.B., *Why, and when, does dynamics tube dilation work for stars?* J.Rheol.,, 2003. **47**: p. 177–198.

32. Marrucci, *Relaxation by reptation and tube enlargement: a model for polydisperse polymers.* J. Polym. Sci. Polym. Phys., 1985. **23**: p. 159–177.

33. Struglinski M.J., G.W.W., *Effect of polydispersity on the linear viscoelastic properties of entangled polymers. 1. Experimental observation for binary mixtures of linear polybutadiene,* . Macromolecules, 1985. **18**: p. 2630–2643.

34. Watanabe H., I.S., Matsumiya Y., Inoue T., *Test of full and partial tube dilation pictures in entangled blends of linear polyisoprenes.* Macromolecules, 2004. **37** p. 6619–6631.

35. H., W., *Viscoelasticity and dynamics of entangled polymers.* Prog. Polym.Sci., , 1999. **1999** p. 1253–1403.

36. Flanco Zhuge, J.B.C.-A., Fustin,Evelyne van Ruymbeke ,Jean-Francois Goh, *Synthesis and Rheology of Bulk Metallo-Supramolecular Polymers from Telechelic Entangled Precursors.* Macromolecules, 2017. **50**: p. 5165-5175.

37. Goldansaz, *Dynamics and Microstructure of Entangled Supramolecular Networks*. 2016, Uclouvain.

38. Hawke, A., Van.Ruymbeke, *Viscoelastic properties of linear associating poly(n-butyl acrylate) chains.* Rheol. , 2016. **60**: p. 297-310.

39. Mark Burnworth, L.T., Justin R. Kumpfer1, Andrew J. Duncan, Frederick L. Beyer, Gina L. Fiore, Stuart J. Rowan& Christoph Weder, *Optically healable supramolecular polymers.* Nature, 2011. **472**: p. 334-339.

40. Jirˇı´ Podesˇva, J.ı.D., Jirˇı´ Speˇva´ cˇek, Petr Sˇ teˇpa´ nek, and Peter Cˇ ernoch, *Supramolecular Structures of Low-Molecular-Weight Polybutadienes, as Studied by Dynamic Light Scattering, NMR and Infrared Spectroscopy.* Macromolecules, 2001. **34**: p. 9023-9031.

41. Sheppard, N., *Hydrogen Bonding*. 1959, London: Pergamon Press.

42. Lewis, C.L.S., K.; Anthamatten, M., *The Influence of Hydrogen Bonding Side-Groups on Viscoelastic Behavior of Linear and Network Polymers.* . Macromolecules 2014. **47 (2)**: p. 729-740.

43. Muller, M.S., U.; Stadler, R. , *Influence of Hydrogen Bonding on the Viscoelastic Properties of Thermoreversible Networks: Analysis of the Local Complex Dynamics.* Polymer, 1995. **36**(3143-3150).

44. Muller, M.D., A.; Seidel, U.; Balsamo, V.; Iv´an, B.; Spiess, H. and R. W.; Stadler, *Junction Dynamics in Telechelic Hydrogen Bonded Polyisobutylene Networks.* Macromolecules 1996. **29 (7)**: p. 2577-2583.

45. Stadler, C.H.a.R., *Multiphase thermoplastic elastomers by combination of covalent and association chain structures: 2. Small-strain dynamic mechanical properties.* POLYMER, 1990. **31**: p. 819-825.

46. Zhang, Z., C. Huang, R. A. Weis, and C. Quan, , *"Association energy in strongly associative polymers,"* J. Rheol. . **61**: p. 1199–1207 (2017).

47. Ruymbeke, E.V., *Special Issue on Associating Polymers.* Journal of Rheology, 2017. **61**: p. 1099-1104.

Chapter2: Experimental techniques and protocols

2.1-^{1}H-NMR AS A CHARACTERIZATION TOOL

Proton Nuclear Magnetic Resonance (^{1}H NMR) Spectroscopy is a powerful method used in the determination of the structure of unknown organic compounds. The ^{1}H NMR spectrum of an organic compound provides information concerning:

- the number of different types of hydrogens present in the molecule.

- the relative numbers of the different types of hydrogens.

- the electronic environment of the different types of hydrogens.

- the number of hydrogen "neighbor" a hydrogen has.[48]

There are three isotopes of hydrogen used in NMR spectroscopy: ^{1}Hydrogen, ^{2}Deuterium and ^{3}Tritium. Each isotope resonates at a very different frequency for example if ^{1}H resonates at 400 MHz then ^{2}H resonates at 61.402 MHz. Only one isotope is observed at a time because the spectrometer transmits and receives over a very limited frequency range. The chemical shift ranges for all three nuclei are virtually identical and can be used for preliminary analysis but there the similarity ends. ^{3}Tritium is not commonly measured by NMR because it is radioactive.[49]

Each type of signal has a characteristic chemical shift range as it shown in Fig. 1.3.

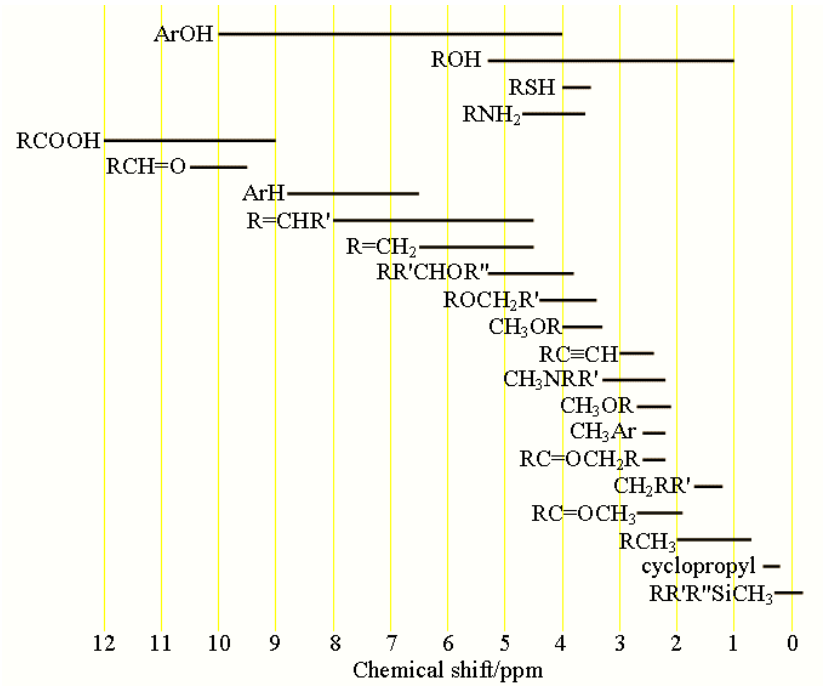

Figure2.1- chemical shift range of different species in NMR.[49]

2.1.1-^{1}Hydrogen (Proton) NMR

The ^{1}D ^{1}H (Proton) NMR experiment is the most common NMR experiment. The proton (^{1}Hydrogen nucleus) is the most sensitive nucleus (apart from tritium) and usually yields sharp signals. Even though its chemical shift range is narrow, its sharp signals make proton NMR very useful. NMR services provides proton NMR along with many other NMR techniques.

A typical analysis of a ^{1}H NMR spectrum may proceed as follows:

The number of protons of each type in the spectrum of a pure sample can be obtained directly from the integrals of each multiplet. This is only true if the multiplets are well separated and do not overlap the solvent or residual water signals and provided that the molecule is not undergoing slow conformational exchange. A routine NMR spectrum yields integrals with an accuracy of +/-10%. Accuracies of +/-1% can be achieved by increasing the relaxation delay to five times the longitudinal relaxation time (T_1) of the signals of interest. Where multiplets overlap, the total integral of the spectral region may be used.[48, 49]

2.2-RHEOMETRY AND MEASUREMENT PROTOCOLS

2.2.1-Measurement Procedure

In order to relate stress and strain, rheology is a powerful tool. In this Section, we briefly present the different rheometers which can be used to measure the viscoelastic properties of a sample under shear or elongation, and their respective advantages. In particular for this project, we used oscillatory shear rheometry in order to study the specific supramolecular system behaviors and more precisely the way the chains relax according to the composition of the samples. To obtain these data, a rotational rheometer is used. The operating mode of the rheological experiments carried out will also be described. Indeed, some operating conditions must be respected. Operating conditions concern both the stabilization of the sample and the experiments.

First of all, it is interesting to note that there are two distinct types of rheometrers which differ according to the geometry of the applied stress. Rheometers using the shear stress are called "rheometers of shear" while rheometers applying an extensional stress are quoted as "extensional rheometers". Among the shear rheometers another classification can be made between capillary rheometers and rotational rheometers. Therefore, the three main categories of rheometers are;[20]

• **The Capillary rheometer**, also called viscometer, it is the main device used to determine the viscosity of the material in shear. This piston-die system is used to measure the viscosity of molten polymers as function of temperature and rate of deformation. Its functioning is based on the extrusion principle where the polymer, liquefied by heat, is forced by a piston to flow into a cylinder through a capillary die. The movement of the piston at variable speeds makes it possible to determine the shear rates and to develop the viscosity curve. For those measurements, it is important to have a good knowledge of the dimension of the system.

In conclusion, it is noted that "*capillary rheometers are useful for determination of melt viscosity at shear rates well above those accessible in rotational rheometer. However, at some shear rate, pressure and temperature variations become important and must be taken in account in the analysis of data. Also, the occurrence of slip may limit the shear rate at which data can be obtained*." wrote John M Dealy.[20]

The capillary rheometry also makes it possible to evaluate the processes: swelling at the die exit, breaking of the rod, slipping on the wall, flow stress with or without flow, resistance of the extruder, etc .

• **The Rotational rheometer** is the second type of shear rheometers. It is the one used in this master thesis to collect the rheological measurements which will be explained more in details.

• **The Extensional rheometer** imposes an extensional loading to the material. The measurements obtained as a response to a stretching deformation are more difficult than those obtained by a shear deformation. In the extensional rheometry, the study of melt behaviour can be made by using uniaxial, biaxial and planar extensional flows but, in general, only the two first ones are used. The rheometer presented in Figure 2.2 is also called "Sentmanat Extensional Rheometer" and gives a uniaxial stretching. The device presents two cylinders, one of them being rotated by the rheometer motor while a gear train drives the slave drum. The sample is clamped to the cylinders at its ends. Given the great deformation undergone by the material, the extensional rheometry is usually used in non-linear regime. With a specific geometry, extensional rheological measurements can be carried out on a rotational rheometer. The contrary is not possible. As long as deformation are small enough to be in the linear regime, it is also possible to convert the measurements carried out in extensional tests into shear data and vice-versa thanks to relationships found, based on the generalized model of Maxwell.[6, 16, 20]

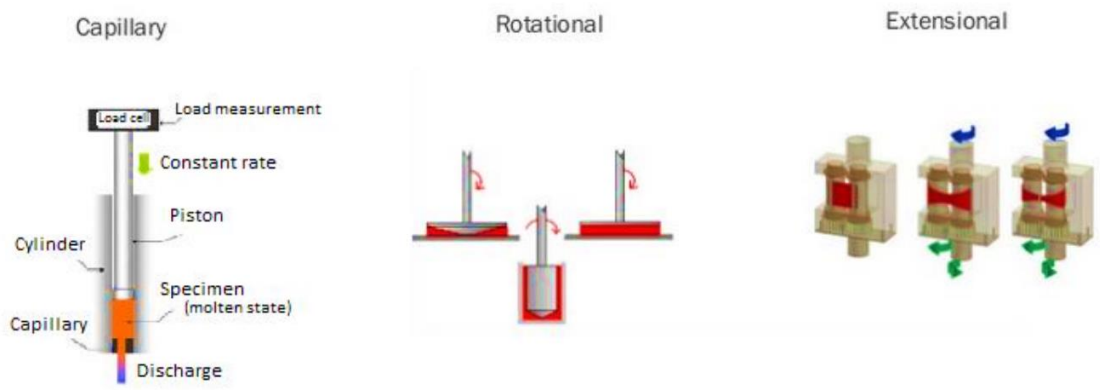

Figure 2.2- There are three main rheometers to measure the rheological properties. They are respectively from left to right capillary, rotational and extensional rheometers. The first two rheometers apply a shear stress and the last one is an example of extensional rheometer and corresponds to an extension loading of the material.[12]

2.2.2-Rotational rheometer

Rheometers can be of two types: controlled-stress and controlled-strain. A controlled-stress rheometer applies a torque to either control the stress at a desired level or to drive the strain to a desired amount. In this kind of rheometer the material is placed between two surfaces: a bottom surface, which is fixed, and a top surface, called the geometry, which rotates. In the controlled-stress rheometer, the torque or stress is the independent variable and is applied to the geometry. In the controlled-strain rate rheometer, the material is placed between two plates. The bottom plate moves at a fixed speed and the torsional force produced on the top plate is measured. Hence, for this case, the strain rate is the independent variable and the stress the dependent one. Here it is worth noting that a controlled-stress rheometer is a better approach for determining yield stress. With these instruments, the stress can be increased in a gradual,

controlled way until the yield point is reached. With controlled-strain instruments, the yield point has to be exceeded before the corresponding stress can be determined .Figure 2.3 shows a schematic representation of the geometry and the moving parts in a controlled-stress instrument.

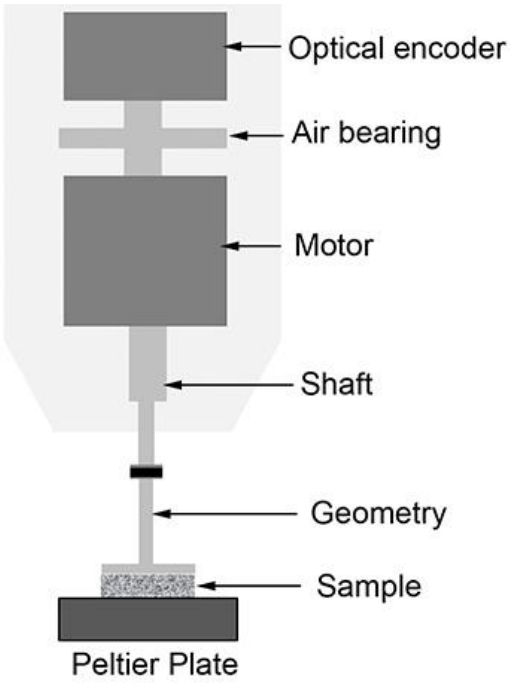

Figure 2.3- Schematic diagram of a stress controlled rheometer main unit.[50]

All the rheological measurements in this master thesis have been performed with a stress-controlled rotational rheometer MCR 301 (Anton Paar). It is a rotational rheometer with a shear loading of material. The Frequency range is between 10^{-5} – 10^{2} Hz and temperature range is between -40 – 200°C ± 0.01°C (Peltier-control). shear rate range10^{-5} – 10^{4} s^{-1} can be adjust between these range too.

various geometries are available:

- cone-plate (CP50): R = 25 mm; α=0.991°,sample volume: 0.6 ml
- plate-plate (PP25): R = 12.5 mm, sample volume for 1mm gap: 0.5 ml

This rheometer allows a good accuracy in linear regime but also in the field of non-linear rheology. [50]

The geometry plate-plate was used; it is one of the two plates is in rotation to give the shear stress. measurements for linear samples have been carried out with a plate-plate geometry.

2.2.3-Operating conditions

This section presents the loading and the experimental protocols. The experimental study presents three main steps for each temperature; an equilibrium phase, a strain sweep test followed by a frequency sweep test. In general, we used the plate-plate geometry of 8 mm. Therefore, the steps described below correspond to the experiments realized with the plate-

plate geometry. The final gap based on amount of material must be between 0.1mm and 0.3mm and stay unchanged during all experiments.

• **Equilibrium phase**: it is very important to give time to the sample so that it can reach its equilibrium and have a good homogeneity. The sample being prepared with 1 or 2 equivalents of transition metal ions, the metallo-ligand complexes required time to be formed. During the sample loading, two equilibrations must be realized; the instrument equilibration and the sample equilibration. The instrument is first of all equilibrated without the sample. To do that, we fix the instrument gap at zero with a command called the Zero Fixture a first time at room temperature. During that command, the device brings down its upper geometry until contact with the lower geometry and thus the obtaining of a normal force. This step is necessary in order to avoid facing big forces or damaging the instrument. The "gap", the distance between the bottom of the geometry and the top of the Peltier plate, might change due to changes in the temperature. When using temperature ramps it is important to compensate for any thermal expansion or contraction by performing a temperature calibration together with a bearing friction correction. The so-called "zeroing the Gap" is not a calibration, but rather a positioning of the geometry to tell the instrument where "0" is. Every time that a geometry is removed or the instrument turned on, the gap needs to be "zeroed". When zeroing the Gap is selected, the geometry is brought into contact with the Peltier plate. If sand paper is used, zero gap must be checked with the sand paper attached to the base and geometry and Peltier plate. Then we set the temperature at 60 °C and let it stabilizing for 20 minutes except for polymers without ions that the temperature is high enough to get any signal data. As a precaution, this operation is carried out each time when the sample is changed. Loading the sample also is important; So, we should avoid the problems like leaving some free space under the spinel or the material should not touch the spinel because it would make problem at low temperatures and frequencies. By playing a bit with final gap we can obtain a perfect sample without bubbles.[6, 20, 27]

• **Strain sweep test** during this test by applying a constant frequency and changing the strain the linear regime can be obtained. Repeating this test must show similar data and if there would be any problem it can be also an indication of a problem in sample loading or the sample is non-equilibrium state. As This test was performed for all the samples and shows 5% strain is a reasonable far away point from non-linear regime.

• **Frequency sweep test:** in a "frequency sweep" test the frequency is ramped between a minimum and a maximum value. A sweep between 0.1 to 10 Hz is a good first option. In a frequency sweep, the user needs to select one variable to be controlled: torque (µN·m), oscillation stress (Pa), the displacement (rad), or the %strain. This test gives us some information about the polymer behavior. To obtain reproducible results, it is essential that the sample is homogenized and stabilized beforehand. To ensure that it is well the case, this test was repeated three times at a specific temperature (here 60 °C). This test is performed three times in a row, at least for this temperature. The frequency sweep test is a shear dynamic measurement performed by a sinusoidal loading. During this test, the frequency of the loading is progressively changed while the load is stress controlled with a constant strain of 5%. By progressively varying the frequencies, we can have access to the viscoelastic response as function of the frequency, in other words, we obtain G'(ω) and G"(ω) according to the range

of the frequencies probed. Indeed, a relationship allows us to link the value of the storage and loss moduli to the complex stress of the sample. The data obtained by SAOS (small amplitude oscillatory shear) measurements realized in the strain-controlled way, answers to a sinusoidal behavior**.** In the next sections more details about each experiment based on nature of sample are explained.[20]

References:

1. Gregory R. Fulmer, A.J.M.M., *NMR Chemical Shifts of Trace Impurities: Common Laboratory Solvents, Organics, and Gases in Deuterated Solvents Relevant to the Organometallic Chemist.* organometllalics, 2010. **29**: p. 2176–2179.

2. http://chem.ch.huji.ac.il/nmr/techniques. *NMR techniques*.

3. Larson, J.M.D.R.G., *Structure and Rheology of Molten Polymers*. 2005, Munich: Hanser.

4. Guillet, P., *Metallo-Supramolecular Block Copolymers: From Synthesis to Smart Nanomaterials*. 2008, Uclouvain.

5. BLOND, J., *Rheology of metallo-supramolecular model polymer based on telechelic poly(n-butyl acrylate)s and metal-ligand interactions*. 2017, uclouvain.

6. Ruymbeke.E, B.C.a.v., *Rheometry and Polymer Processing*, in *MAPR 2018*. 2018.

7. *Controlled-Stress Rheometry*. Available from: http://lipidlibrary.aocs.org/Biochemistry/content.cfm?ItemNumber=40883.

8. E. van Ruymbeke, L.B., S. Coppola, S. Righi, D. Vlassopoulos, *Decoding the viscoelastic response of polydisperse star/linear polymer blends.* Journal of Rheology, 2010. **54**.

Chapter 3: Synthesis of Linear Supramolecular Polymer

Outline:

This chapter aims at the description of the polymer synthesis involved in the supramolecular systems studied. The study of the linear supramolecular formed by metallo-ligand associations requires the functionalization of polymer which will also be described completely here. In this chapter, the protocol to follow with the different steps to get those systems would be described. A characterization of intermediate molecules would also be provided.

3.1-PREPARING SUPRAMOLECULAR POLYMERS

Polybutadiene was first prepared in the early years of the 20th century by methods as sodium-catalyzed polymerization of butadiene. However, the polymers produced by these methods and also by the later free-radical emulsion polymerization techniques did not possess the properties which made them desirable rubbers because the architecture of the backbone was not precisely controllable. With the development of the Ziegler–Natta catalyst systems in the 1950s, it was possible to produce polymers with a controlled stereo regularity, some of which had useful properties as elastomers.

Polymers containing 90–98% of a cis-1,4-structure can be produced using Ziegler–Natta catalyst systems based on titanium, cobalt or nickel compounds in conjuction with reducing agents such as aluminum alkyls or alkyl halides. Useful rubbers may also be obtained by using lithium alkyl catalysts but in which the cis content is as low as 44%.

The structure of cis-1,4-polybutadiene is very similar to that of the natural rubber molecule. Both materials are unsaturated hydrocarbons but, whereas with the natural rubber molecule, the double bond is activated by the presence of a methyl group, the polybutadiene molecule, which contains no such group, is generally somewhat less reactive. Furthermore, since the methyl side group tends to stiffen the polymer chain, the glass transition temperature of polybutadiene is consequently less than that of natural rubber molecules.

This lower Tg has a number of ramifications on the properties of polybutadiene. For example, at room temperature polybutadiene compounds generally have a higher resilience than similar natural rubber compounds. In turn this means that the polybutadiene rubbers have a lower heat build-up and this is important in tire applications. On the other hand, these rubbers have poor tear resistance, poor tack and poor tensile strength. For this reason, the polybutadiene rubbers are seldom used on their own but more commonly in conjunction with other materials. For example, they are blended with natural rubber in the manufacture of truck tyres and, widely, with SBR in the manufacture of passenger car tires. The rubbers are also widely used in the manufacture of high-impact polystyrene.[1]

In this section, bulk supramolecular polymer prepared from a hydrogenated polybutadiene based on bearing the terpyridine end-functionalized group and different metal ions, to highlight the difference of this supramolecular polymer from a well-established-supramolecular system based on theories.

3.1.1.-An Introduction to hydrogenated, hydroxylated polybutadiene and its properties

Hydrogenated, hydroxylated polybutadiene with molecular weight of 3 kg/mol, Tg, -55°C number-average functionality is 1.9 kindly donated from Cray Valley(KRASOL, HLBH-3000) It is an odorless, water clear, saturated aliphatic liquid. The saturated nature of the resin provides light and weather-stability, enabling formulators to develop coatings that will not yellow or lose their critical mechanical properties, such as flexibility, adhesion, elongation, and strength.

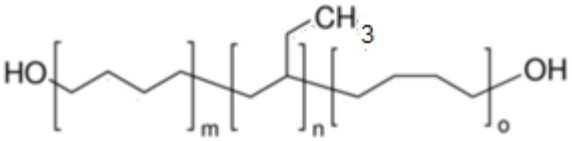

Figure 3.1- Hydrogenated, hydroxylated polybutadiene (Mn=3kg/mol, hydrogenation extent, % >98)

There has been increasing interest in segmented polyurethanes based on polybutadiene soft segments. The low moisture permeability of these materials makes them more suited for certain applications than the more conventional polyether or polyester based polyurethanes, despite inferior abrasion resistance and tensile and tear strength. Another useful application of the polybutadiene-based materials is as electrical potting and encapsulating compounds. [2]

In light of the earlier work on phase segregated poly- urethane systems, one very interesting feature of the polybutadiene-containing polyurethanes is the complete elimination of hydrogen bonding to the soft segment due to the hydrocarbon nature of the butadiene backbone. By restricting hydrogen bonding to the hard segments only in this way, phase segregation is promoted. such materials provide a system for studying the role played by micro phase separation in determining polyurethane properties, in the absence of inter-phase hydrogen bonding. Therefore, in the ideal case of a linear polybutadiene-containing polyurethane, with the absence of inter-phase hydrogen bonding and crystallinity, properties will depend on the extent of phase separation and the organization of hard and soft domains.[3]

Anionic polymerization technology has been used for the production of KRASOL® polybutadienes. This method permits the production of well-defined linear polymeric products of a specific microstructure, with exactly set molecular weight in a narrow range and with reactive functional groups built-in on both ends of polymeric chains. These characteristics distinguish this product significantly from similar liquid butadiene polymers, produced by other technologies, such as by radical polymerization. It contains nearly one hundred percent of polymer molecules with two functional groups. Besides the main proportion of bifunctional macromolecules (min. 92%), KRASOL contain only small amounts of monofunctional polymer and polymer without functional groups. This is important point, as in the next chapter it would be assumed that all the chains are bifunctional so by adding proper amount of metal ions they should make a long chain by associations through metal ligand coordination although the correctness of this assumption would be investigated by rheological characterization and available models.

A significant feature of the hydrogenated polybutadiene of this sample is its specific microstructure. Roughly two thirds of the butadiene molecules are polymerized in the 1,2-configuration, which means that the polymers contain approximately 65% vinyl groups in their chain. This places it in the medium or medium high content of vinyl structures according to established classification. This feature is significant for its chemical reactivity, processing

properties and final properties of products made from it. It affects the viscosity of liquid polybutadiene, its glass transition temperature, thermos oxidation stability, resistance to UV radiation and other properties. In addition, hydrogenation preferentially took place in the pendant vinyl groups, as could be expected since these groups are more accessible for reaction. Mango and Lenz, who showed that the rate of hydrogenation of the pendant vinyl double bonds was greater than that of the internal double bonds. In addition, it was seen that hydrogenation in the 1,4-units preferentially took place in the cis units. Crystallization may be possible if long enough sequences of methylene units are present but the random placement of the hydrogenated vinyl groups probably precludes any extensive crystallinity in these prepolymers.[2, 4, 5]

3.2-FUNCTIONALIZATION PROCESS

Functionality determination: The hydroxyl values of the HTPB's can be determined by a procedure suggested by ARCO Chemical Co. The hydroxyl groups were acetylated with an excess of acetic anhydride in pyridine. The amount of reagent which reacts with the sample was determined by titrating the excess hydrolyzed anhydride and resulting acetic acid with alcoholic potassium hydroxide. The hydroxyl value was reported as the milli equivalents of hydroxyl groups per gram of material. The average functionality was then determined by multiplying the number of equivalents per gram by the molecular weight of the HTPB for each HTPB.[6]

Functionalization process: Two strategies to substitute the hydroxyl group with terpyridine was tried. The first strategy was direct substation of hydroxyl group through a nucleophilic reaction with 4′-Chloro-2,2′:6′,2″-terpyridine which high conversion was not obtained. The second strategy to increase the conversion of functionalization was to susbsitute the Hydroxyl group with better leaving groups like toluenesulfonyl and later substituting the leaving group with terpyrdine species as 2,6-Bis(2-pyridyl)-4(1H)-pyridone. This strategy was successful and it lead to complete conversion of reaction. Although during these procedure other critical parameters for example solvent, temperature, duration of reaction and etc. were fully investigated and optimized. These Steps will be explained thoroughly in this chapter.

3.2.1-First strategy of Functionalization, direct substitution

Nucleophilic substitution reactions occur when an electron rich species, the nucleophile, reacts at an electrophilic center attached to an electronegative group, the leaving group, that can be displaced as shown by the general scheme:

Figure 3.2 nucleophilic substitution reaction.

The electrophilic center can be recognized by looking for the polar σ bond due to the presence of an electronegative substituent (for example C-Cl, C-Br, C-I and C-O) Nucleophilic substitution reactions are an important class of reactions that allow the interconversion of

functional groups. In this step 4′-Chloro-2,2′:6′,2″-terpyridine as an electrophilic center was used with NaOH to replace with hydroxyl group.

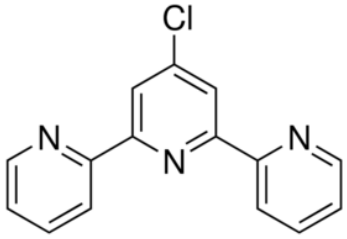

Figure 3.3-Chemcial structure of 0—1-4′-Chloro-2,2′:6′,2″-terpyridine

4′-Chloro-2,2′:6′,2″-terpyridine (Cl-terpy) is a tridentate ligand that contains a terpyridine (tpy) site with a Cl site at the 4′-position. It coordinates with various metal ions through these two sites to form different coordination polymers.

Procedure: The reaction was started with 1 equivalent of polymer (1 gr.) with 2 equivalents of 4′-Chloro-2,2′:6′,2″-terpyridine (0.178 gr.) and 2 equivalents of NaOH (0.026 gr.) in the relevant amount of Toluene (50 mL) at 65 °C, under purge of N_2; After 48 hours it was stopped. Toluene was removed and, the polymer was dissolved in DCM and washed with water then it was precipitated in methanol. Later the precipitated polymer was kept under high vacuum for 24 hours to remove all the solvent.

To study the yield of the reaction the ^{1}H-NMR (500 Hz, in deuterated chloroform) spectra of starting hydrogenated, hydroxylated polybutadiene and of the sample after 48hours of reaction in Toluene were compared.

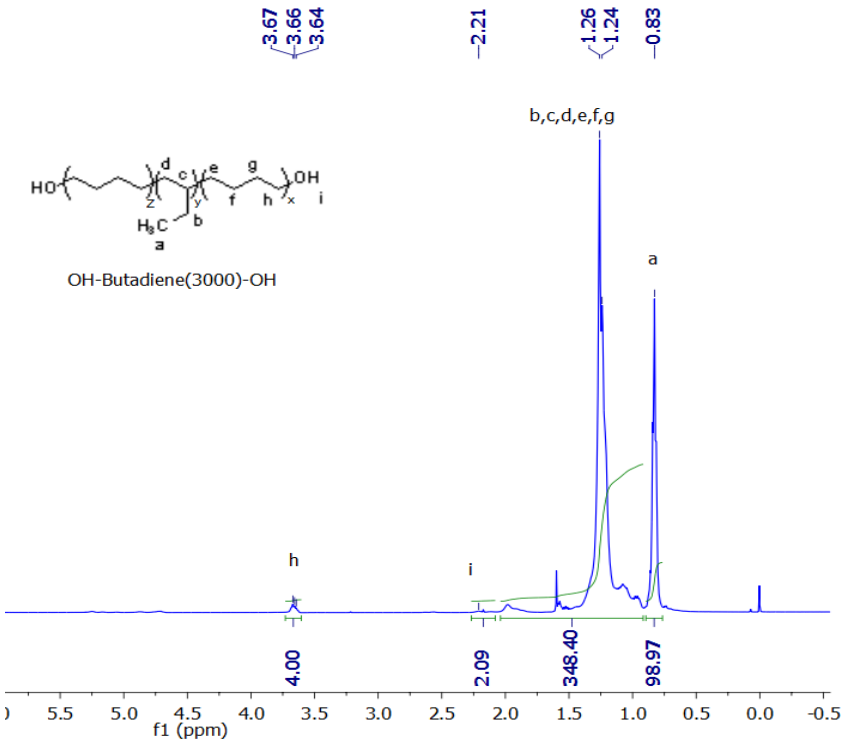

Figure3.4- ^{1}H NMR (500 Hz, in deuterated chloroform) spectrum of the hydrogenated, hydeoxylated polybutadiene 3kg/mol

In this spectra by computing number of the protons in (-CH_3) and other protons in the back bone the ratio of 65% vinyl groups in the initial sample can be observed.

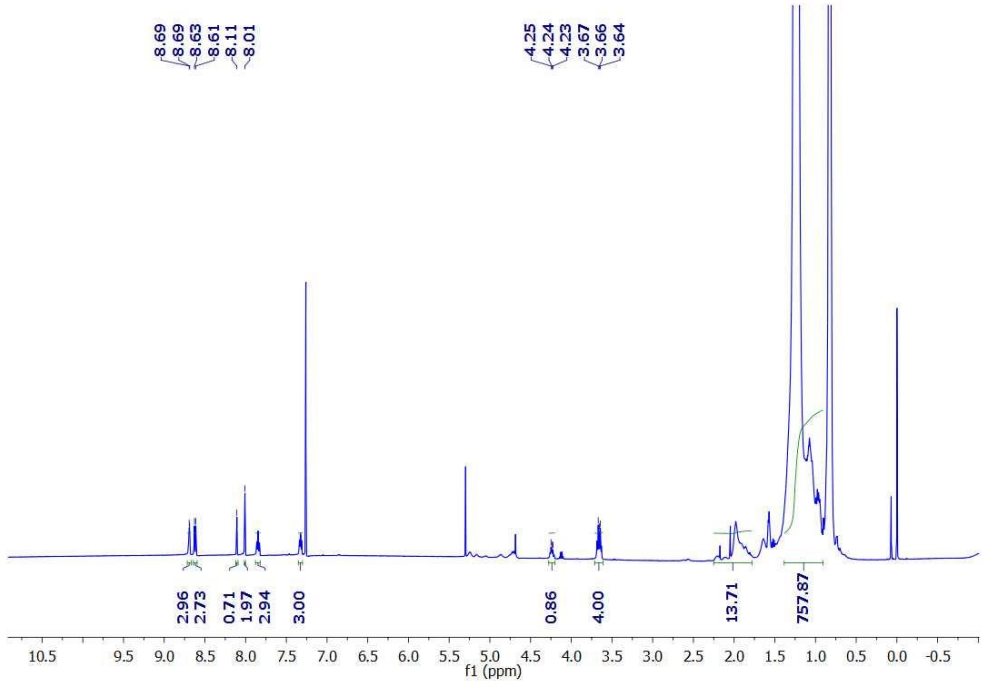

Figure3.5- ^1H NMR (500 Hz, in deuterated chloroform) spectrum of the hydrogenated, hydeoxylated polybutadiene 3kg/mol after 48 hours of reaction (20% conversion)

By comparing the aromatic proton peaks (7-9 ppm) in Figure 3.5 it is obvious that the reaction has a very low conversion (20%, obtained by ratio the intensities of the peak at 4.25 (ppm) and at 3.75(ppm) corresponding to protons of CH_2-O; During substation of hydroxyl groups by terpyridine they would shift to higher frequency) therefor, another possible synthesis should be investigated.

3.2.2-Second strategy of functionalization

As it was observed in previous section the reaction did not lead to 100% conversion. since the first strategy did not provide desired results we tried to "reverse" the strategy; we transformed the PB chain-end into good leaving group (by tosylation) and we used a tpy derivative as nucleophile because in nucleophilic substitution reactions of alkyl halides (R-X) and alcohols (R-OH), the range of substitution reactions can be increased by utilizing the tosylates (R-OTs) which is an alternative method of converting the -OH to a better leaving group. [7]

Tosylation of hydroxyl-functionalized substrates is an important transformation to activate hydroxyl groups, thus yielding substrates for further nucleophilic substitution in various fields of organic syntheses. In general, the treatment of alcohols with tosyl chloride and, a amine base in an organic solvent is a conventional method to prepare tosylates.[7]

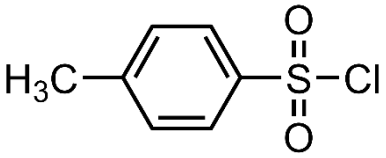

Figure 3.6- chemical structure of toluenesulfonyl

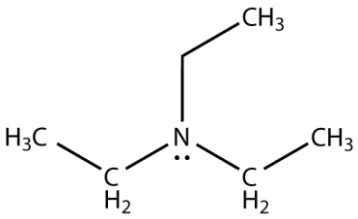

Figure 3.7- chemical structure of Triethylamine

Procedure: The reaction started with the same situation in two different solvents. The reaction of HPBD-$(OH)_2$ of 1 equivalent (5 gr.) with 10 equivalents of Toscl (3.164 gr) and 20 equivalents of Triethylamine (4.614 mL) in the appropriate amount of Toluene (80 mL) and for the second one in THF (80 ml) at 70 °C under purge of N_2 was run for 48 hours. Solvent was removed by a rotary evaporator then the remaining product was dissolved in dichloromethane and washed with water three times and one time with braine solution. The organic phase was then dried with sodium sulfate, and the solvent was removed under vaccum. The polymer was finally precipitated twice in pure methanol. Polymer was dried under high vacuum for 48 hours.

^{1}H-NMR analysis (500 Hz, in deuterated chloroform) which proved a 100% of conversion as it shown in Fig.3.8. Consequently, the PBD-$(OTs)_2$ with perfect degree of functionality was obtained.

The same procedure was followed for other reaction in THF to test the influence of the solvent. Due to bad solubility of the polymer in THF the conversion was only around 60% .

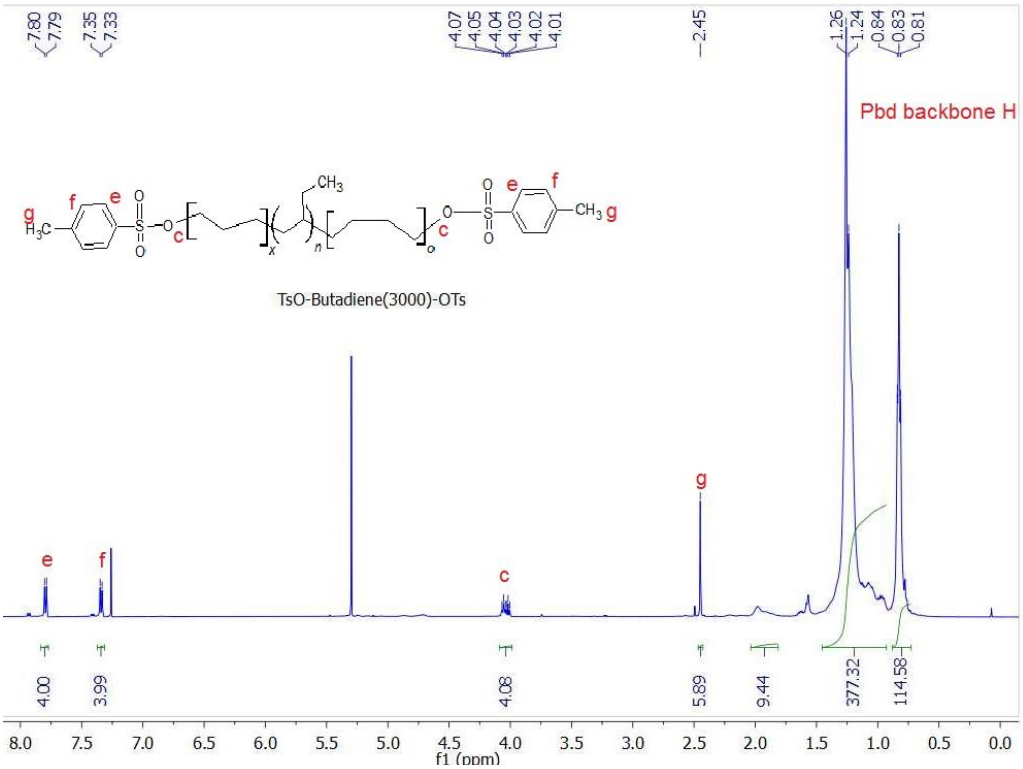

Figure 3.8- 1H NMR (500 Hz, in deuterated chloroform) spectrum of PBD-$(OTs)_2$

After obtaining the PBD-$(OTs)_2$, the second step to subsititution of the OTs group by the terpyridine ligand could be perfomed the schematic of reaction is shown at Fig 3.11.

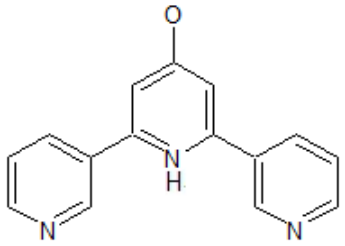

Figure 3.9- the chemical structure of 2,6-Bis(2-pyridyl)-4(1H)-pyridone

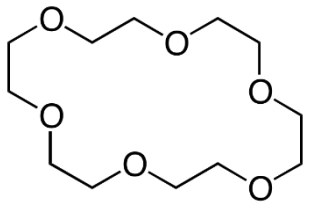

Figure 3.10-the chemical structure of 2-18-Crown-6

Procedure:4 equivalents of 2,6-Bis(2-pyridyl)-4(1H)-pyridone (0.74 gr.) 4 equivalents of K_2CO_3 (0.413 gr.) 1 equivalent of polymer (2.5 gr.) and 1 equivalent of 18-crown-6 (160 µL)

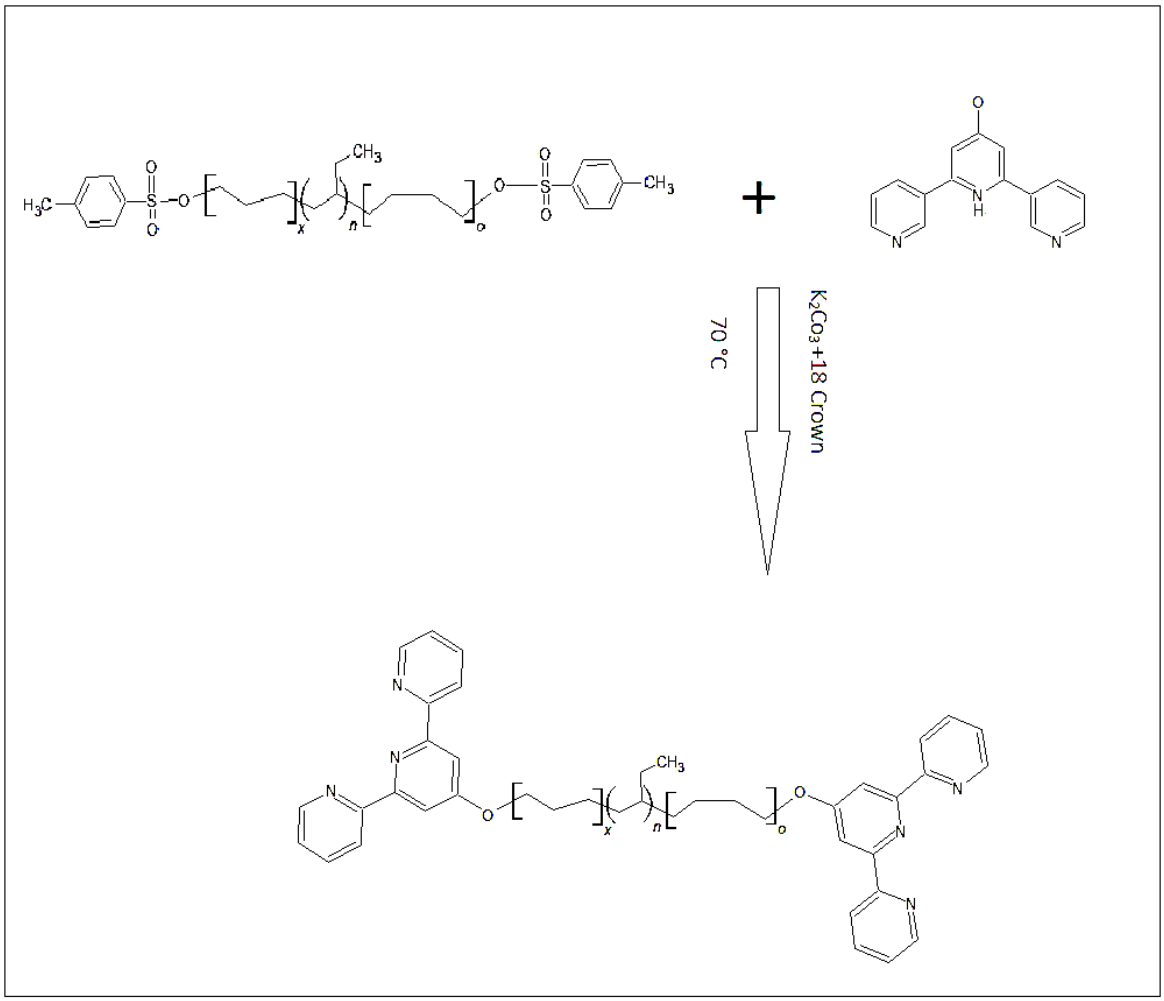

Figure 3.11- The schematic of the reaction of substituting the OTs groups by the terpyridine ligand.

were dissolved in Toluene (60 mL). The temperature was fixed at 70 °C under purge of N_2 and the reaction was run for 48 hours.

The same procedure of washing and precipitation as described in previous section was followed. The final material was characterized by ^{1}H-NMR and the spectrum showed a successful reaction with functionalization degree 100%. (Fig.3.12)

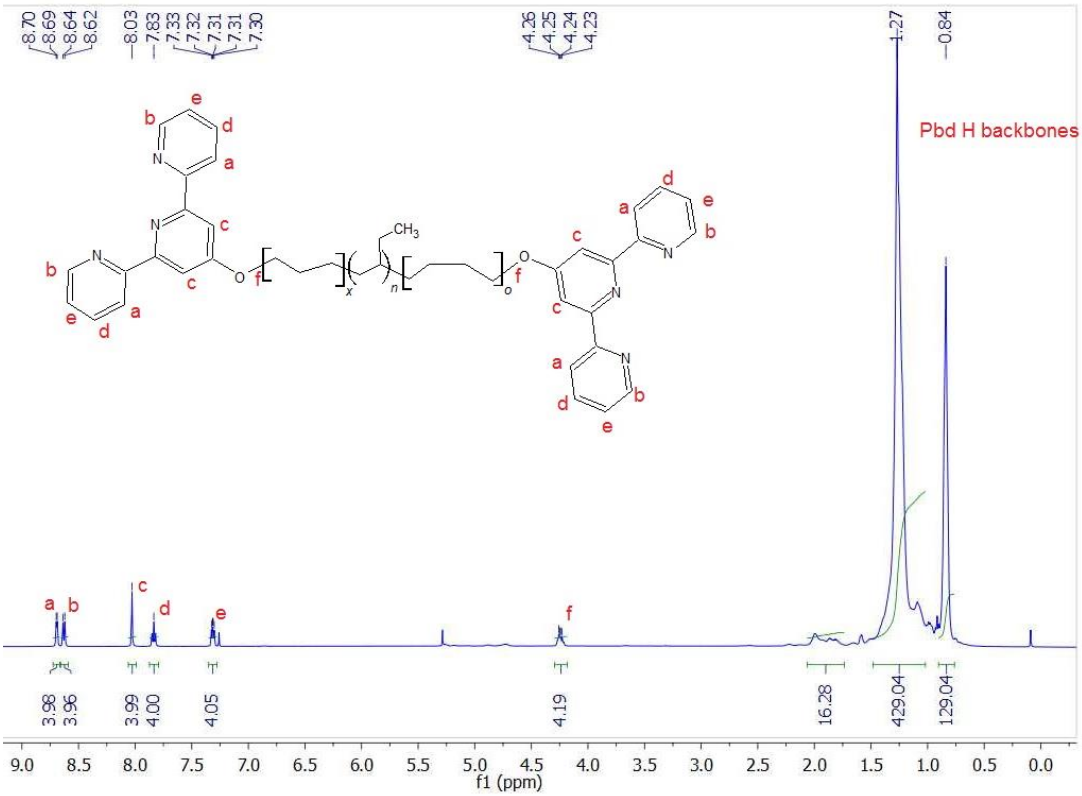

Figure 3.12- ^{1}H NMR (500 Hz, in deuterated chloroform) spectrum of PBD-(tpy)$_2$

3.3-PREPARING METALLO-SUPRAMOLECULAR POLYMERS OF PB(TPY)$_2$

In order to have clear vision in the next chapter about the effect of the metal ion nature and the effect of their amount compared to the amount of terpyridine ligands, four different samples were prepared. These samples will help us to understand these parameters the effect of these parameters.

Two different metal salts were selected and we prepared samples containing 1 and 2of metal ions compared to the polymer chain (i.e. respectively 0.5 and 1 equivalent with respect to terpyridine ligand). The solubility of metal salts and of the polymer is crucial and different solvents were thus tested to find suitable candidates.

The first metal salt Zinc di(bis(trifluoromethylsulfonyl)imide) (Synonym: $Zn(NTf_2)_2$,>95%) was used. NTFs counter ion here is well soluble in chloroform which would be used for dissolving of the polymer. Bistriflimide (NTf_2^-) was chosen as the counterion because of its thermal stability and non-coordinating nature.[8] The second metal salt was Cobalt di(bis(trifluoromethylsulfonyl)imide) (Synonym: $Co(NTf_2)_2$,>95%) .

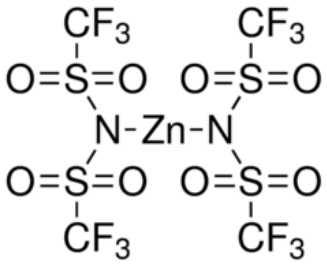

Figure 3.13- Chemical structure of Zinc di[bis(trifluoromethylsulfonyl)imide]

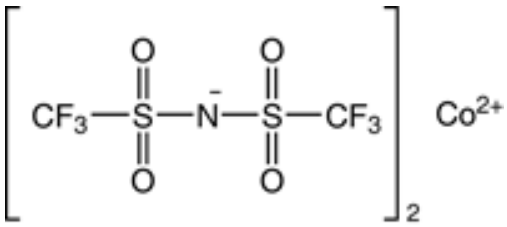

Figure 3.14- Chemical structure of Zinc di[bis(trifluoromethylsulfonyl)imide]

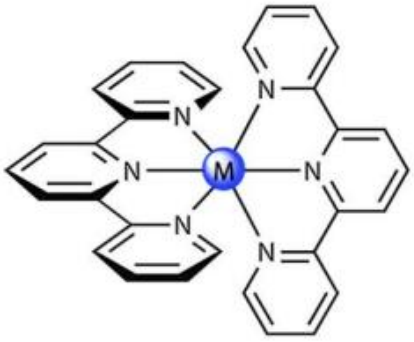

Figure 3.15- Terpyridine complex.[9]

The mixing procedure: To prepare one equivalent sample of PBD(tpy)$_2$-Zn, 35.7 mg of Zinc di(bis(trifluoromethylsulfonyl)imide) was solved in 200 µL of acetonitrile and 200 mg of polymer were solubilized in chloroform (500 µL). Under stirring the polymer solution was kept at 40 °C and metal solution was added slowly, letting the metal ions to form the metal-ligands bonds. The combination of equimolar amounts of Zn(NTf$_2$)$_2$ and PBD(tpy)$_2$ in solution caused a rapid viscosity increase, indicative of supramolecular assembly. The solution was stirred for 10 minutes and no phase separation happened during this mixing or even after stopping the stirring. The solvent was then removed under reduced pressure and the sample was kept under high vacuum for 24 hours.The same procedure was repeated to prepare the two equivalent sample of PBD(tpy)$_2$-Zn.

To prepare the one equivalent sample of PBD(tpy)$_2$-Co, 35 mg of Cobalt di(bis(trifluoromethylsulfonyl)imide) were solved in 200 µL of acetonitrile and 200 mg of polymer solubilized in 500 µL of chloroform under stirring. The polymer solution was kept in 40 °C and metal solution was added slowly, letting the metal ions to form the metal-ligands bonds. The solution was stirred for 10 minutes and as some phase separation happened during this stirring by adding extra amount of chloroform (100 µL) it disappeared and homogenous solution was obtained and even after stopping the stirring no phase separation occurred. The solvent was then removed by reduced pressure and the sample was kept under high vacuum for 24 hours. Some small pink regions that showed aggregation of metal salts and phase separation appeared after vacuum. Therefore, this region was washed with acetonitrile. The same procedure was repeated to prepare two equitant sample of PBD(tpy)$_2$-Co.

Figure 3.16 shows the obtained Zn and Co supramolecular polymers.

Figure 3.16- Final sample of PBD(tpy)$_2$-2eq-Zn (left) and PBD(tpy)$_2$-2eq-Co (right).

3.7-Experimental section:

First strategy Materials: 4′-Chloro-2,2′:6′,2″-terpyridine from TCI, Sodium hydroxide (reagent grade 97%, powder) from Sigma Aldrich and dried Toluene (max. 0.005% H_2O) from Merck were used.

Second strategy Materials: 4-toluensulfonyl chloride (CAS-number:98-59.9) and dried Toluene both from Merck and Triethylamine (≥99.5%- 471283) from SIGMA-ALDRICH was used. 2,6-Bis(2-pyridyl)-4(1H)-pyridone (>98.0%-(HPLC)(T)) from TCI chemical, K_2CO_3 (>99.995%) from Sigma Aldrich, 18-crown-6 and dried Toluene (max. 0.005% H_2O) both from Merck were used.

Mixing procedure Materials: Zinc di(bis(trifluoromethylsulfonyl)imide) (Synonym: $Zn(NTf_2)_2$,>95%) was obtained from Sigma Aldrich. Cobalt di(bis(trifluoromethylsulfonyl)imide) (Synonym: $Co(NTf_2)_2$,>95%) was also obtained from Sigma Aldrich.

References:

1. Brydson, J.A., *Plastics Materials*. 1999: Elsevier.

2. A.F. Puchkov, I.A.N., A.V. Nistratov, O.O. Tuzhikov, V.F. Kablov, and S.V.L. P.N. Orlyanskaya, and D.V. Pyl'nov, *Polyurethanes with different molecular weight characteristics as materials for assessing the damaging effects of ozone.* International Polymer Science and Technology, 2014. **42**: p. 22-25.

3. C. G. Seefried, J.V.K.a.F.E.C., *Thermoplastic urethane elastomers. II. Effects of variations in hard-segment concentration.* J. Appl. Polym. Sci., 1975. **19**: p. 2493-2495.

4. *cray-valley-products-for-polyurethane-lpbd*, in *USA*, C. Valley, Editor. 2013.

5. Lenz, L.A.M.a.R.W., *Hydrogenation of unsaturated polymers with diimide.* Makromol. Chem., 1973. **13**: p. 163.

6. Ramey, K., *"Characterization of R-45M, Final Report".* in *AFRPL-TR.* p. 74-64.

7. George W. Kabalka, M.V., and Rajender S. Varma, *Tosylation of Alcohols.* Tosylation of Alcohols, 1986. **51**: p. 2386-2388.

8. Mark Burnworth, L.T., Justin R. Kumpfer1, Andrew J. Duncan, Frederick L. Beyer, Gina L. Fiore, Stuart J. Rowan& Christoph Weder, *Optically healable supramolecular polymers.* Nature, 2011. **472**: p. 334-339.

9. Guillet, P., *Metallo-Supramolecular Block Copolymers: From Synthesis to Smart Nanomaterials*. 2008, Uclouvain.

Chapter 4: Rheology Results

Outline:

In this chapter the result of the rheological characterization of the samples will be fully discussed. First, the effect of functionalization and later the effect of association which created by phase separation and metal-ligand coordination will be studied. Finally, by putting all of these measurements and information together a clear perspective of the whole phenomena of the chains dynamic will be obtained.

Results:

4.1-VISCOELASTIC PROPERTIES OF LINEAR ENTANGLED METALLO-SUPRAMOLECULAR POLYMERS

In this section we present the linear viscoelastic properties of supramolecular assemblies obtained by adding different amounts of metal ions into linear PB$(tpy)_2$ building blocks end-functionalized by a terpyridine group (see chapter 3).

Since the building blocks are linear, it is expected that long linear assemblies, made of several building blocks, are formed. In such a case, the elasticity of these supramolecular assemblies should be mainly governed by the entanglement dynamics of the building blocks, while the relaxation time of these systems should be dominated by the supramolecular interactions, by adjusting the amount of metal ions, the length of the linear assemblies should be varied, with direct influence on the relaxation time.

On other hand, due to possible secondary supramolecular interactions such as phase sepraration of the complexes (see section 1.5), a second, low frequency plateau could be observed for these supramolecular assemblies. Indeed, in such a case the associated or phase-separated domains act as branching points for the supramolecular assemblies and consequently, a fraction of the sample cannot flow anymore, giving rise to this second plateau.

Aggregation of the junctions as it is shown in Figure 4.6 is responsible for different behavior from initial sample. In other words, the supramolecular samples consist of a biphasic structure. The main phase is the PB linear chain, while part of the metal-ligand complexes forms clusters together with the metal salts. Thus, the chain-ends of a given building block (i.e. the functionalized PB with a mass 3kg/mol) can in principle act as chain extenders (by the formation of the complexes) as well as form be part of clusters of complexes, acting as crosslinking points.

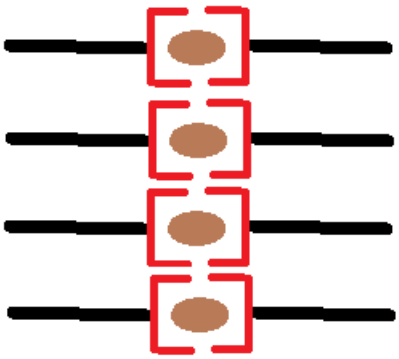

Figure 4.1-Aggregation of metallo-supramolecular junctions.

Within such scenario, it seems interesting to investigate if the addition of metal ions above the 1:2 metal ion/terpyridine stoichiometric ratio allows promoting the creation of such secondary supramolecular interactions to lead to the reversible gelation of the system. By comparing the rheological behavior of $PB(tpy)_2$ samples, without any ions, we aim at determining the influence of these possible extra supramolecular bonds and the role of excess of metal ions.

4.1.1- Reference and Functionalized PB

We first study the viscoelastic properties of the reference sample which is hydrogenated, hydroxylated polybutadiene with molecular weight of 3 kg/mol. In the following, we refer to it as "IndPBD". We compare its properties to the properties obtained after functionalization of the end groups with terpyridine ligands. The measurements were done under the same conditions to compare the effect of functionalization. Results are shown in Figure 4.2. . A deviation is observed between the reference and the functionalized sample.

As observed by Hilger et al. (see section 1.5) this deviation from the expected behavior may still happen because of polar terpyridine end-groups can form associations. First, as it can be observed that the flow regime, characterized by the slopes 1 and 2 in the low frequencies domain can be seen for the reference sample. Indeed, the Rouse relaxation of the chains takes place until full relaxation of the chains as the molecular weight is below the limit of entanglements so no plateau would be observed. The measurement on the $PBD(OH)_2$ and $PBD(tpy)_2$ was done between -20 °C and 10 °C (interval of 10 °C). Above 10 °C getting signals of G' is difficult since the samples become too liquid like and starts to flow. On other hand, below -20 °C the samples might get close to T_g and it would start to increase the normal force or it might induce crystallization which is not favorable at all. For the range of temperatures explored, a master curve could be built, which followed Time-Temperature Superposition (TTS) very well.

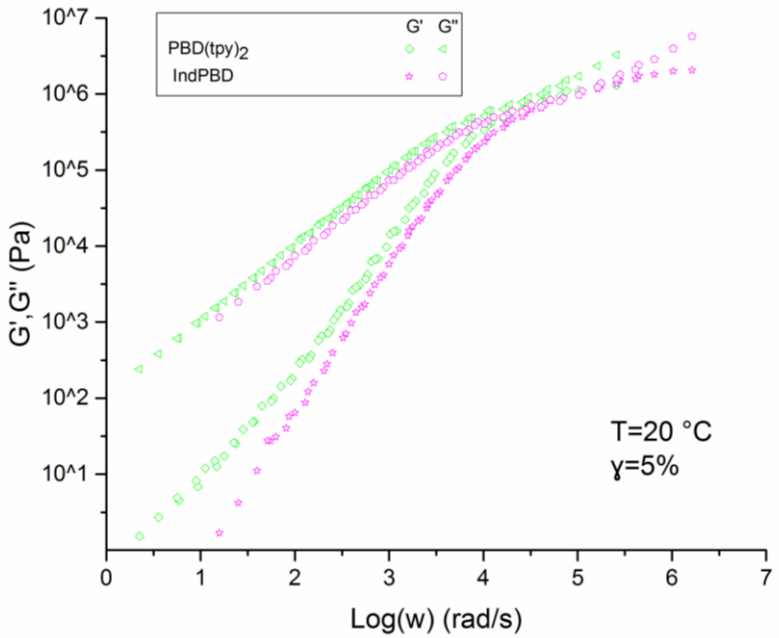

Figure 4.2- Linear rheology master curves at 20 °C of linear bifunctional PBD(tpy)2 and $PBD(OH)_2$ (melts)

Then, we can also observe that significant difference appears between the viscoelastic response of the two samples. In order to understand it, it is essential to notice that the hydrogenated,

hydroxylated polybutadiene also has different behavior from linear polybutadiene as explained in chapter 1 because low-molar-mass polybutadienes, as well as their hydrogenated analogues, form hydrophobic domains which contribute to the existence of supramolecular clusters detectable by dynamic light scattering. These domains, and hence also the clusters, gradually and reversibly disintegrate with increasing temperature for original polybutadienes but persist in their hydrogenated derivatives.[1]

The deviation of the PBD(tpy)$_2$ from PBD(OH)$_2$, behavior especially in the flow regime can prove that the terpyridine group form aggregation and there could be phase separation between terpyridine groups and the polybutadiene backbones. In addition, it is important to notice that the polymer chains have a low molecular weight around 3kg/mol and both terpyridine groups at the chain-ends have a molecular weight around 466 g/mol which is non-negilible. This probably explains the slower relaxation of the functionalized sample, compared to its precursor. Furthermore, terpyridine groups have much bigger steric effects compared to hydroxyl ones. To go further in analysis of the curves, one can compare these experimental results to the predicted data obtained based on the tube model (see Section 1.4). As shown in Figure 4.3, it is possible to determine material parameters to accurately describe the viscoelastic properties of PBD(OH)$_2$. However, based on these parameters, the model cannot properly capture the behavior of PBD(tpy)2. Since the deviation is already seen at high frequency, one cannot exclude some difference in Tg value between the two samples.

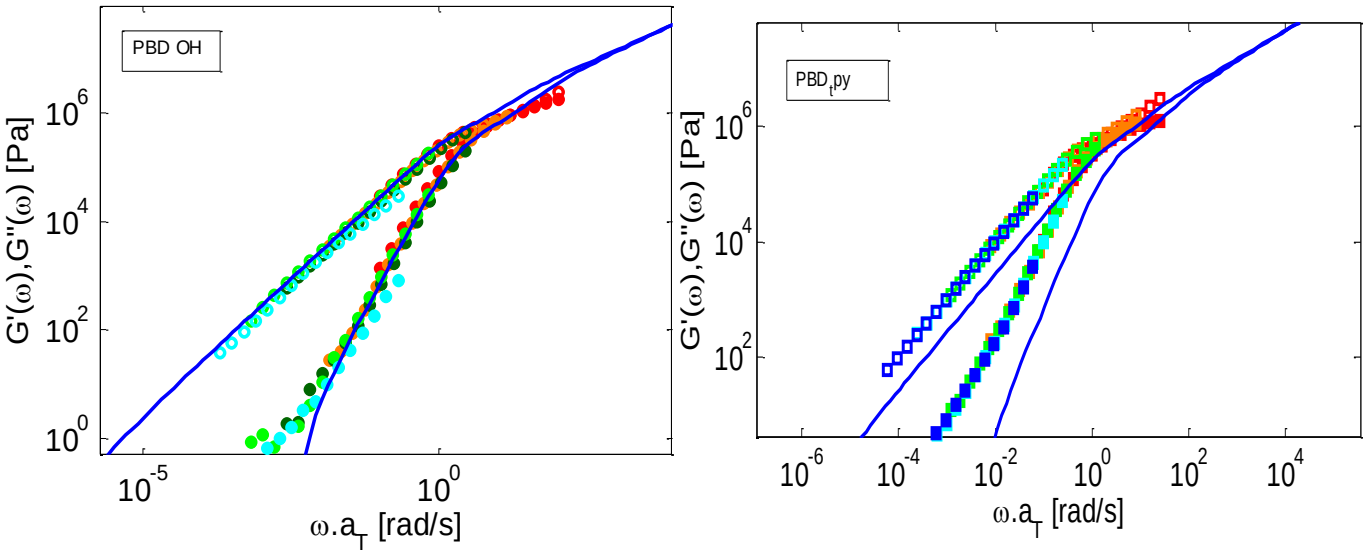

Figure 4.3- Comparison of experimental data with tube models prediction of PBD(OH)$_2$ (left) and PBD(tpy)$_2$ (Ref. sample: Mw=3000g/mol, G^0_N= 1,8MPa; M_e=1650; τ_e=0.15s)

4.1.2-Metallo-supramolecular of PBD(tpy)$_2$

We now add metal ions in the polymer of PBD(tpy)$_2$ in order to obtain longer assemblies. When the stoichiometric amount of metal ions is added to PBD(tpy)$_2$, the idealistic case of the formation of a single super-long entangled supramolecular chain loop as represented in Figure 4.4 is to be reached. However, in the real case bifunctional associating polymers rather self-assemble into assemblies containing few or several building blocks, and of various lengths (see Fig. 4.4-b). This high PDI in the length of the supramolecular assemblies leads to a large

spectrum of relaxation time also as already mentioned phase separation of the end-groups might have critical influence as it was observed in previous section. [2]

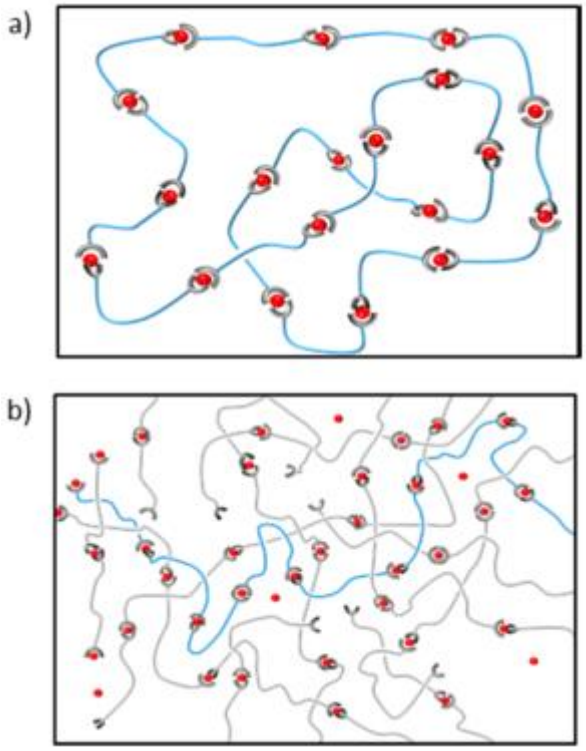

Figure 4.4- (a) Idealistic schematic view of an entangled super-long supramolecular polymer loop from linear bifunctional polymers end functionalized with a sticker at each extremity. (b) Schematic view of different associating configurations from linear associating bifunctional polymers resulting in a large distribution in supramolecular polymer sizes.[2]

The first measurement of supramolecular samples was performed between -30 °C and 50 °C. At the beginning the frequency sweep at high temperature (60 °C) was repeated several times to let the samples homogenized and get to equilibrium state. The first sample that was investigated contains 1 equivalent of Zn. Results are shown in Figure 4.5.

The master curve of PBD-1eq-Zn was obtained through manual shifting of data. The data followed the TTS, although in some region there were difficulties that would be discussed later. The measurement was repeated again once more to check the repeatability of experiment and it was completely successful. Later the shift factors of the reference sample were used to obtain the master curve so it can provide better information.

Although zinc is considered as a labile ion (meaning that zinc bis-terpyridine complex lifetime is short), associating units which keep switching between free and

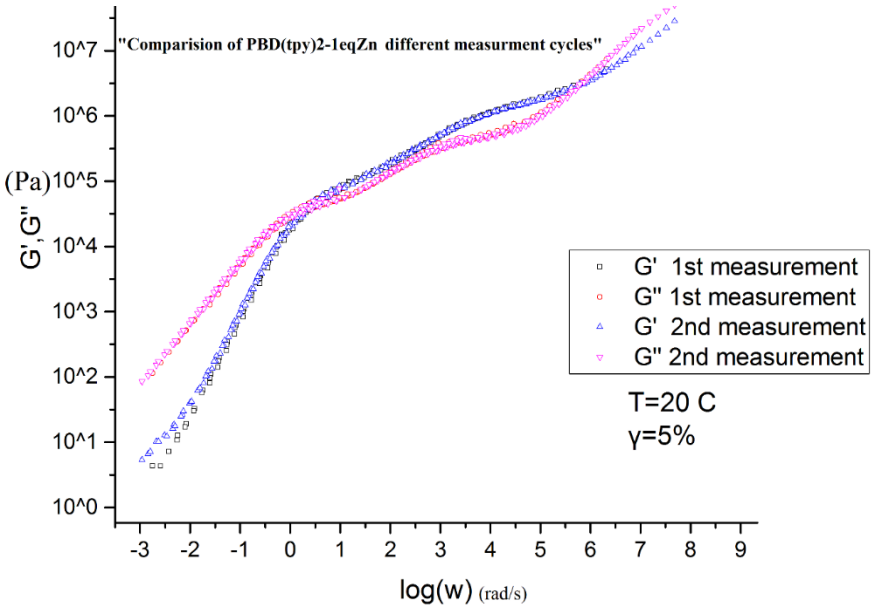

Figure 4.5- Linear rheology curves at 20°C of linear bifunctional PBDtpy2-1eq-Zn (melts)two

attached states clearly affect the rheological properties before going through the flow regime. Indeed, the sample shows a two-steps relaxation, with relaxation times much longer than the ones of the precursor. The first relaxation, taking place at a frequency of around 10^3 rad/s, can be attributed to relaxation of the larger assemblies, formed by the association of several linear PBD(tpy)2 units. Indeed, their relaxation time is much longer than the average lifetime of the bifunctional precursor.

In order to quantify the amount of building blocks involved in these assemblies, we used the tube model in order to determine what is the average molar mass of the chains that we should use in order to correctly describe this first peak of relaxation. As shown in Figure 4.6, a linear polymer with a molar mass of 10 kg/mol gives a good description of this first peak. This means that in average, the linear assemblies contains slightly more than 3 polymer PBD(tpy)2.

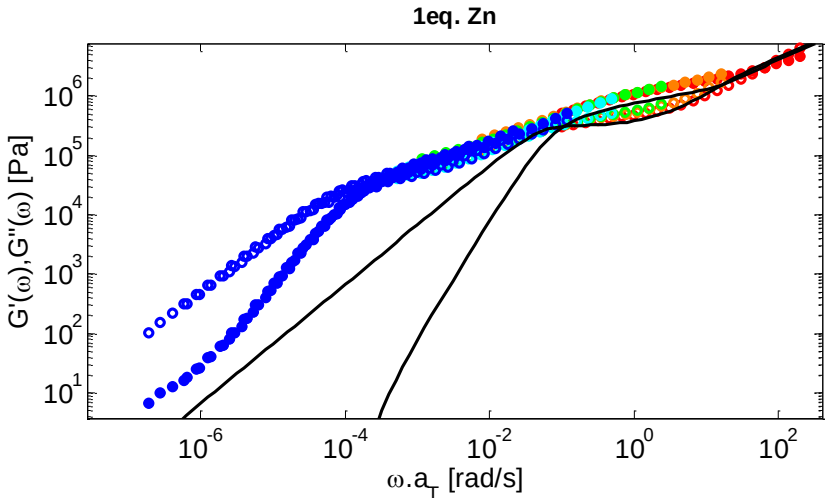

Figure 4.6-Tube model prediction of PBD(tpy)2-1eq-Zn first peak with a linear PB polymer with a molar mass of 10 kg/mol (black curve) T=-30 °C.

Before going on it should be mentioned that by adding different metal ions into functionalized polymer (containing star and linear chains) a gel would be created. A critical gel, in the definition of Chambon and Winter has the storage and loss moduli parallel and proportional to the angular frequency to 0.5. This slow and regular decrease should occur on the whole frequency range for the limit of the critical gel. This behavior is the illustration of a complicated relaxation process. Indeed, there is not a unique relaxation time but more an infinite spectrum of relaxation times. It is consistent with an infinite and regular relaxation which give straight and parallel lines. With a physical association which has a typical life time, it looks not possible to obtain such critical gel. However, it is possible that before the final relaxation time which is probably linked to the life time of the association, the behavior is gel-like.[3]

On the other hand, the second, low-frequency, relaxation process cannot be attributed to the relaxation (by reptation) of the long linear assemblies. Indeed, there is no reason that these assemblies form two different populations, with relaxation times separated by several order of magnitude. Therefore, based on the above discussion, we attribute this slow relaxation process to phase separation of the metal-ligand complexes, with the phase-separated domains acting as branching points for the linear assemblies, since the fraction of molecular segments trapped between two of these domains is not able to disentangle and relax.

Interestingly, one can observe in Figure 4.6 that a second Rouse-like regime appears at intermediate frequencies, i.e. between 10 and 100 rad/s similar behavior has already been observed in literature, for example in Hawke et al.[4] in the case of entangled sticky chains and was attributed to the slow motion of the molecular segments trapped between two sticky domains, exploring their surrounding at the rhythm of the entanglement/disentanglement of the free chains and dangling ends.

We believe our sample behaves similarly, containing a fraction of linear assemblies which are free to move and reptate, as well as assemblies which have one or more complexes involved in a (phase separated) cluster. While the assemblies with only one complex trapped into a cluster are still able to disentangle through fluctuations process (see section 1.5), the ones with two or more complexes belonging to phase-separated domains cannot relax by reptation or fluctuations (Fig.4.7).

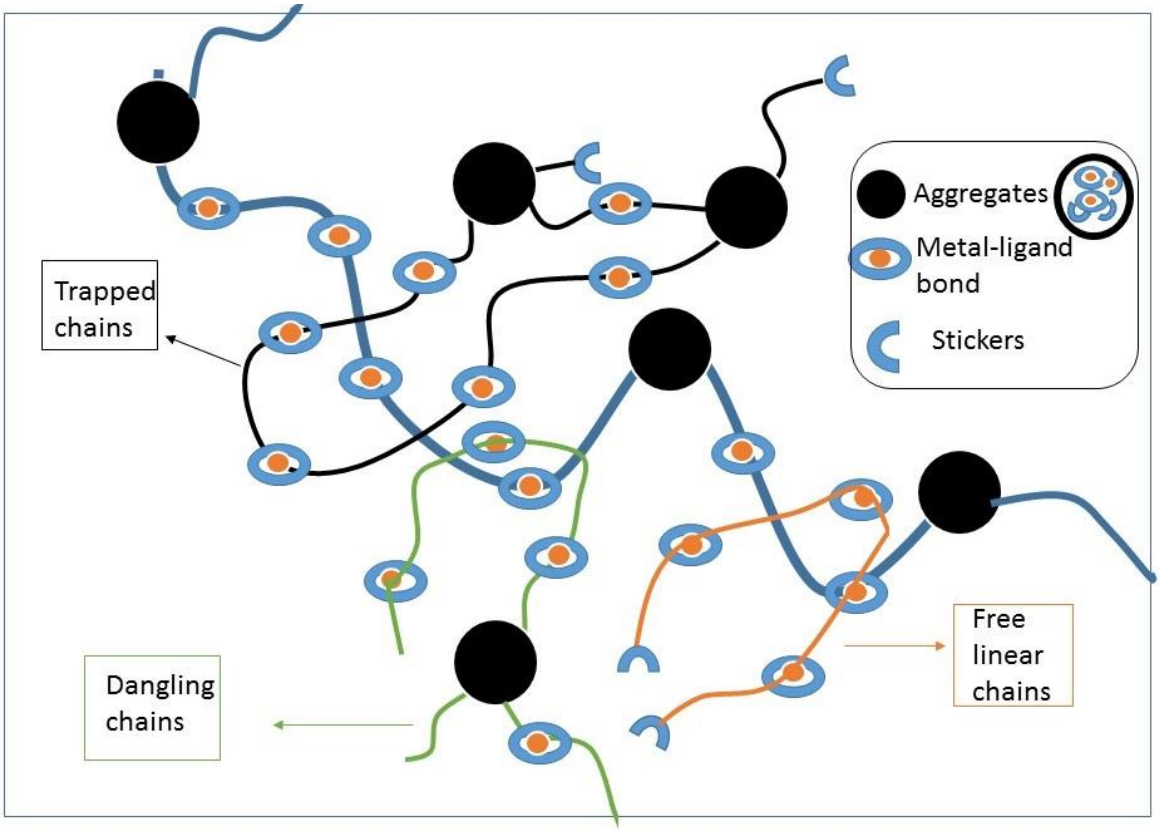

Figure 4.7 Schematic illustration of the adopted physical picture. Aggregates (clusters) composed of terpyridine groups with metal- ligands bonds are shown as filled circles. It is surrounded by free linear chains not attached to aggregations, dangling chains that are only attached to one cluster, and trapped chains that are connected to at least two cluster.

However, with time, they can explore larger and larger surrounding, since most of the chains with which they are entangled are able to move and disentangle. This process is represented in Figure 4.8.

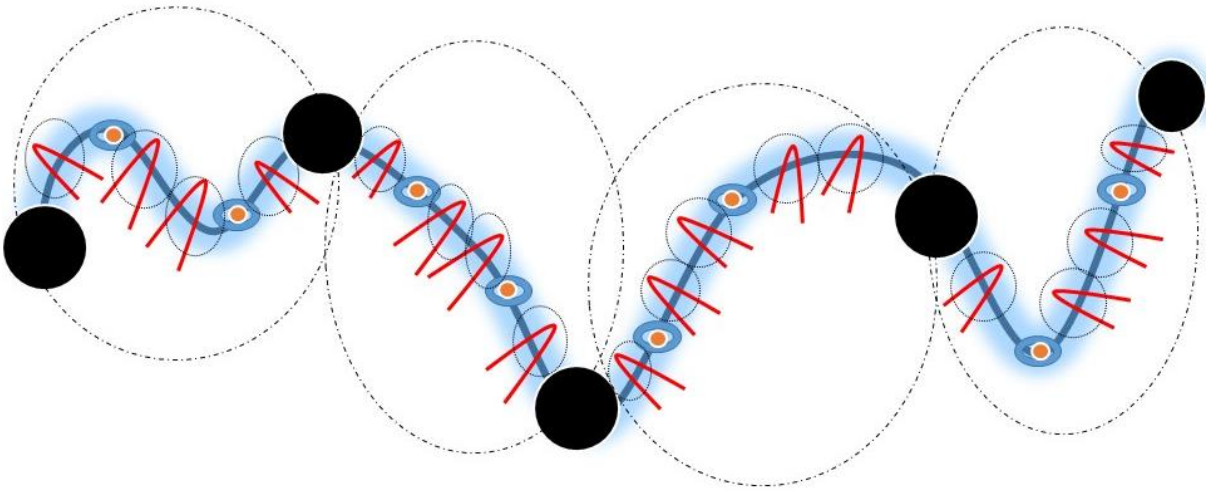

Figure 4.8- Cartoon of the relaxation mechanisms of a probe chain (dark blue line). Aggregates (clusters) composed of terpyridine groups with metal- ligands bonds are shown as filled circles: At early timescales, the mobile components (red lines) are still entangled with the probe chain. With time the "relaxation blob" increase from these entanglements to blobs to the blobs defined by both sticky junctions and aggregations. Relaxation occurs via pure Rouse motion only.

This picture is tested in Figure 4.9, in which we consider two populations of chains: the first one is made of linear assemblies of mass equal to 10 kg/mol, while the second is a fraction of chains with infinite relaxation time. Thus, this last population can only relax by these Rouse motions dominated by the motions of the linear assemblies. We let the proportion of the two populations as a fit parameter. Of course, the real composition of the sample is expected to be more complex since the presence of dangling ends should be also taken into account. Furthermore, since no relaxation mechanism is proposed for describing the terminal relaxation of the trapped chains, this approach cannot be valid at low frequency, at which the sample starts to flow. However, the proposed description allows us to obtain a first estimation of the proposed picture. Results are shown in Figure 4.9. A good description of the data has been obtained.

Considering 10 wt% of the chains being trapped between two clusters (see the red curves). While a more quantitative agreement between experimental and theoretical data would require a more accurate sample description, this result allows us to validate the molecular picture proposed here. the building blocks self-assemble through metal-lingand interaction into linear assemblies containing 3 or 4 building blocks, and around 10 wt% of these assemblies are trapped between aggregates.

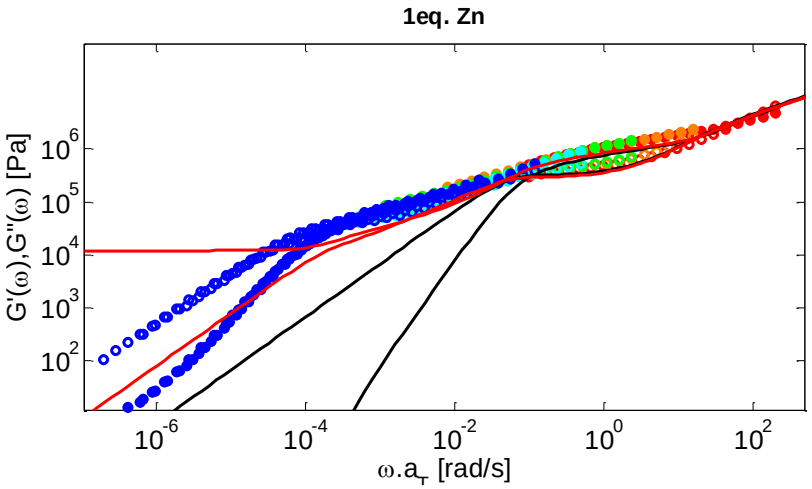

Fig 4.9- Tube model prediction of PB-1eq-Zn chains with two populations of chains: the first PB with 10kg/mol and the second one with infinite relaxation time. Description obtained by considering 10 wt% of the chains being trapped between two clusters.

Still, the terminal regime of the figure needs to be discussed: it is observed that a low frequency, the chains finally flow.

The origin of this relaxation is not clear since it could be due to several mechanisms. First this relaxation could be due to breaking of the complexes. Second, it could be due to detachment of a complex from the phase separated domains. In the first case when complex breaks the bonds along the self-assemblies trapped between two aggregates, the self-assembly can then relax as two self-assembled arms attached to the aggregates. The other possibility is that the micro-phase domains start to separate because the complex try to escape from the clusters. However, the necessary time for a complex to dissociate from a cluster is probably longer than the lifetime of a complex. In such a case, breaking of the complexes should be the main mechanism which allows the sample to flow.

We now extend this discussion to the other samples containing 1 or 2 eq. of Zn or Co ions. All the experimental data that have been obtained from different temperatures are gathered below and all the cases would be study separately. Except the polymer without ions all other data were measured between 0.1 to 200 rad/s and 5% shear rate. In the Fig. 4.10 and Fig4.11 the data between -30 °C to 50 °C are shown. By having a general look at the measurements of supramolecular polymers, we find out that two plateaus and two relaxation times are present for each sample of supramolecular and the curves are following almost the same trend. In addition, we can understand easily that changing the nature of metal ions or adding an excess amount of it leads to a different viscoelastic property. By measuring at low temperatures, we can get information about local dynamic of the chains. From -20 °C the first plateau can be observed. It shows a plateau modulus around 10^6 (Pa) which is common for the entangled PB polymers. By increasing temperature, the PBD$(tpy)_2$ starts to flow while the metallo-supramolecular behave differently. The first relaxation time is longer than initial sample due to presence of metal ligand bonds and forming longer linear chains which produce entanglements with other chains. As the metal-ligand coordination between terpyridine and Co is more stable than Zn, the 1eq of Co sample has a more elastic behavior compared to Zn. By decreasing the frequency at 0 °C the level of first plateau is decreasing slowly as a sign of existence of different relaxation times. The second plateau is observed for all the samples but in this regime the samples (2eq Zn) with excess amount of ion behaves more elastic as the size and number of clusters are increasing and the relaxations of the chains are more difficult. From 20 °C the second cross over can be observed and as the temperature is increasing the samples will show the second relaxation which might be due to breaking of complexes or detachments of micro-domains. Above 30 °C the supramolecular samples start to flow. In the next section we try to obtain the master curves of the samples based on this experimental data which can provide better information.

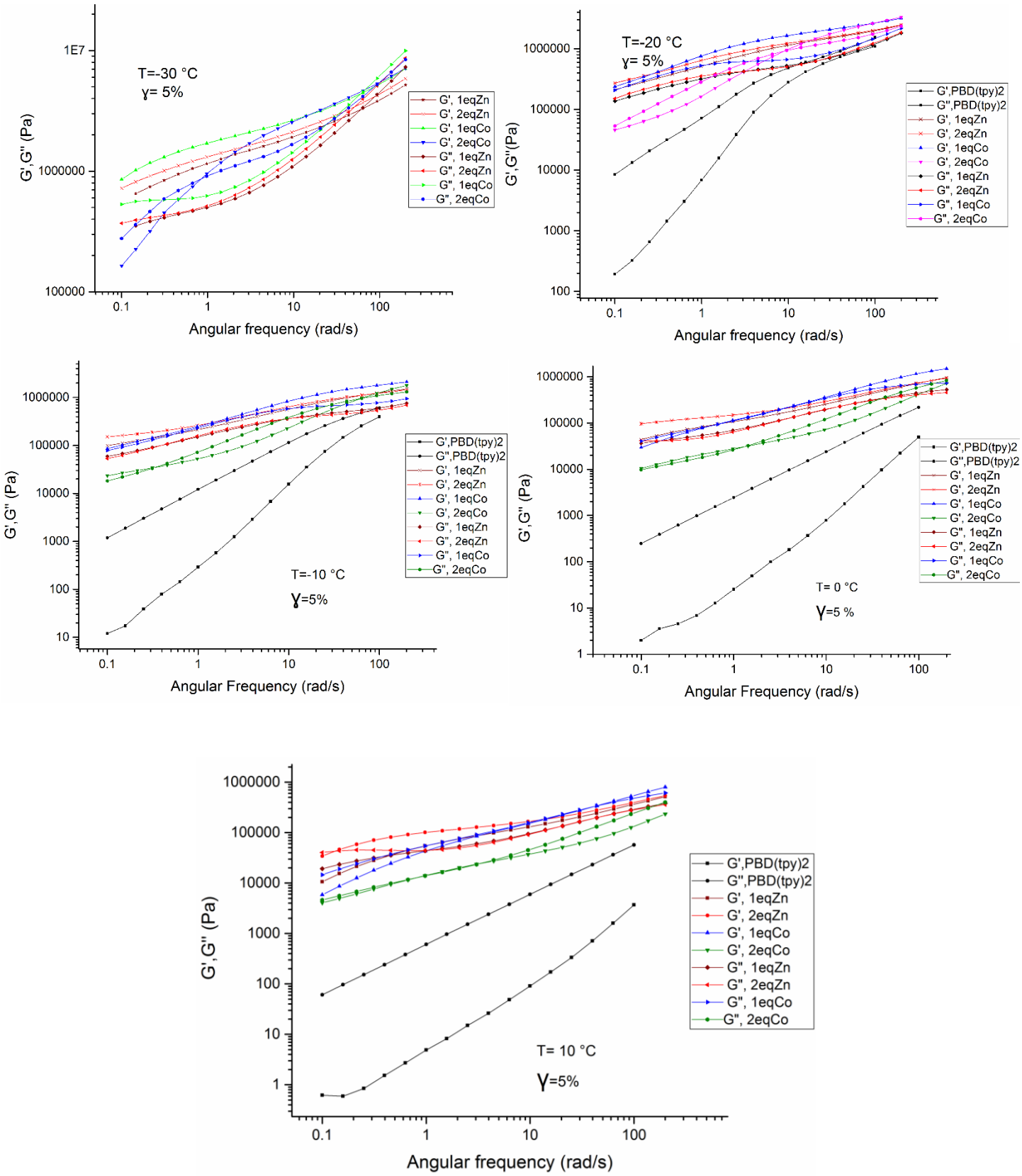

Figure 4.10- LVE experimental data of different metallo-supramoleculars at temperatures between (-30 °C-10 °C)

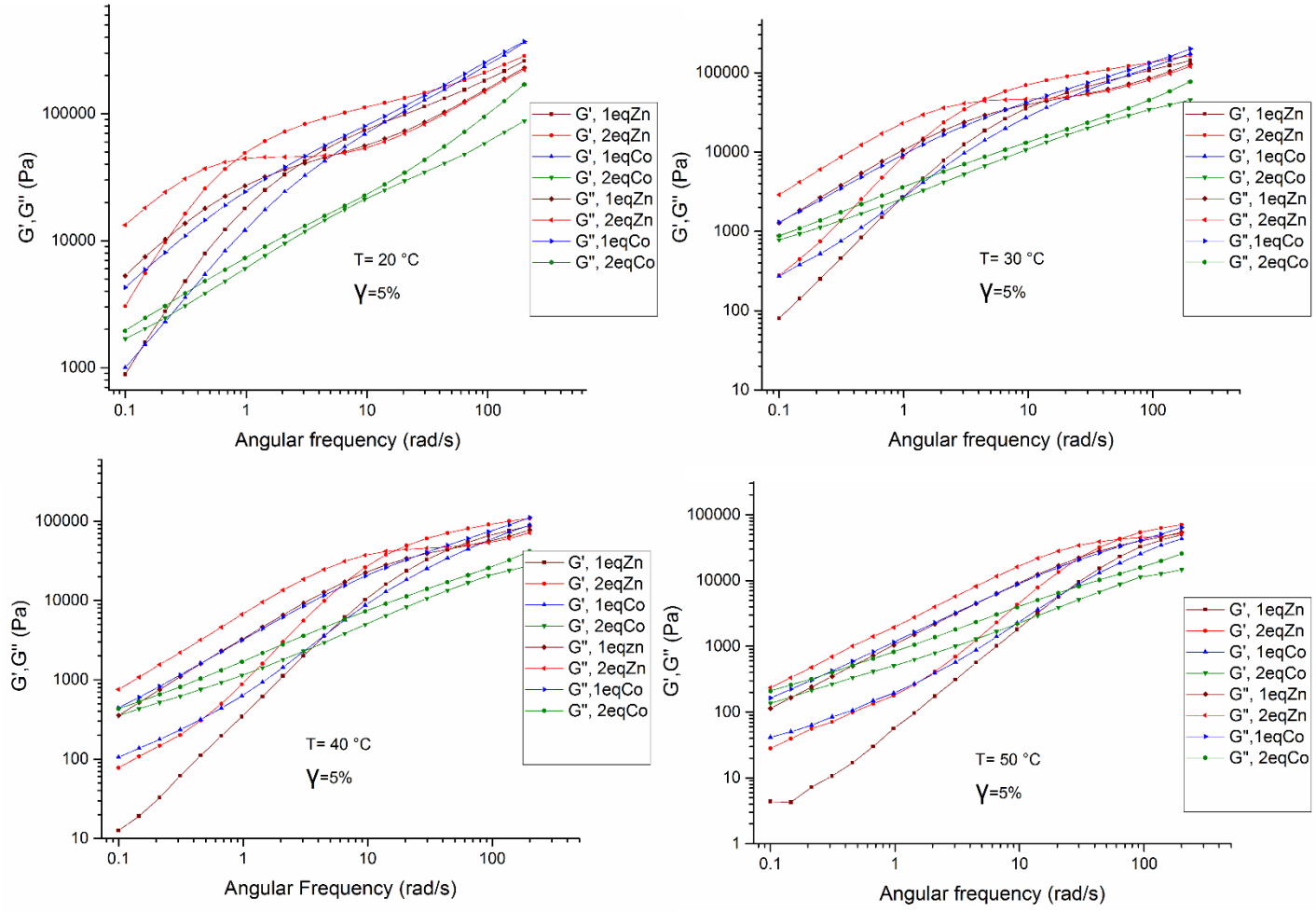

.

Figure 4.11- LVE experimental data of different metallo-supramoleculars at temperatures between (20 °C-50 °C).

4.2-MASTER CURVES AND THERMO-RHEOLOGICAL COMPLEXITY:

The master curves of the reference sample PBD(tpy)$_2$ and the PBD-1eq-Zn are shown in Fig.4.13. They are obtained using the horizontal shift factors, a_T, presented in Fig.4.12. In case of the reference sample "IndPBD" (green line) these shift factors almost exhibit a Williams-Landel-Ferry (WLF) behavior (black line), C_1= 9.42, C_2= 100 K and T_0= 243 k (the so-called reference temperature). In the case of PBD(tpy)$_2$ there are difference in the shift factors which is also another indication of terpyridine group changing the nature of dynamics governing the polymer behavior.

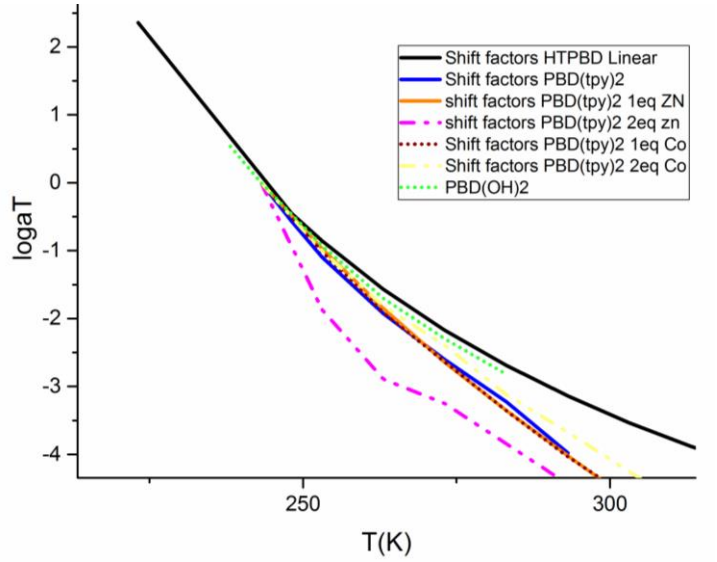

Figure 4.12- horizontal shift factors for the reference and other metallo-supramolecules.

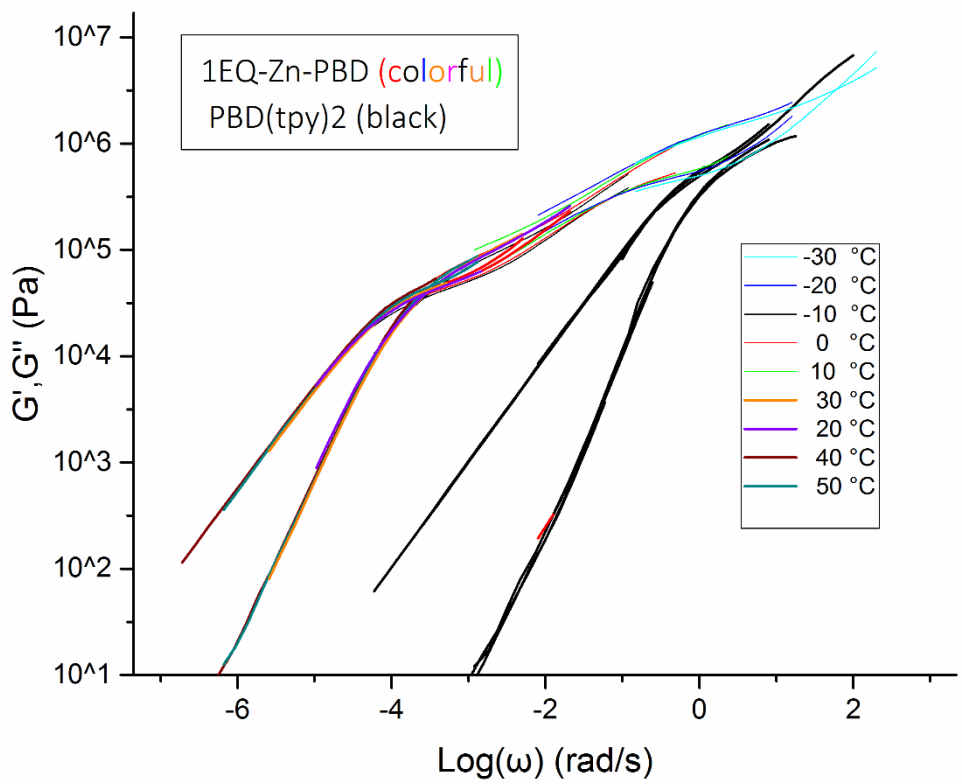

Figure 4.13- The master curves of the reference sample and the PBD-2eq-Zn at T=243.15 k.

On the other hand, adding metal ions in the functionalized sample only slightly affects these shift factors, which are found to be close to ones of sample $PBD(tpy)_2$. The large deviation observed with the sample containing 2eq of Zn can be attributed to a different behavior at 243.15 K, i.e. the temperature which has been selected as the reference temperature. Indeed, if another temperature would have chosen, the shift factor curve would have shown a good match with the other curves, for all temperature apart from 243.15K.

In the following, the master curves of the transient networks have been built based on the shift factors used for the reference. In such a case, we can assume that they are only correct for the

temperature influence of the segmental dynamics of the chains, not for the sticker dynamics. Example is shown in Figure 4.13, which shows the comparison between the viscoelastic response of the functionalized PB sample, with and without adding Zn metal ions in stoichiometric amount. It is observed that this response of the transient network shows a thermos-rheological behavior, which is often the case for supramolecular polymers: by changing the temperature, the amount and dynamics of the supramolecular bonds is affected, which is not taken into account in the shifting parameters. Here, we observe that this complex behavior mainly takes place at intermediate frequency, between the two different rubbery plateaus. As already discussed the first (high frequency) relaxation and drop of the plateau is similar to the reference polymer but relaxation needs more time. It can be justified as metal ions would lead to the formation of metal-ligand coordination giving different lengths of supramolecular polymer chains. The terminal relaxation of the assemblies seems to slow down when the temperature is decreased producing thermo-rheological complexity (TRC) at intermediate and low frequencies. This can be explained as followed: when decreasing temperature, the lifetime of the metal-ligand complexes is increased. Therefore, the association probability of the building blocks is increased, which leads to the formation of longer assemblies, characterized by a longer relaxation time. From this observation, we conclude that the complex formation is temperature-dependent.

On other hand, the second relaxation process which takes place at low frequency, does not seem to be sensitive to temperature and no thermos-rheological behavior is observed in this region. Nevertheless, it is important to note that in this range of temperature, the shift factors deviate from the WLF equation, in a similar way as for the PBD$(tpy)_2$ sample (see Figure 4.12.)

Building a master-curve (Figure 4.14) for the PBD-2eq-Zn supramolecular is more delicate since this sample manifests higher TRC also at intermediate frequencies. The relaxation time of the free linear assemblies as well as the level of the second plateau, which is directly related to the proportion of sample trapped between two phase-separated clusters, is strongly affected by temperature. Again, in order to follow a consistent approach, the data of the PBD-2eq-Zn sample have been shifted according to the shift factors of the reference and PBD $(tpy)_2$ samples.

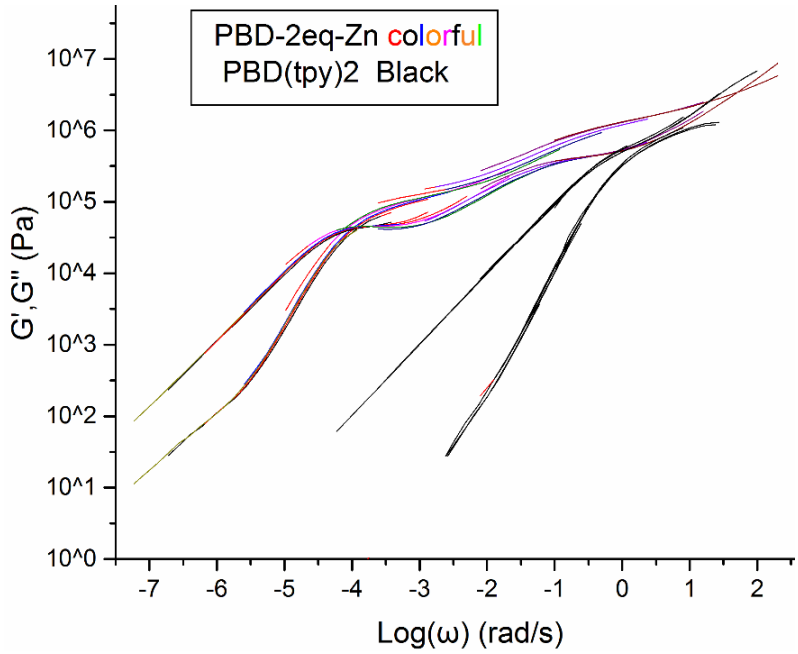

Figure 4.14- The master curves of the reference sample and the PBD-2eq-Zn at T=243.15 k.

In Figure 4.15 both samples of PBD 1 and 2 equivalent of Zn can be compared in one diagram.

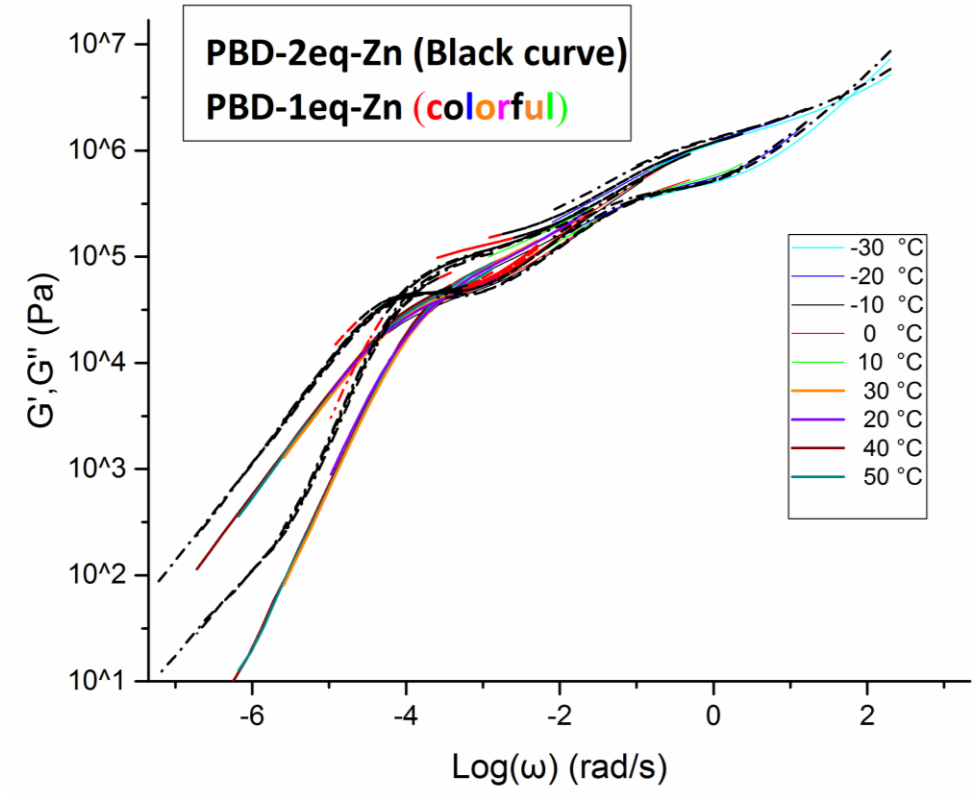

Figure 4.15- The comparison of the master curves of the the PBD-1eq-Zn and the PBD-2eq-Zn at T=243.15 k.

At high frequency both curves superimpose very well and have the same region and level of first plateau, which is mainly dominated by the entanglements of the assemblies. Furthermore, the relaxation time associated to the free assemblies is similar, meaning that the length of the assemblies (or equivalently, the probability for the PB chain extremities to be part of metal-ligand complexes) is not very sensitive to the amount of metal ions (as long as their proportion is equal or above the stoichiometric amount). The main difference between the samples is observed in the second plateau where in the intermediate region the TRC is increasing and the crossover also shifts to lower frequencies. So, this diagram is providing very useful information. As the amount of metal ions has been doubled for each sticker, the proportion of chain segments trapped between two phase-separated clusters is increasing. Furthermore, it is observed that the terminal relaxation time of the sample is also delayed. This is probably due to the fact that the larger probability of the complexes to be trapped in a cluster is related to the formation of bigger structures, as represented in the Fig. 4.16. Consequently, these bigger cross-linked assemblies need more time to dissociate and finally flow.

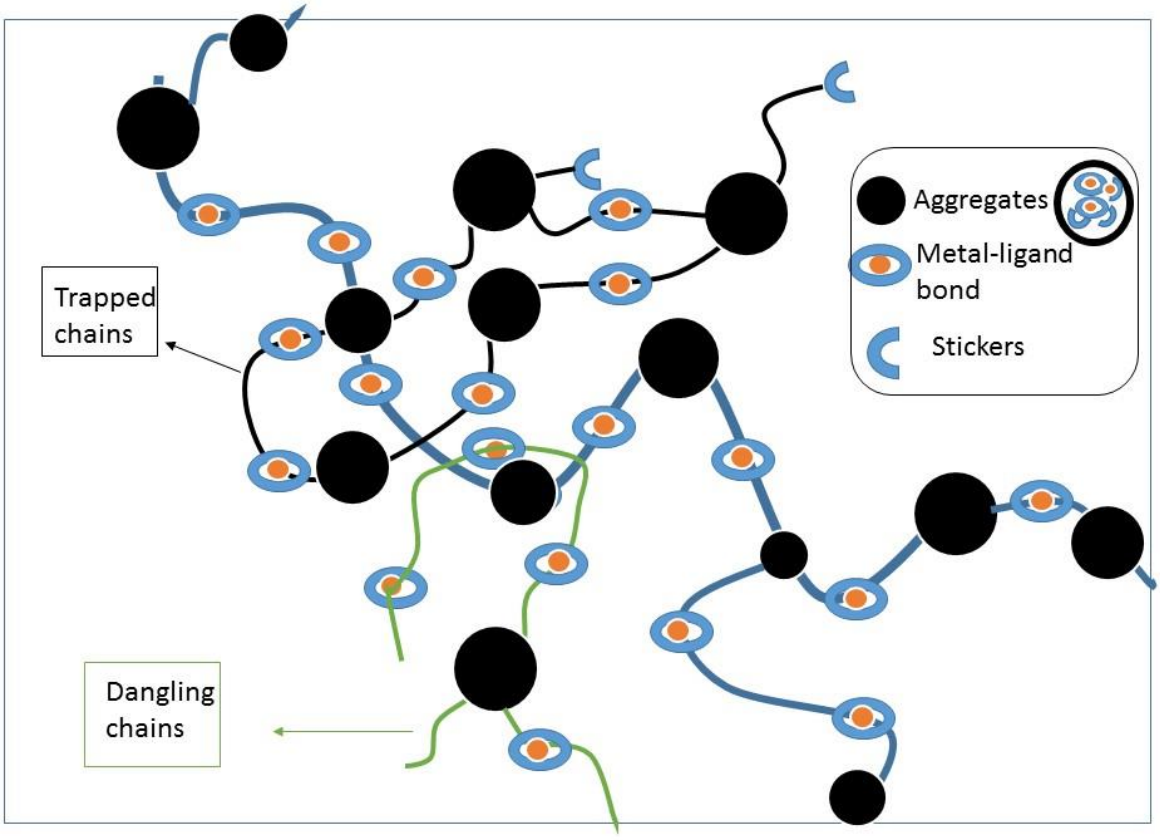

Figure 4.16- Schematic illustration of the effect of increasing the metal-ions amount. Doubling the amount of metal ions leads to larger probability of the complexes to be trapped in a cluster which is related to the formation of more and bigger structures.

In the ideal case, we would expect having shorter linear assemblies due to the formation of mono-complexes acting as the extremities of the assemblies, as illustrated in Figure 4.17. This was, for example, observed in a research about highly tunable systems presented by Brassinne et al., who study the linear viscoelastic properties of ultrahigh molecular weight polymers sparsely decorated with chelating ligand in aqueous solution, adding metal ions to this sample

leads to the creation of a reversible network, thanks to the formation of metal-ligand complexes. By playing with the nature and proportion of metal ions, the molar mass of the backbone, and the temperature, the authors demonstrate that it is possible to control its dynamics, with a terminal relaxation time. In particular, they show that adding metal ions in excess compared to their stoichiometric amount speeds up the reversible dynamics of the bonds.[5]

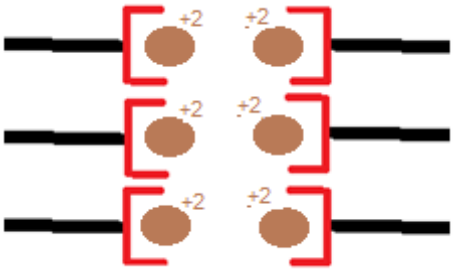

Figure 4.18- Terpyridine stickers containing metal ions in each one.

However, this is not observed with our system. Adding an excess of ions enhances the formation of aggregates, rather to create mono-complexes.

Overall these data validate the assumption that a phase separation is happening. Despite the fact that Zn is quite labile, its lifetime seems long enough to observe the relaxation of the linear assemblies through reptation process rather than by complex dissociation. Only at lower frequency, they start to dissociate and associate again, allowing the complex branched structures to be destroyed. By adding the double amount of ions shorter the complex formation stays similar but the structure of the clusters is changing. The bigger the clusters, the best is the chains cohesion, leading to longer terminal relaxation times, but also take much longer to equilibrate.

Now we investigate and discuss the effect of changing the nature of metal ions and using a stronger one. In the case of Co even after preparing the samples phase separation was visible. As mentioned in the chapter 3, part of the ions was lost during the sample preparation. Therefore, the exact proportion of Co ions is not known, being certainly lower than the target proportions of 1eq or 2eq.

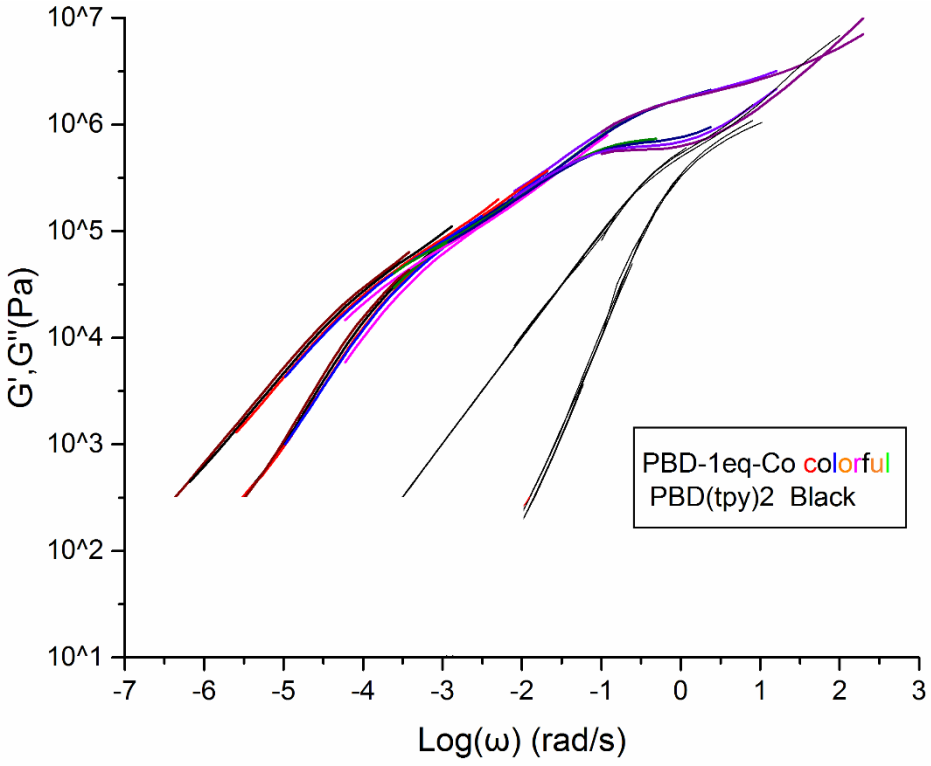

Figure 4.19- The master curves of the reference sample and the PBD-1eq-Co at T=243.15 k.

The comparison of the viscoelastic properties of 1eq of Zn and 1eq of Co is shown in (Figure 4.20). It shows that in the sample containing Co, TRC is increasing, most probably due to more stable association between stickers and metal ions.

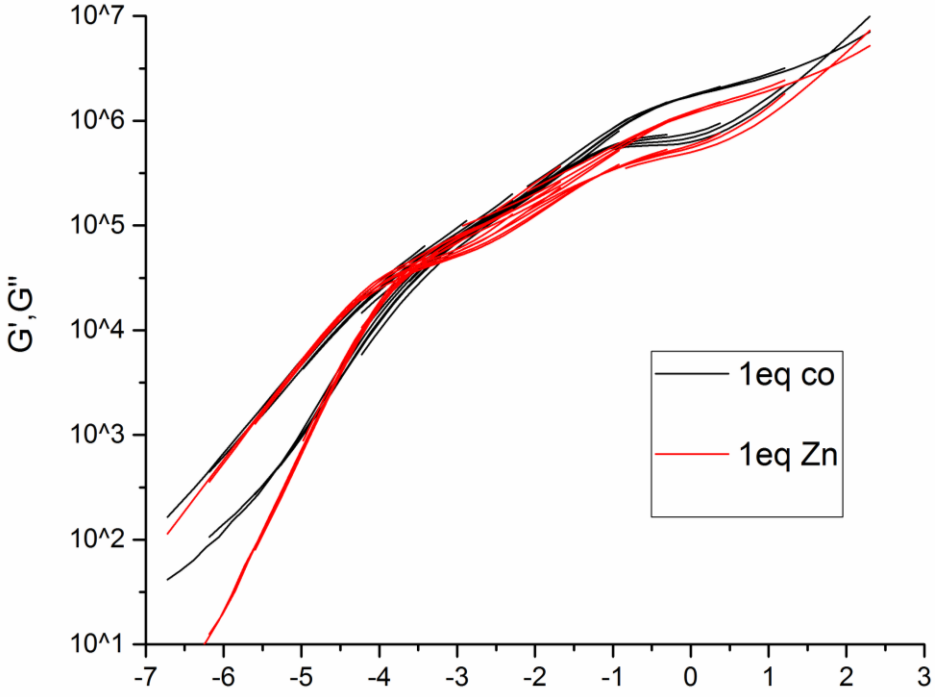

Figure 4.20- Comparison of The master curves of PBD-1eq-Zn and the PBD-1eq-Co at T=243.15 k.

The figure also shows that the Co and Zn 1eq. samples do not superimpose at high frequencies. It is possible to conclude that the sticky group association with Co can also affect the local dynamics of the chains. The TRC at low and intermediate frequency has increased which can be an indication that clusters that clusters have been formed are structurally stronger.

In Figure 4.21, we show the results obtained by adding 2eq Co. During the preparation of this supramolecular polymer, the amount of phase separation increased even more. Again, the pink regions were washed with solvent to obtain a homogenous sample. It is completely obvious that TTS has failed and TRC has increased a lot.

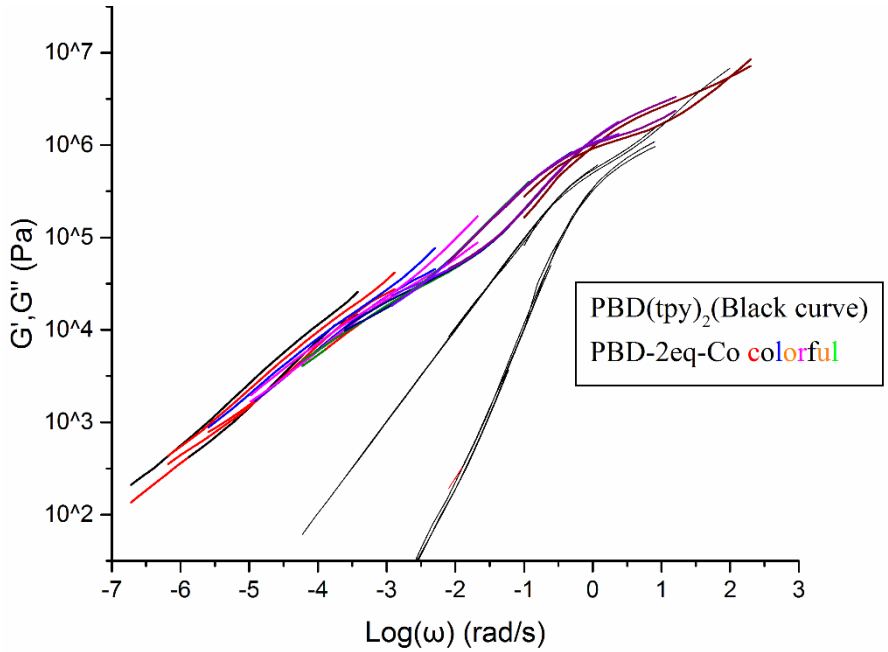

Figure 4.21- The master curves of the reference sample and the PBD-1eq-Co at T=243.15 k.

The viscoelastic properties of this sample are rather unusual: while the short relaxation time of the first relaxation peak seems to indicate that a fraction of the sample is relaxing as short dangling ends or short linear assemblies, the sample is also characterized by a very long power law relaxation at low frequency, with G' and G" decreasing with a slope of around ½.
The origin of this behavior is not clear. A possible explanation would be the combination of shorter self-assemblies (due to the appearance of mono-complexes) with creation of very big structures, due to an enhance in formation of aggregates, which take a very long time to decompose into smaller and smaller structures. Also by comparison to 2eq-Zn, as it is shown in Figure 4.22, we observe that the amount of dangling ends or linear chains is larger with Co than with Zn ions, while the terminal time is longer with the Co.

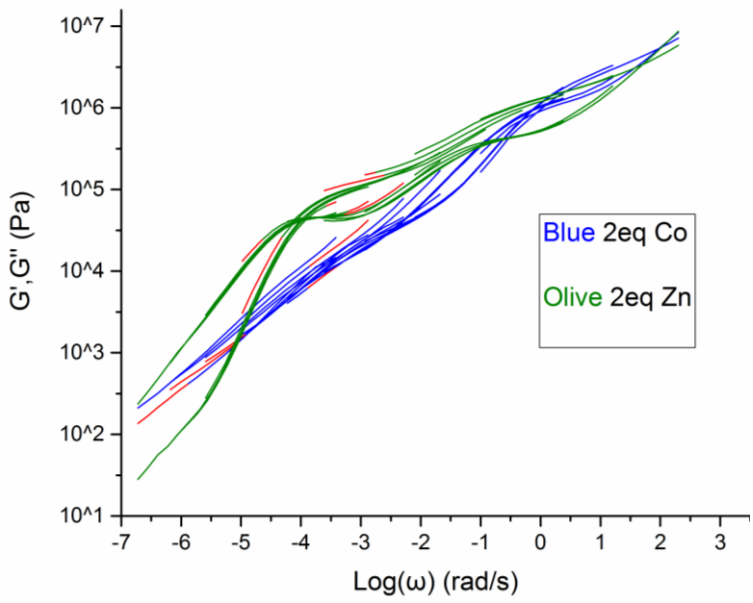

Figure 4.22- Comparison of The master curves of PBD-2eq-Zn and the PBD-2eq-Co at T=243.15 k.

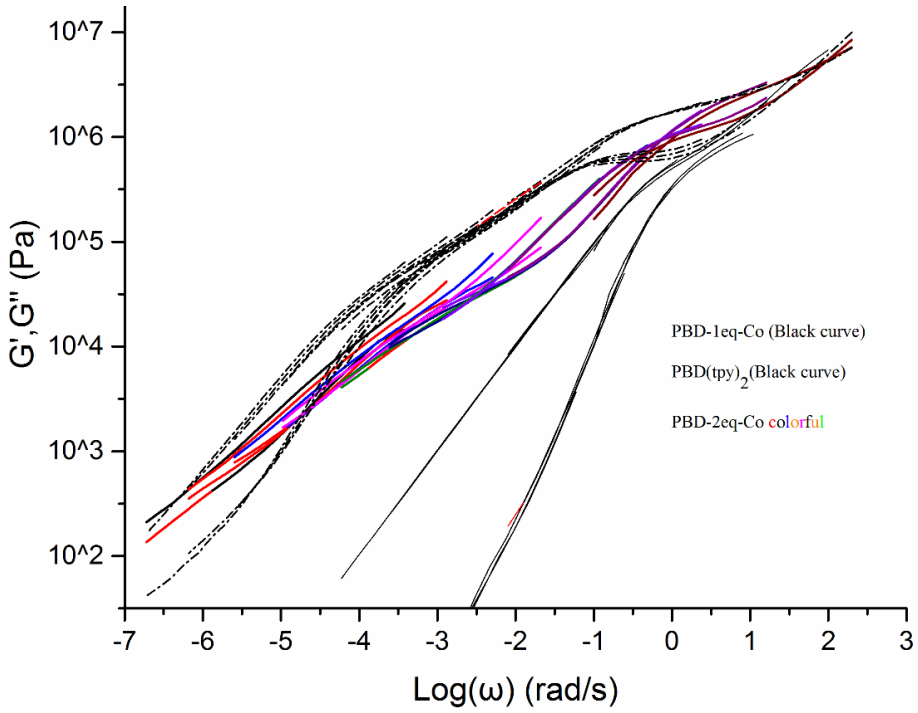

Figure 4.23- Comparison of The master curves of PBD-2eq-Co and the PBD-1eq-Co at T=243.15 k.

In order to validate our picture of large branched and complex assemblies, Small-angle X-ray scattering (SAXS) and transmission electron microscopy (TEM) studies of these supramolecules should be performed. Due to lack of time these tests were not obtained, but definitely they are essential to provide more clear picture of the sample structure.

4.3-CONCLUSION:

By investigating four different samples the dynamic of metallo-supramolecular chains of hydrogenated terpyridine-terminated polybutadiene and different metal ions (1 and 2 eq. of Zn and Co) were investigated. The master curves of the transient networks were built based on the

shift factors of PBD(tpy)$_2$ and considering that they are only correct for the temperature influence of the segmental dynamics of the chains, not for the sticker dynamics. For all samples, it was observed that the response of the transient network shows a thermo-rheological behavior specially at intermediate frequencies, which is often the case for supramolecular polymers. By adding an excess amount of ions, especially in case of Co, this TRC increased because the lifetime of the metal-ligand complexes increased too. In addition, by studying all the samples two plateaus were observed. We conclude that the first relaxation happens due to fast motion of the free linear assemblies, followed by the slower (Rouse) motion of the molecular segments trapped between two aggregates made of several metal-ligand complexes.These molecular segements , explore their surrounding at the rhythm of the entanglement/disentanglement of the free chains and dangling ends. The second (terminal) relaxation is not clear since it could be due to several mechanisms. Most probably, this relaxation is due to breaking of the complexes along the self assemblies.However, it could also be due to the detachment of a complex from the phase separated domains. This relaxation time increased by increasing the amount of metal ions as the number and size of clusters are increasing.In case of Zn despite the fact that Zn is quite labile, its lifetime seems long enough to observe the relaxation of the linear assemblies through reptation process rather than by complex dissociation. Only at lower frequency, they start to dissociate and associate again, allowing the complex branched structures to be destroyed. In case of Co, the phase separation happened during preparation of samples therefore the targeted amount of metal-ion in sample was not achieved. Although by comparison to Zn samples the amount of dangling ends or linear chains is larger with Co than with Zn ions, while the terminal time is longer with the Co ions.

References:

1. Jirˇı´ Podesˇva, J.ı.D., Jirˇı´ Speˇva´ cˇek, Petr Sˇ teˇpa´ nek, and Peter Cˇ ernoch, *Supramolecular Structures of Low-Molecular-Weight Polybutadienes, as Studied by Dynamic Light Scattering, NMR and Infrared Spectroscopy.* Macromolecules, 2001. **34**: p. 9023-9031.

2. Flanco Zhuge, J.B.C.-A., Fustin,Evelyne van Ruymbeke ,Jean-Francois Goh, *Synthesis and Rheology of Bulk Metallo-Supramolecular Polymers from Telechelic Entangled Precursors.* Macromolecules, 2017. **50**: p. 5165-5175.

3. Winter, F.C.H.H., *Analysis of Linear Viscoelasticity of a Cross-Linking Polymer at the Gel Point.* Journal of Rheology, 1986. **30**: p. 367-382.

4. Hawke, A., Van.Ruymbeke, *Viscoelastic properties of linear associating poly(n-butyl acrylate) chains.* Rheol. , 2016. **60**: p. 297-310.

5. Brassinne, J., A. Cadix, J. Wilson, and E. van Ruymbeke,, *"Dissociating sticker dynamics from chain relaxation in supramolecular polymer networks—The importance of free partner!,".* J. Rheol, (2017). **61**: p. 1123–1134.

Rue Archimède, 1 bte L6.11.01, 1348 Louvain-la-Neuve, Belgium **www.uclouvain.be/epl**